

# **Hypoxia-induced gene expression in murine alveolar macrophages**

Inauguraldissertation

zur Erlangung des Grades eines Doktor der Medizin  
des Fachbereichs Humanmedizin  
der Justus-Liebig-Universität Gießen

vorgelegt von Zeev Israeli  
aus Ayelet haschachar, Israel

Gießen 2009

Aus dem Institut für Pathologie  
des Universitätsklinikums Gießen und Marburg, Standort Gießen

Leiter: Prof. Dr. Schulz

Gutachter: Prof. Dr. Fink

Gutachter: PD Dr. Hänze

Tag der Disputation: 02.02.2009

---

## I Table of contents

I	Table of contents .....	I
II	Abbreviations .....	V
III	Declaration .....	VII
<b>1</b>	<b>Introduction .....</b>	<b>1</b>
1.1	Oxygen sensing	1
1.1.1	What is the oxygen-sensing protein?	1
1.1.2	Oxygen signalling	3
1.2	Hypoxia and its influence on the cell	3
1.2.1	The hypoxia- inducible factor 1 (HIF-1)	3
1.2.2	Nuclear Factor kappa B and hypoxia	6
1.3	Transcriptional mechanisms in acute lung injury	8
1.3.1	Therapeutic targets for acute lung inflammation	10
1.4	Hypoxia and alveolar macrophages	12
1.4.1	Activation of alveolar macrophages by hypoxia and lipopolysaccharide	12
1.4.2	The effects of hypoxia on the adhesiveness of AM	14
1.4.3	Phagocytosis and ATP levels in alveolar macrophages in hypoxia	15
1.5	DNA Array technology	16
1.5.1	What is a Microarray?	17
1.5.2	How are Microarrays produced?	17
1.5.3	How are Microarrays used?	18
1.5.4	The Microarray technique and some of its problems	19
1.5.5	Array technology applications	22
1.5.6	Limitations of Microarrays	23

---

1.6 Aim of this work	23
<b>2 Materials and Methods .....</b>	<b>24</b>
2.1 Small Materials	24
2.2 Instruments	24
2.3 Reagents and Kits	26
2.3.1 Bronchoalveolar lavage and cell lysis	26
2.3.2 RNA extraction	26
2.3.3 DNase treatment of total RNA	26
2.3.4 Labelling of cDNA	27
2.3.5 Column chromatography	27
2.3.6 Preparation of the cDNA for hybridisation	27
2.3.7 Stripping the Arrays membranes	27
2.3.8 cDNA synthesis from total RNA using RT enzyme (for PCR)	27
2.3.9 Real-time PCR	28
2.3.10 Agarose gel electrophoresis	28
2.3.11 Immunohistochemistry	28
2.3.12 Primers for TaqMan PCR	29
2.4 Methods	31
2.4.1 Animal model of hypoxia	31
2.4.2 Bronchoalveolar lavage (BAL)	31
2.4.3 Isolation of RNA from alveolar macrophages (AM)	32
2.4.4 DNase treatment of total RNA	33
2.4.5 Spectrophotometry of isolated RNA	33
2.4.6 Synthesis of radiolabelled cDNA using oligo (dT) primers	34
2.4.7 Column chromatography	35
2.4.8 Array hybridisation	36

---

2.4.9	Exposure of the phosphoimager plates to the membranes	37
2.4.10	Stripping cDNA from the Atlas arrays	38
2.4.11	Image analysis and data processing	38
2.4.12	Real-time PCR	40
2.4.13	cDNA synthesis from total RNA using RT enzyme	43
2.4.14	Agarose gel electrophoresis	46
2.4.15	Immunohistochemistry	47
<b>3</b>	<b>Results.....</b>	<b>52</b>
3.1	Bronchoalveolar lavage	52
3.2	Hybridisation results	53
3.3	Arrays analysis	54
3.4	PCR results	58
3.5	Immunohistochemistry	61
<b>4</b>	<b>Discussion .....</b>	<b>65</b>
4.1	Methodical aspects and limitation of the study	65
4.2	Genes selected for immunohistochemistry	67
4.2.1	Vimentin	67
4.2.2	Integrin $\beta$ 2	72
4.2.3	CD 74 antigen	79
<b>5</b>	<b>Summary .....</b>	<b>81</b>
<b>6</b>	<b>Zusammenfassung .....</b>	<b>83</b>
<b>7</b>	<b>References .....</b>	<b>85</b>
<b>8</b>	<b>Curriculum Vitae.....</b>	<b>93</b>

---

**9 Acknowledgments.....94**

---

## II Abbreviations

AEC	alveolar epithelial cells
AM	alveolar macrophages
AP	alkaline phosphate
APAAP	alkaline phosphatase anti alkaline phosphatase
ARDS	acute respiratory distress syndrome
BAL	bronchoalveolar lavage
BM	blood monocytes
bp	base pair
CD	cluster of differentiation
cDNA	complementary DNA
DNA	deoxyribonucleic acid
g	gram
h	hour(s)
HIF-1	hypoxia inducible factor 1
HRE	hypoxia responsive element
ICAM	intercellular adhesion molecule
IF	intermediate filaments
IL	interleukin
l	litre
LFA-1	leukocytes function-associated antigene-1
LPS	lipopolysaccharide
m	milli ( $10^{-3}$ ) or meter(s)
M	Mol
min	minute
$\mu$	micro ( $10^{-6}$ )
MCP-1	monocyte chemoattractant protein-1
MF	microfilaments
MT	microtubules
MIP	macrophages inflammatory protein
mRNA	messenger RNA
NF-kB	nuclear factor kappa beta
nm	nanometer
PCR	polymerase chain reaction
PMN	polymorpho- nuclear cells
RNA	ribonucleic acid
ROS	reactive oxygen species
RT	reverse transcriptase
SDS	sodium deodecylsulfate
SSC	sodium chloride sodium citrate
TGF- $\beta$	transforming growth factor- $\beta$

---

TNF	tumour necrosis factor
VCAM	vascular cell adhesion molecule
VEGF	vascular endothelial growth factor



### **III Declaration**

Ich erkläre: Ich habe die vorgelegte Dissertation selbständig, ohne unerlaubte fremde Hilfe und nur mit den Hilfen angefertigt, die ich in der Dissertation angegeben habe. Alle Textstellen, die wörtlich oder sinngemäß aus veröffentlichten oder nicht veröffentlichten Schriften entnommen sind, und alle Angaben, die auf mündlichen Auskünften beruhen, sind als solche kenntlich gemacht. Bei den von mir durchgeführten und in der Dissertation erwähnten Untersuchungen habe ich die Grundsätze guter Wissenschaftlicher Praxis, wie sie in der „Satzung der Justus-Liebig-Universität Gießen zur Sicherung guter wissenschaftlicher Praxis“ niedergelegt sind, eingehalten .

# 1 Introduction

## 1.1 Oxygen sensing

An adequate supply of oxygen is essential to all higher organisms; it serves as the terminal electron acceptor in mitochondrial oxidative phosphorylation. Moreover, several enzymatic processes require molecular oxygen as a substrate. Therefore, oxygen supply must be optimised by tight regulation of ventilation, haemoglobin saturation levels and systemic oxygen transport. Changes in oxygen concentration (hypoxia, hyperoxia or anoxia) can cause a wide range of adaptive responses at the systemic, tissue and cellular levels.

Molecular and metabolic cell responses to hypoxia show a universal pattern of an ability to cope with a reduction in available energy, caused by the limitation in oxidative phosphorylation. Adaptive strategies help to accommodate for actual level of ATP and to maintain the normal cell function (Lopez-Barneo *et al.*, 2001; Michiels, 2004). A common feature is an increasing abundance and activity of enzymes responsible for anaerobic glycolysis and decreasing activity of ATP consumers such as Na<sup>+</sup>/K<sup>+</sup>-ATPase. Additionally, different organs respond to low oxygen tension by regulating the expression of unique sets of genes responsible for organ-specific functions.

Even slight reduction in normal oxygen concentrations can cause the induction of specific genes involved in mammalian oxygen homeostasis such as erythropoietin or vascular endothelial growth factor. Investigations of such hypoxia-inducible genes performed in many different cultured cell lines suggest that every mammalian (perhaps even every vertebrate and insect) cell possesses one or several oxygen-sensing mechanism(s), i.e. a molecular oxygen sensor. However, the mammalian cellular oxygen sensor is not yet known.

### 1.1.1 What is the oxygen-sensing protein?

As there is no assay available to identify directly the oxygen sensor among the hundreds of known oxygen-binding proteins, many different candidate proteins have been suggested in the

past to play this role in addition to their known or proposed functions. A few of them will be shortly mentioned-

One of the most important models trying to handle the oxygen sensor is that of the *haem oxygen sensor*. Since so far all proteins capable of binding oxygen contain iron, it is not surprising that the hypothesis has become widely spread, that one of these proteins is probably the oxygen sensor (Goldberg *et al.*, 1988). Indeed, many findings support this model; the induction of erythropoietin gene expression can be induced not only by hypoxia, cobalt (and to a less extent nickel and manganese) salts proved to do that as well. This finding suggests that the ferrous haem iron was replaced by the non-oxygen binding cations. According to this model, this locks the oxygen sensor in the deoxy conformation. Further support to the haem hypothesis was provided by the finding that iron chelators, such as desferrioxamine, are also capable of mimicking hypoxia (Ho *et al.*, 1996; Wang *et al.*, 1993); blockers of haem synthesis abolished both hypoxic and cobalt –dependant erythropoietin induction.

Although many evidences are in favor of this *haem oxygen sensor* model, some discrepancies remain. For example, the flavoprotein cytochrome P450 reductase inhibitor Mesalyl inhibited hypoxia-, cobalt- and desferrioxamine –dependant induction of the erythropoietin gene, but did not induce the hypoxia inducible factor 1 $\alpha$  (HIF-1 $\alpha$ , see below) and the vascular endothelial growth factor (VEGF) gene.

The cytochrome  $b_{558}$ /NADPH oxidase complex, that generates superoxide in the plasma membrane of phagocytes and B-lymphocytes, is just another one of the well-known candidates. Interestingly, subunits of this complex were also found in oxygen-sensing cells of the carotid body and pulmonary neuroepithelial bodies. However, it was demonstrated that in cell lines derived from patients suffering from chronic granulomatous disease, in which one of the subunits of the cytochrome  $b_{558}$ /NADPH oxidase complex is defective, the oxygen-regulated gene expression is normal (Wenger *et al.*, 1996). This finding was later demonstrated using knock-out mice lacking a subunit of this cytochrome (Archer *et al.*, 1999). Taking these evidences into account, we can probably conclude that this complex is not likely to be the *universal* oxygen sensor.

Other promising candidates are the major oxygen-consuming organelle of the cell- the mitochondria, or some of the mitochondrial cytochromes. But because the respiratory electron transport chain blocker potassium cyanide cannot induce erythropoietin gene expression

(Goldberg *et al.*, 1988; Tan *et al.*, 1991) the role of the mitochondria and its cytochromes remains unclear.

Taken together, and without mentioning some other possible candidates, the search for the oxygen-sensor protein is not yet over.

### **1.1.2 Oxygen signalling**

Reactive oxygen species (ROS), such as superoxide and peroxide are known to serve as signal transducers in several systems. Because oxygen is the main component of these molecules, it seems obvious that their concentration depends upon the environmental oxygen concentrations, making them candidates for signal transduction in hypoxia. Many findings are truly supporting this assumption- a close relationship between oxygen and hydrogen peroxide concentration in hepatoma cells; hydrogen peroxide sequestration could mimic hypoxia and addition of hydrogen peroxide inhibited hypoxic induction of erythropoietin. In contrast, cardiomyocytes increase their production of ROS following exposure to hypoxia (Vanden Hoek *et al.*, 1998). Antioxidants inhibited this increase in levels of ROS and also blocked hypoxic inhibition of cardiomyocyte contraction.

To sum up, there is no common consensus about whether ROS concentrations decrease or increase following exposure to acute hypoxia, but meanwhile more and more studies indicate an increase of ROS under hypoxic conditions (Weissmann *et al.*, 2006; Yamamoto *et al.*, 2006).

## **1.2 Hypoxia and its influence on the cell**

### **1.2.1 The hypoxia- inducible factor 1 (HIF-1)**

Compared with the relative lack of information on the oxygen sensor and its signal-transduction pathways, much more is known about the target of these putative signalling mechanisms. In 1995 Semenza and co-workers discovered HIF-1 on the basis of its ability to bind to a hypoxia-response element (HRE) in the 3' flanking region of the erythropoietin gene.

HIF-1 is a ubiquitously and constitutively expressed heterodimeric transcription factor, composed of a  $\alpha$  subunit unstable under normoxia and a common  $\beta$ /ARNT (aryl hydrocarbon receptor nuclear translocator) subunit. While ARNT is abundantly expressed and almost not affected by the oxygen partial pressure, the stabilisation of its  $\alpha$  subunit is hypoxia-induced.

HIF-1 $\alpha$  cannot be detected above a critical oxygen partial pressure (which is highly tissue dependant) when it is subjected to a rapid ubiquitination and proteasomal degradation. Only hypoxic exposure or addition of hypoxia-mimicking reagents (e.g. cobalt chloride or iron chelators) leads to increase HIF-1 $\alpha$  protein levels and hence to activation of HIF-1 -dependant target genes.

### **1.2.1.1 Stabilisation of HIF-1 $\alpha$ under hypoxic conditions**

Once stabilized, HIF-1 $\alpha$  translocates to the nucleus guided by a nuclear localization signal present in the C-terminus (Kallio *et al.*, 1998). This translocation occurs not only under hypoxic conditions but also under normoxia, suggesting that it occurs without the need of any further hypoxia-dependant signals. After translocated, HIF-1 $\alpha$  heterodimerises with ARNT, and the resulting HIF-1 complex binds to the sequence of the hypoxia response element (HRE) present in oxygen- regulated target genes (see Figure 1).

Although HIF-1 $\alpha$  is regulated mainly by the oxygen partial pressure, other factors modulate its stability and its trans-activation activity. Post-translational modifications (mainly phosphorylation) of HIF-1 $\alpha$  are essential for full transcriptional activation and stabilization of the HIF complex. Extensive phosphorylation of the HIF-1 $\alpha$  by the MEK-1/p42/p44 MAPK pathway enhances the transcriptional activity of HIF-1. As such, addition of a MEK-1 inhibitor does not alter the hypoxic stabilization or DNA-binding ability of HIF-1  $\alpha$  but it inhibits the trans-activation ability of HIF-1 $\alpha$ , thereby reducing the transcriptional activity of HIF-1 target genes (Hur *et al.*, 2001; Richard *et al.*, 1999).

### **1.2.1.2 HIF-1 $\alpha$ under normoxic conditions**

The von Hippel Lindau tumour-suppressor protein (pVHL), a subunit of a multiprotein complex harboring E3 ubiquitin ligase activity, is responsible for regulating cellular levels of HIF-1 $\alpha$  (Maxwell *et al.*, 1999). The pVHL directly interacts with the oxygen dependant degradation (ODD) domain of the HIF-1 $\alpha$ . The key enzymes controlling the oxygen-

dependant step in this degradation cascade are specific HIF-1 $\alpha$  -proline hydroxylase that require Fe (II) as co-factor as well as dioxygen and 2-oxoglutarate as co-substrates. HIF-1 $\alpha$  is hydroxylated at two proline residues that are highly conserved amino acid within the ODD domain. Under normoxic conditions, prolyl hydroxylation enables the specific interaction of pVHL with HIF-1 $\alpha$ , whereas under hypoxic conditions, prolyl hydroxylation does not occur, preventing pVHL binding and the degradation of HIF-1 $\alpha$ .

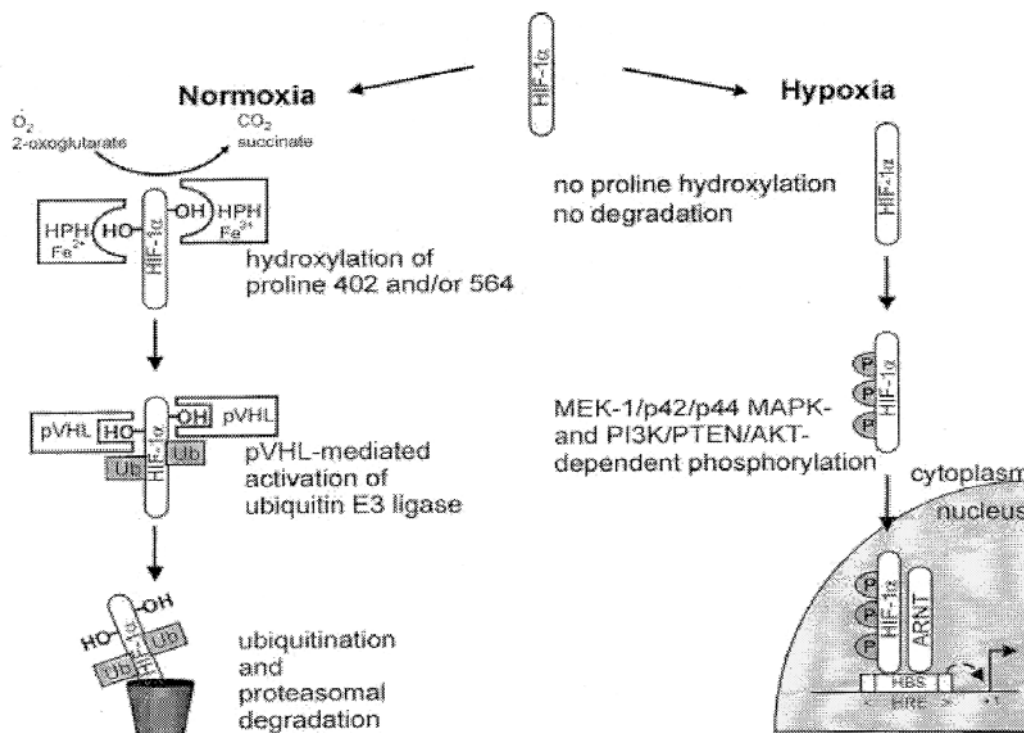


**Figure 1 Hypoxia-dependant function of HIF-1.** Taken from (Hofer *et al.*, 2002)

Probably the most commonly cited example of HIF-1 inducing human genes expression in response to hypoxia is that of erythropoietin. It activates erythropoiesis to enhance the systemic oxygen transport capacity. Because iron is a limiting factor in haem formation, erythropoiesis is sustained by increased expression of transferrin and transferrin receptor to enhance iron supply to erythroid cells.

At the local level, HIF-1 activates vascular endothelial growth factor (VEGF), the most powerful inducer of angiogenesis, as well as one of its receptors (Flt-1). The clinical relevance of this two target genes, mostly these of VEGF is enormous, because it might be applied to

treat ischemic diseases like coronary artery disease, or on the other hand, fighting tumours by preventing them to secrete angiogenetic factors, required for their growth.

Local blood circulation is also controlled by modulation of the vascular tone through the production of NO (via nitric oxide synthase), CO (haem oxigenease 1), endothelin-1, adrenomedullin or activation of the  $\alpha$ 1B adrenergic receptor.

At the cellular level, loss of ATP production in the mitochondria is compensated by anaerobic glycolysis. Therefore, glucose uptake (glucose transporters) and glycolysis (glycolytic enzyme) are up regulated by HIF-1. In addition, HIF-1 activates Insulin like growth factor 2 (IGF-2) and some of the IGF- binding proteins (IGFBPs). Figure 2 demonstrates some of the most important HIF-1 regulated genes. Genes are listed with regards to their activity.

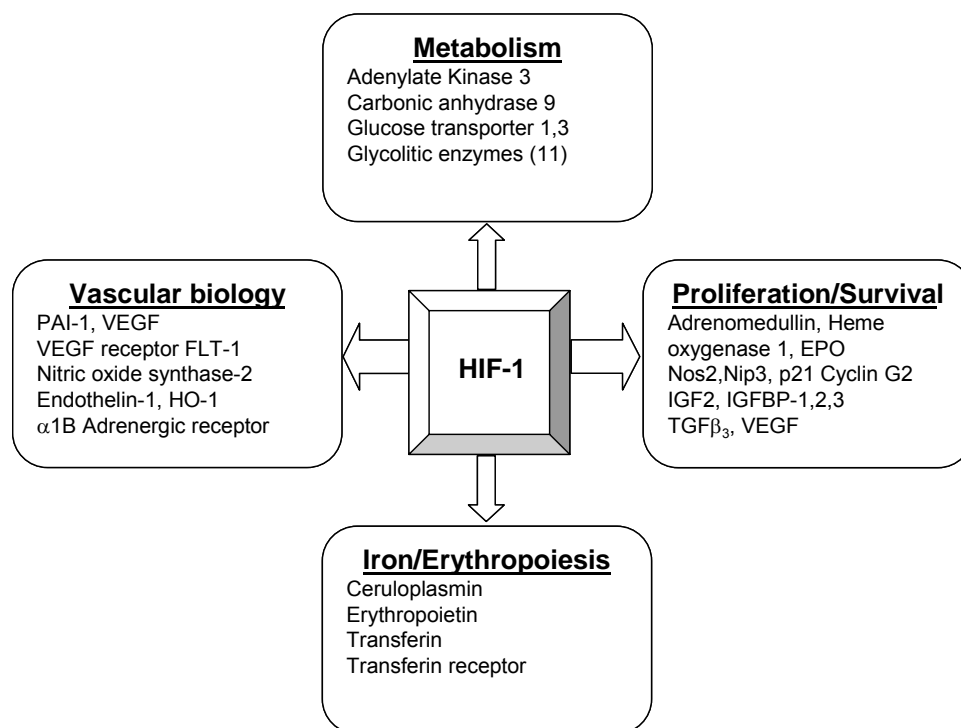


**Figure 2 HIF target genes.** EPO= Erythropoietin; HO= Haeme oxygenase; IGF= Insulin like growth factor; IGFBP= IGF binding protein; NOS= Nitric oxide synthase; PAI= Plasminogene activator inhibitor; TGF= Transforming growth factor; VEGF= Vascular endothelial growth factor.

### 1.2.2 Nuclear Factor kappa B and hypoxia

Nuclear factor (NF) -  $\kappa$ B, named following its original description in B-cells, is one of the critical transcription factors required for maximal expression of many cytokines involved in the pathogenesis of acute lung injury. It functions to enhance the transcription of a variety of

genes, including cytokines and growth factors, adhesion molecules, immunoreceptors, and acute-phase proteins. Its activation is necessary for an intact host defence response, whereas excessive activation of NF- $\kappa$ B results in overly of exuberant inflammatory injury of lungs and other organs.

**Table 1 Genes involved in lung injury regulated by NF- $\kappa$ B.** Taken from (Fan *et al.*, 2001)

Family	Genes
Tumour necrosis factor	TNF- $\alpha$ ,TNF- $\beta$
Interleukins	IL-1 $\beta$ ,2,6,8,12
Chemokines	MIP-1,MIP-1 $\alpha$ ,MCP,GRO- $\alpha$ , $\beta$ , $\gamma$
Cell adhesion molecules	ICAM-1,VCAM-1,E-Selectin
Colony-stimulating factor	G-CSF,GM-CSF
Transcription factors and subunits	I $\kappa$ B- $\alpha$ , NF- $\kappa$ B- precursor p100,105
Acute-phase proteins	C-Reactive Protein, Lipopolysaccharide binding protein
Interferons	IFN- $\beta$
Others	NO Synthase, Tissue Factor, Phospholipase A2, Cyclooxygenase-2

Under resting conditions, NF- $\kappa$ B functions in regulating the expression of genes involved in normal immunologic response such as the generation of antibody light chains and other immunoregulatory molecules (Sen *et al.*, 1986; Weih *et al.*, 1995).

### 1.2.2.1 Regulation of NF- $\kappa$ B

NF- $\kappa$ B is normally sequestered in the cytoplasm through its association with an inhibitory  $\kappa$ B (I $\kappa$ B), which masks the nuclear translocation signal and thus prevents NF- $\kappa$ B from entering the nucleus. NF- $\kappa$ B activation represents the terminal step in a signal transduction pathway leading from the cell surface to the nucleus. On exposure of the cell to activation factors, the I $\kappa$ B protein is phosphorylated on serine 32 and serine 36, ubiquitinated, and degraded in proteasomes. After being freed from association with I $\kappa$ B, the NF- $\kappa$ B complex moves to the nucleus where it binds to specific sequences in the promoter/enhancer regions of target genes, (see Table 1).

A wide variety of extracellular stimuli can trigger the activation of NF- $\kappa$ B. In response to infection (activation through rhinovirus, bacterial LPS), cytokines (TNF- $\alpha$ , IL-1 $\beta$ ), lipopolysaccharide (LPS) and ionising radiation, the NF- $\kappa$ B complex is activated and translocated to the nucleus. An interesting and controversial stimulus of NF- $\kappa$ B is achieved by reactive oxygen species (ROS). Data stretching back a decade, suggests that the application of



oxidant stressors such as H<sub>2</sub>O<sub>2</sub> to cell culture increase NF-κB activity and that addition of antioxidant compounds or up regulation of cellular antioxidant systems prevent this effect. However, oxidants effects seem to be also cell specific. In lymphoid and monocytic cells, prior administration of antioxidant results in suppression of the NF-κB response to Tumour necrosis factor-α (TNF-α) or Interleukin 1β (IL-1β). In epithelial cell lines, antioxidant pre-treatment did not have such effect. (Bonizzi *et al.*, 1999),(Bonizzi *et al.*, 1996) (Brennan *et al.*, 1995)

Further evidence for the complexity of NF-κB regulation is given by other studies (Bonizzi *et al.*, 1999), demonstrating different, cell specific pathways leading to inhibitory κB (IκB) degradation and NF-κB activation by IL-1. IL-1β stimulation of lymphoid cells generates ROS, which are required for IκB degeneration and NF-κB activation. The source of generated ROS (in these cells) is the 5-lipoxygenase enzyme. In monocytic cells, ROS is also generated in response to IL-1 stimulation, but this time the source of ROS was the NADPH oxidase complex.

In recent years, we have just begun to understand the role of AM in mediating lung injury, directly or indirectly through the release of different cytokines and transcription factors such as NF-κB. New studies (Hirani *et al.*, 2001; Madjdpour *et al.*, 2003) demonstrate the hypoxia-dependant activation of AM and the cascade following this activation with an increased binding activity of NF-κB and transcription of some of the cytokines that their transcription is NF-κB-dependant (TNF-α, MCP-1, MIP-1β, ICAM-1, and IL-8). Another work gives some further insight to the way in which hypoxia-dependant activation of AM leads to cytokine release. The scientists exposed murine macrophages to hypoxia and analysed the levels of macrophages inflammatory protein-2 (MIP-2) (Zampetaki *et al.*, 2004). They demonstrated both at the mRNA and the protein level a hypoxia induced increase of MIP-2. Furthermore, their results indicate that the hypoxic signal for induction of MIP-2 gene expression is implemented through enhanced NF-κB activity.

### **1.3 Transcriptional mechanisms in acute lung injury**

Lung injury occurs as a result of a cascade of cellular events initiated by either infectious or non-infectious inflammatory stimuli. An elevated level of pro-inflammatory mediators

combined with a decreased expression of anti-inflammatory cytokines is a critical component of lung inflammation.

As mentioned previously, a key player in the molecular cascade leading to pulmonary injury is the transcription factor nuclear factor  $\kappa$ B (NF- $\kappa$ B). For this reason its activation and regulation is tightly regulated by a complicated signalling cascade. The mechanism leading to lung injury and the involvement of NF- $\kappa$ B and AM will be shortly discussed:

**Endothelial activation-** In lung injury, endothelial adhesion molecules have a role in recruiting inflammatory cells such as neutrophils and lymphocytes from the circulation to the injured area. NF- $\kappa$ B regulates the expression of several genes that encode adhesion molecules such as ICAM-1, VCAM-1, and selectin-E. Cytokine induced cell-surface expression of E-selectins. VCAM-1, ICAM-1 and the secretion of IL-8 as well as of other chemokines are regulated at the transcriptional level in endothelial cells by the binding of NF- $\kappa$ B to its target site in the nucleus. Treatment with antioxidant down-regulate the NF- $\kappa$ B-dependant expression of these molecules (Chen *et al.*, 1995).

**Neutrophils accumulation-** Acute lung injury is characterized by the accumulation of neutrophils in the lungs, accompanied by the development of interstitial edema and an intense inflammatory response. A study made by neutropenic mice proved that an endotoxemia or haemorrhage-induced lung edema was significantly reduced in these animals, verifying the important role of neutrophils in lung damage. In addition, activated NF- $\kappa$ B contributes to lung neutrophils accumulation and expression of TNF- $\alpha$ , MIP-2, and IL-1 $\beta$  mRNA in lung neutrophils (Shenkar *et al.*, 1999).

**NF- $\kappa$ B and apoptosis-** It is suggested that NF- $\kappa$ B has a role in apoptosis, probably by regulating the expression of genes important in regulating cell death. In particular, increased NF- $\kappa$ B activation results in decreased apoptosis and increased cell life span. This effect of NF- $\kappa$ B activation is a potential determinant of acute lung injury. An increased number of activated neutrophils that generate ROS and pro-inflammatory cytokines are present in the lungs of patient with ARDS, and these neutrophils have decreased rates of apoptosis. In experimental models of acute lung injury secondary to haemorrhage or endotoxemia, NF- $\kappa$ B was activated in the lungs and apoptosis was reduced in neutrophil population (Parsey *et al.*, 1999). Thus, increased survival of pro-inflammatory neutrophils in the lungs of ARDS patients secondary to NF- $\kappa$ B activation may perpetuate the pulmonary inflammatory response.

**The role of AM-** Due to their strategical location, at the air-tissue interface in the alveoli and alveolar duct, AM are the first cells to be encountered by inhaled antigens and organisms in the lower respiratory tract. They should not only be seen as cells capable of phagocytosis; when activated they function as potent secretor cells, making them very important in regulating inflammatory reactions in the lung. The mechanism of NF- $\kappa$ B activation during lung inflammation injury is known to require TNF- $\alpha$  and IL-1 $\beta$ , which operate as autocrine/paracrine stimulation of AM. AM activation is generally an initial event in the genesis of lung inflammatory reactions. Lentsch et al. showed that early activation of AM occurred in an NF- $\kappa$ B-dependant manner (Lentsch *et al.*, 1997). Furthermore, NF- $\kappa$ B activation in AM in vivo occurred before NF- $\kappa$ B activation in whole lung tissue and depletion of AM attenuated NF- $\kappa$ B activation in whole lung and decreased the bronchoalveolar lavage fluid content of pro-inflammatory mediators. These findings suggest that the products of activated AM such as TNF- $\alpha$  are essential in stimulating nuclear translocation of NF- $\kappa$ B in other lung cell type. AM are necessary for maximal NF- $\kappa$ B activation in response to endotoxin (Koay *et al.*, 2002). A depletion of AM showed a reduced total lung NF- $\kappa$ B activation and lower TNF- $\alpha$  concentration in lavage fluids. In addition, neutrophils recruitment (total neutrophils counts in BAL) was markedly reduced in AM-depleted lungs. Madjdpour et al. showed similar effects on the NF- $\kappa$ B levels after AM elimination in hypoxia-dependant AM activation (Madjdpour *et al.*, 2003). Although the importance of NF- $\kappa$ B in cytokine transcription has been established in animal model, only a few published studies have demonstrated a role for NF- $\kappa$ B in human AM. While the basal activation of NF- $\kappa$ B in AM of healthy volunteers appeared to be minimal, it has been reported that NF- $\kappa$ B in AM from patient with ARDS is highly activated (Schwartz *et al.*, 1996).

### **1.3.1 Therapeutic targets for acute lung inflammation**

The regulation of inflammation by cytokines involved an intricate balance of pro-and anti-inflammatory mediators. Many anti-inflammatory cytokines released in lung tissue are already well known (i.e. IL-4, IL-6, IL-10, IL-1RA, IL-11, IL-13, and TGF- $\beta$ ). Only some of them have been shown to be involved in lung injury via interaction with NF- $\kappa$ B. Because of the central role of NF- $\kappa$ B in conducting lung injury, it is interesting to focus on some options to interfere the activation of NF- $\kappa$ B. These options could very well become the target of future

drugs aimed to regulate and minimize lung injury. Some of these therapeutic approaches are discussed below.

Studies using a model of intrapulmonary deposition of IgG immune complex in rats to cause AM activation have identified IL-10, IL-6, IL-13, and IL-1RA as endogenous regulators of the inflammatory lung injury. Exogenously administered IL-10, IL-4, or IL-13 greatly attenuated the lung injury induced in this model (Lentsch *et al.*, 1997). It was also demonstrated that both IL-10 and IL-13 inhibited nuclear localization of NF- $\kappa$ B in AM and lung tissue in a manner associated with preserved expression of I $\kappa$ B- $\alpha$  protein. These findings suggest that IL-10 and IL-13 reduce lung inflammation by preventing degradation of I $\kappa$ B- $\alpha$ , thus inhibiting the activation of NF- $\kappa$ B.

TGF- $\beta$ , a pleiotropic cytokine/growth factor, is believed to play a critical role in the modulation of inflammatory events. DiChiara *et al.* demonstrated that endogenous TGF- $\beta$ 1 inhibited the expression of the pro-inflammatory adhesion molecule E-selectin in vascular endothelium exposed to inflammatory stimuli (DiChiara *et al.*, 2000). The inhibitory effect occurred at the level of transcription of the E-selectin gene and was dependant on the action of Smad proteins, a class of intracellular signalling proteins mediating the cellular effects of TGF- $\beta$ 1. Moreover, this work demonstrated that Smad-mediated effects in endothelial cells resulted from a competitive interaction between Smad proteins activated by TGF- $\beta$ 1, and NF- $\kappa$ B activated by inflammatory stimuli. This data demonstrates another way in which the pro-inflammatory function of NF- $\kappa$ B can be regulated (namely by application of TGF- $\beta$ 1) and eventually used as a therapeutically measure.

Lung injury is the final step in a complex cascade initiated by either infectious or non-infectious inflammatory stimuli. Better understanding of these complicated, well regulated events, are crucial for developing new and efficient therapeutic ways that may specifically inhibit transcription signalling, and thus giving physicians new weapons to better cure lung injury of their patients. NF- $\kappa$ B and other pro-inflammatory mediators (some of which are secreted directly from AM) are without any doubt the key for achieving this goals and will be therefore in the centre of interest of future studies.

## 1.4 Hypoxia and alveolar macrophages

### 1.4.1 Activation of alveolar macrophages by hypoxia and lipopolysaccharide

The lung is an important target organ for systemic inflammatory mediators released after major trauma and severe infection. Local activation of resident cells in the lung interstitium and alveolus, primarily alveolar macrophages (AM), leads to elaboration of several pro-inflammatory cytokines such as tumour necrosis factor- $\alpha$  (TNF- $\alpha$ ), interleukin 1- $\beta$  (IL-1 $\beta$ ), IL-8 and macrophages inflammatory protein (MIP). These mediators act in concert to promote neutrophil sequestration by activating endothelial cell adhesion molecule expression and to induce migration of neutrophils into the interstitium where they propagate inflammation and injury through the release of reactive oxygen species and proteolytic enzymes. The release of mediators and the imbalance between pro- and anti-inflammatory factors is a critical component of lung injury.

AM are often found in hypoxic environments such as large granulomas, lung abscesses, and lung segments with a low ventilation-perfusion ratio. Systemic inflammatory processes, like acute respiratory distress syndrome (ARDS) also expose AM to hypoxia. It was of great interest than, to try and explore the effects of hypoxia on the release of pro-inflammatory cytokines from AM.

Hempel et al. have demonstrated that hypoxia decreases the gene transcription and synthesis of prostaglandin H synthase 2 (PGHS-2) in response to LPS, resulting in decreased prostaglandin E<sub>2</sub> (PGE<sub>2</sub>) synthesis (Hempel *et al.*, 1994). It was also demonstrated that PGE<sub>2</sub> decreases the release of TNF- $\alpha$  and IL-1. Taking these two findings together it is not surprising that under hypoxia (O<sub>2</sub><0,05%), LPS- stimulated AM markedly increase the release of IL-1 and TNF- $\alpha$  (Hempel *et al.*, 1996), suggesting that the release of these two inflammatory proteins under hypoxia was, at least partially regulated by the decrease of PGE<sub>2</sub>. When PGE<sub>2</sub> synthesis was inhibited by indomethacin, an increase in the release of TNF- $\alpha$  and IL-1 was also the result.

Another potential explanation of the increase in cytokines release during hypoxia involves an important transcription factor mentioned before, NF-kB. Fact is that many genes involved in

lung injury are regulated by NF- $\kappa$ B. TNF- $\alpha$  and IL-1 $\beta$  are only two of these genes, some other are listed in Table 1. Leeper-Woodford et al. have demonstrated this mechanism and the possible influence of hypoxia on NF- $\kappa$ B. LPS-exposed AM in hypoxia have shown enhanced expression of NF- $\kappa$ B compared with normoxia, and again higher levels of TNF- $\alpha$  and IL-1 $\alpha$ + $\beta$  (Leeper-Woodford *et al.*, 1999). They have found increased p65 and Rel-c isoform of NF- $\kappa$ B in the LPS-stimulated AM exposed to acute hypoxia (1.8 % O<sub>2</sub>; after 2 hours), with the p65 isoform appearing to be the most dominant one in this macrophages system. Another interesting study of (Koong *et al.*, 1994) demonstrated that hypoxia caused activation of NF- $\kappa$ B by inducing tyrosine phosphorylation of I $\kappa$ B, an important proximal step that precedes its dissociation from the NF- $\kappa$ B complex before transcriptional activation.

Taken together, these studies suggest that the release of pro-inflammatory mediators from LPS- triggered AM in acute hypoxia is regulated by the hypoxia-dependant activation of NF- $\kappa$ B.

Hirani and colleagues have focused mainly on the influences of hypoxia on interleukin 8 (IL-8), expressed and secreted by AM (Hirani *et al.*, 2001). IL-8 is a potent neutrophil chemokine, secreted mainly by AM and known to play an important role in acute respiratory distress syndrome (ARDS). After 2 hours exposure of AM to hypoxia, IL-8 protein secretion was double compared to normoxia, but significantly lower than that induced by LPS, a finding supported by other studies that suggest hypoxia induces only a mild lung injury, compared with LPS inducing a more severe injury (see below). Since hypoxia also induced a rapid up regulation of IL-8 mRNA, (as rapidly as 30 minutes post exposure to hypoxia), the effects of hypoxia on transcription factors known to implicate in the regulation of IL-8 were also studied. Hypoxia increased the DNA binding activity of AP-1, C/EBP but not of NF- $\kappa$ B. The binding activity of these 3 transcription factors was measured 15 and 30 minutes after hypoxia exposure. In contrast, (Madjdpour *et al.*, 2003) demonstrated a higher binding activity for NF- $\kappa$ B, ( when measured 1 or 2 hours post-hypoxia exposure), which may suggest that the hypoxia dependant activation of NF- $\kappa$ B can be first detected after 60 min or later.

The last work (Madjdpour *et al.*, 2003) further exposed the role of AM and NF- $\kappa$ B in response to acute hypoxia. Unlike many other studies about AM, they were activated solely by hypoxia and not by LPS allowing to focus and isolate the direct effects of hypoxia on AM. Rat lungs were exposed to a FiO<sub>2</sub> of 0.1 over a short period of time (1-8h). An increase in the number of the AM in the bronchoalveolar lavage was shown between 1 and 8h (max. between

2-6h), resulting in AM accumulation. On the level of inflammatory mediators, DNA-binding activity of NF- $\kappa$ B and expression of mRNA for HIF-1 $\alpha$ , TNF- $\alpha$ , intercellular adhesion molecule-1 (ICAM-1), MIP-1 $\beta$  and monocyte chemoattractant protein-1 (MCP-1) were increased. All the mediators listed above, except HIF-1 $\alpha$ , are considered to be NF- $\kappa$ B regulated genes, and thus giving more data to support the thesis that hypoxia activates NF- $\kappa$ B and so the release of cytokines. The second part of this work should also evaluate whether AM were truly the source of mRNA of the inflammatory mediators. Performing a macrophage depletion they could show that AM were indeed the source of these mediators. The only mediator not affected by macrophage depletion was the MCP-1, suggesting that epithelial cells rather than macrophages are the main source for MCP-1.

In conclusion, this study demonstrated that acute hypoxia results in inflammatory changes in the lung representing a mild lung injury (compared with other inflammatory changes, for example LPS), whereby alveolar macrophages are the main effector cells during this inflammatory process.

#### **1.4.2 The effects of hypoxia on the adhesiveness of AM**

Polymorphonuclear leucocytes (PMN) play a major role in mediating hypoxic injury. Both *in vitro* and *in vivo* studies have indicated that during hypoxia, adherence of neutrophils to endothelial cells is increased. It is interesting then, to try and understand the role of hypoxia in recruiting immune cells to fight lung damages.

Alveolar epithelial cells (AEC) are targets for hypoxia in the alveolar space in pathologic conditions, such as hypoventilation. AEC are also a major component in the recruiting of PMN and AM since they express some of the adhesion molecules. Two of these molecules should be mentioned because of their role in binding immune cells.

The intercellular adhesion molecule-1 (ICAM-1) is an adhesion molecule of the immunoglobulin superfamily and has two  $\beta_2$ -integrin ligands on leucocytes. Interactions between ICAM-1 and  $\beta_2$ -integrins are a key step in emigration of leucocytes to sites of inflammation. A second member of the immunoglobulin superfamily is the vascular cell adhesion molecule-1 (VCAM-1) that interacts with integrin  $\alpha_4\beta_1$ . The primary role of this molecule is the promotion of lymphocytes and macrophages adhesion.

Beck-Schimmer et al. have exposed rat AEC to hypoxia (5% O<sub>2</sub>) for short periods of time ranging from 0,5 to max. 8 hours and investigated the effects on these two adhesion molecules (Beck-Schimmer *et al.*, 2001). They demonstrated not only an increase on mRNA level and protein level, but also an increase in adherence of neutrophils and AM to these adhesion molecules. To specify the adhesion patterns of these two cell populations they used ICAM-1 and VCAM-1 antibodies to block the adhesion. The adhesion of AM to AEC was blocked to 95% using anti-VCAM-1 antibodies, while the neutrophils adhesion blocked to 83% using anti-ICAM-1 antibodies. Based on these findings, we can conclude that VCAM-1 is the adhesion molecule most important for the adhesion of AM, whereas ICAM-1 for the adhesion of neutrophils.

Of interest are also the findings that the up regulation on mRNA level for ICAM and VCAM were time limited (only during the first hour), and the protein up regulation being limited to 4-6 h of hypoxia.

Compared with other experimental systems of lung inflammation, such as LPS-induced injury, there was a less intense increase of the mRNA and protein for ICAM-1 during hypoxia; AEC under LPS stimulation showed a 700% increase of mRNA for ICAM-1 whereas hypoxia only led to an 80-90% up regulation. This finding is also supported by other works, showing similar results (Madjdpour *et al.*, 2003).

### **1.4.3 Phagocytosis and ATP levels in alveolar macrophages in hypoxia**

With its location in the oxygen-rich environment of the lung airways, the pulmonary alveolar macrophages may utilise primarily oxidative phosphorylation for energy production in activities like phagocytosis. Some studies could also demonstrate that AM having greater O<sub>2</sub> utilisation, higher activities of cytochrome oxidase and lower glycolytic enzyme activities than peritoneal macrophages.

Leeper-Woodfore et al. exposed AM to hypoxia (1.7%) and measured ATP levels and phagocytosis activity (Leeper-Woodford *et al.*, 1992).

A direct influence of hypoxia on the phagocytotic ability of AM could be demonstrated when AM were exposed to hypoxia and rabbit red blood cells (RBC) at the same time; AM showed a normal phagocytotic activity in the first 30 min (compared with AM exposed to normoxia), followed by a falling of this activity when exposure to hypoxia proceeded. A pre-exposure of



AM to hypoxia for 30 min prior to the incubation with RBC showed a complete blocking of phagocytosis, but they could slowly regain this ability after being exposed for 30 min to normoxia.

The ATP levels of AM were measured 30 and 60 min after exposure to hypoxia. Surprisingly, the level remained at a level comparable to the ATP concentration observed at time 0. The group suggested that although under normoxia the major source of energy for AM is oxidative phosphorylation, under anaerobic conditions AM were able to respond quickly and to shift their energy source to glycolysis.

A similar effect was demonstrated when normoxia and hypoxia-exposed-AM were incubated with RBC. Knowing that phagocytosis is a highly ATP consuming process, it seems reasonable that ATP levels were falling in both cell populations and that the decrease was more dramatically in cells exposed to hypoxia. After 60 min though, ATP levels of hypoxia cells were as high as the levels of normoxia cells. They proposed that the rapid reduction of ATP levels in hypoxia-exposed AM in the first 30 min, induce mechanisms that either conserve or increase cellular ATP in the first 60 min of hypoxia.

Another interesting observations, made by counting the RBC “swallowed” by the AM, was that hypoxia exposed AM were losing or exocytosing some of the previously phagocytosed RBC.

They concluded that the cellular ATP level of AM in a hypoxic environment may only be partially responsible for the phagocytic alteration observed in AM. Moreover, these cells have the ability to maintain their energy depot (at least for a short period of time) by shifting their energy generation to anaerobic form.

## **1.5 DNA Array technology**

With the growing abundance of sequencing data from different organisms, a pressing need has come to develop and apply technologies to perform comprehensive functional analysis. DNA arrays have been developed in response to the need for simultaneous analysis of the pattern of expression of thousand of genes and offer, therefore, great advantages over traditional “single gene” methods.

### 1.5.1 What is a Microarray?

A gene expression Microarray consists of multiple features (spots) of DNA which are used to determine the levels of mRNA expression in a pool of cells. The DNA for each feature is from a gene of interest and is a target for the mRNA encoded by that gene. In general, one may think of a Microarray as a grid of DNA spots. Each spot has a unique DNA sequence, that is specific for one gene's mRNA. Thus, each spot will be hybridised only by its complementary DNA strand. In this way each spot is acting as a target to determinate the levels of a specific mRNA produced by a collection of cells.

The basic idea of using a piece of DNA as a target to determinate the presence of a complementary DNA in a solution was already used; it is the same general technique used in Southern and Northern blots by molecular biologists every day. The large number of DNA probes that is possible to place on a Microarray (the largest Microarray currently contains up to 170,000 spots) makes Microarrays so exciting. It allows to observe the response of the whole genome to various stimuli at once.

### 1.5.2 How are Microarrays produced?

There are, naturally, many different types of Microarray available but there are only two real fabrication methods:

In the first one, commercially available oligonucleotides, named "Gene-Chips" (registered trademark by Affymetrix), are supplied by Affymetrix Inc., Santa Clara, CA. This high-density array of oligonucleotides (25mer oligonucleotides) is synthesised *in situ* (i.e. oligonucleotides synthesised directly on the matrix, usually glass slide) by using photolithographic techniques. The strength of this technology is its ability to detect polymorphism and mutations, thereby making oligotechnology particularly suited for single nucleotide polymorphism (SNP) screens and epidemiological studies. This technology has two main drawbacks- 1). It is very expensive to implement in an academic setting (based on a research from year 2000 only 11% of the labs having Microarrays facilities used exclusively Gene-Chip technology). 2). It has a limited flexibility.

In addition, Affymetrix is not currently promoting co-hybridisations of the two samples being compared, which makes the normalisation of the experimental and control Gene-Chips very

important (more about normalisation see also 2.4.11). Thus, the Affymetrix system does not produce ratios; each target produces primarily an absolute intensity.

The second method is the cDNA or oligonucleotide Microarray technology for competitive hybridisation. cDNA Microarray spots the PCR fragments of cDNA on a glass or plastic slide, or even a nylon membrane (nylon membranes, used in our work, are currently considered to be an “old” technique and are therefore less in use). This method is relatively low in costs and flexible; making it suitable for an academic institution to produce in-house Microarrays with the clones of interest and to perform highly focused in-depth studies. Given the fact that only 10-30% of the human genes are expressed in a given cell, it may not always be necessary to examine the whole genome at once (as made by Affymetrix). In many occasions, in-house Microarrays with well-defined target sequences can effectively address many research questions.

### **1.5.3 How are Microarrays used?**

The basic protocol contains the following steps:

1. Isolating the target and control RNA. RNA may come from any cells. It is important to realise though, that the RNA from tissues or any heterogeneous cells may lead to results that reflect changes in the composition of the sample rather than changes due to the experimental hypothesis. Therefore, a carefully isolation of target and control RNA is asked, avoiding contamination with “unwanted” RNA.
2. RNA labelling. This means performing a reverse transcriptase reaction. In this reaction, dyes that have been linked to a DNA nucleotide are incorporated. When using nylon membranes, DNA is labelled radioactively (for more details see chapter 2.3.4). Otherwise, fluorescent dyes are also widely used.
3. Hybridising the labelled probe to the Microarray. This consists of placing a solution containing the labelled probe on the Microarray to let it hybridise for a period of time, thus, allowing a given probe to find its target on the Microarray and bind to it. Usually this is carried out at a specific temperature, salt concentration, pH etc. to minimise non-specific binding of probes to the target on Microarray.
4. Removing the hybridisation solution and washing the Microarray. The washing can be done at different salt and detergent concentrations to minimise non-specific binding. In general,

solutions with lower salt concentrations weaken the DNA base pairing and are referred to as “more stringent”.

5. Once the Microarray has been washed it is scanned. That means to quantify how much probe bound to the DNA target on the Microarray. Most Microarrays use fluorescent dyes to label DNA, and scanned by a laser, used to excite the fluorescent dye. The photons coming from the dye are captured using lenses to focus the light, and a photo multiplier tube (PMT) is used to quantitate how many photons are being captured. The resulting image is analysed by finding the spot and comparing the differences between chips (if the hybridisation contained only one colour) or the ratio of the two colours in co-hybridisation experiments. Nylon arrays radioactive -labelled are scanned using a Phosphoimager (see chapter 2.4.9) and analysed as described in chapter 2.4.11.

Figure 3 demonstrate scanned images of nylon arrays. Spot intensity is proportional to the number of mRNA copies on the membranes, and can give a “first look” impression of the regulation level of specific genes.

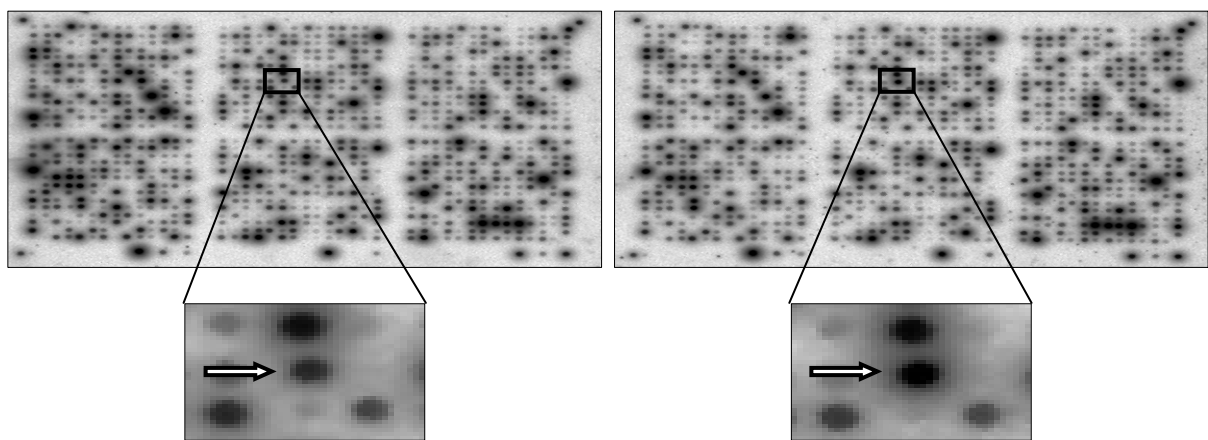


**Figure 3** A phosphoimager scan of two membranes, left normoxia and right hypoxia. Arrows point the difference in spot intensity as can be seen best in the magnification of a single gene below.

### 1.5.4 The Microarray technique and some of its problems

Although being a new and very promising technique, there are substantive technical issues associated with the use of this technology that limit the interpretation of Microarray data. Some of these difficulties are listed below:

- Selection of target genes; a potential problem for cDNA Microarray technology is the cross-hybridisation due to sequence homology, particularly when including several members of the same family. If there is a high homology among the target genes, specific primers need to be designed to target the most divergent regions of these genes.
- DNA concentration; optimum DNA concentration for printing has not been systematically investigated. Accepted concentration for printing varies from 0.1-to 0.5  $\mu\text{g}/\mu\text{l}$ . Investigations show that the concentration of DNA on the slides can significantly affect signal intensity and reproducibility. It should be pointed out that optimal DNA concentration could vary, depending on the expression level of target gene.
- Isolation of RNA; the integrity and purity of RNA is one of the most important factors affecting reproducibility. When comparing two different samples (in this work hypoxia and normoxia) it is actually impossible to guarantee a high and equal quality of RNA in both samples, especially when they are held in different tubes. The same difficulty is also relevant concerning the RNA concentration of the two samples and the efficiency of the labelling. For an effective reproducibility these factors have to be equal in both probes.
- Labelling methods; the labelling method is also a factor affecting reproducibility. When using a fluorescent labelling one should notice that the molecular structure affects the efficiency of incorporation. Cy5 is generally incorporated not as efficient as Cy3, which generates artificial signal bias.
- Hybridisation protocol; the hybridisation conditions, such as probe concentration, ionic strength and temperature, largely depend on the length of DNA fragments present on the array and need to be optimised for a given experiment. It is not possible to present a universal protocol that suites every experiment. The users should perform preliminary experiments to determine which protocol gives reproducible, high-quality hybridisation results. An additional problem when working with nylon membranes, results from the facts that both samples (probe and control) are hybridised in separate hybridisation bottles, making it impossible to maintain exactly the same hybridisation conditions for both.

- Data analysis; this is currently one of the major bottle-necks in the use of Microarray technology and is still at developmental stage. Because there is no gold standard for analysis of Microarray data, valid results and correct interpretation require understanding of the nature of data set, theory, and assumption behind the raw data process. Only few issues will be mentioned here-
  - ❖ Visual examination of the array; prior to data analysis, the first step is to visually examine the array and remove the spots that are not suitable for analysis. It is essential to carefully examine each spot to exclude the unsuitable ones for analysis (for example, spots caused by artefacts).
  - ❖ Background subtraction; image processing software offers several options for background substitution. The option chosen for background subtraction will vary, depending on the uniformity of background. If membranes have a uniform background, mean intensity is a good option for background subtraction; however, if the background pattern is uneven or patchy, the background may be set at the median intensity of a user-defined area of the array.
  - ❖ Data normalisation; in most cases, it is useful to normalise the signal intensity between the two Array compared. This step is especially important if the probes have very different specific activities, or if the arrays analysed have very different levels of signal. Choosing the “global method” (the one used in this work) for normalisation means, that the signal value of all genes on the array are used. This method is best suited for the comparison of similar or identical tissues, because only a small number of genes are expected to be differentially expressed. When divergent tissues are compared, (i.e. many differentially expressed genes are expected), it may be useful to choose only a set of genes for the normalisation (for example take the average intensity value of all the house keeping genes to normalise the results).

In summary, analysing the raw data is a multiple-step process. Because there is no gold standard for each step that suits every experiment, computer software offers options in many occasions. To correctly process raw data, it is important to understand assumptions

underlying each option so that the appropriate data-processing strategy is selected in accordance with experimental design.

### **1.5.5 Array technology applications**

Two chief applications of DNA Microarray technology are described below. Other applications include gene discovery, genotyping, and pathways analysis.

- Analysis of gene expression; gene expression patterns are biologically informative and provide direct clues to function. Correlating changes in gene expression with specific changes in physiology can provide insights into the dynamics of various biological processes in an organism. Array technology can be used, for example, for comparing genes expressed in normal and disease stages; in different tissues or at different developmental stages; analysing the response of cells exposed to drugs or different physiological conditions. In this work, the technology was used to compare the gene expression of alveolar macrophages in hypoxia and normoxia. The array analysis allowed to focus on a small number of genes (target genes), with changes in their expression, and to ignore many other genes which did not show hypoxia-dependant regulation. Knowing the function of these target genes can help understanding the cellular response to hypoxia.
- Monitoring changes in genomic DNA; this application is extremely important in investigating cancer cells, because they often exhibit genomic instability with gene amplification or translocations, or tumour suppresser genes often marked by point mutations or deletion.
- Mutation or polymorphism, in particular single nucleotide polymorphisms (SNP), can be studied within and among species using high density oligonucleotide arrays. These so-called mutation detection arrays consist of oligonucleotides representing all known sequence variants of a gene or collection of genes. Because hybridisation to oligonucleotides is sensitive enough to detect single-nucleotide mismatches, a homologues gene carrying an unknown sequence variation can be screened rapidly for a large number of changes. Examples of mutation detection arrays include p53 gene chip, HIV gene chip and breast cancer BRCA-1.

### **1.5.6 Limitations of Microarrays**

- First, level of mRNA expression does not always reflect protein concentration: therefore, differential RNA expression could have no biological significance.
- Second, the expression data derived from cDNA Microarray are not the end point of the study. In many occasions, it only provides several candidates genes whose functions require further verification and investigation using other techniques like real-time PCR. Thus, the Microarray technique is used as a screening method that is only the first step in understanding biological processes.
- Third, cDNA Microarrays require possession of cDNA clones or prior knowledge of cDNA sequence. Given the fact that only a small number of genomes have been sequenced and many functionally important genes are expressed at low levels and underrepresented in a cDNA library, not all genes can be studied with satisfying quality using this technology.

## **1.6 Aim of this work**

This work aims to extend current knowledge about the mechanism leading to lung damage under hypoxia and in particular on the role of alveolar macrophages in currying out this damage. Using established methods of molecular biology it will try to define genes that are taken part in this complex process and learn more about their activation/depression in alveolar macrophages. The application of different techniques enable the self-control of the obtained data. Additionally, it allows the distinguishing between the influence of hypoxia on genes at the mRNA level and at the protein level.

Moreover, it aims to distinguish between genes that are activated under the influence of acute hypoxia and those activated under chronic hypoxia. For that reason examination of genes was performed after 1 and 21 days of hypoxia.



## 2 Materials and Methods

### 2.1 Small Materials

Atlas Mouse 1.2(II) Array Kit	Clontech (Heidelberg)
Phosphimaging Screen (20x25 cm)	Fuji (Düsseldorf)
Hybridisation bottles (13 ml)	Hybaid (Heidelberg)
Pipettes (1-10 µl, 10-100 µl, 100-1000 µl)	Eppendorf (Hamburg)
Pipette tips (sterile, 10-1000 µl)	Fisher Scientific (Schwerte)
PR-Tubes (15 ml, 50 ml)	GreinerLabortechnik (Frickenhausen)
Optical tubes (0.2 ml) / for TaqMan	Applied Biosystems (Langene)
Tubes (0.2-2.0 ml)	Eppendorf (Hamburg)
Cassettes for Phosphoimaging Screen (24x30 cm)	Kisker (Steinfurt)
Tubes for column chromatography	
QIAquick™ PCR Purification Kit	Qiagen (Hilden)
Microcon YM-100	Microcon (Ireland)
Cannules 20 gauge x1½"	TERUMO (Leuven, Belgium)
Microscope slides	Menzel Glaeser (Braunschweig)

### 2.2 Instruments

AbiPrism™ 7700 Sequence Detector	Applied Biosystems (Foster City, USA)
Autoclave 2540 ELC	Tuettner Systec (Wettenberg)

---

Photospectrometer Uvikon 922A	Kontron Instruments (Milano, Italy)
$\beta$ - $\gamma$ -Detector LB 122	Berthold (Zurich, Switzerland)
Bag sealer	Severin (Sundern)
Hot plate	Ika Labortechnik (Staufen)
Gel electrophoresis chamber	Bächler (Hölstein)
Hybridisation oven (rotating)	Hybaid (Heidelberg)
Phosphorimager FUJIX BAS 1000	Fuji (Düsseldorf)
Vortex Type REAX 2000	Heidolph (Schwabach)
UV Transilluminator	Bachofer (Reutlingene)
Liquid scintillation counter	Hidex (Straubenhardt)
Thermoblock TDB-120	Kisker (Mühlhausen)
Trio-Thermoblock TB-1	Biometra (Göttingene)
Microwave	Bosch (Stuttgart)
Scales PM 480	DeltaRange <sup>R</sup> Mettler (Giessen)
Water bad GFL 1012	GFL (Burgwedel)
Centrifuges: Biofuge 15R	Heraeus Sepatech (Hanau)
Biofuge pico	Heraues Instruments (Hanau)
Centrifuge 5415D	Eppendorf (Hamburg)
Cytocentrifuge Cytospin	Thermo Shandon (Pittsburgh, USA)
Microscope	Olympus (Hamburg)
Cryostat (Cryocut Jung CM 3000)	Leica (Bensheim)

## 2.3 Reagents and Kits

### 2.3.1 Bronchoalveolar lavage and cell lysis

Phosphate Buffered Saline (PBS) with 5mM EDTA:

NaCl	Carl Roth (Karlsruhe)
KCl	Merck (Darmstadt)
EDTA	Sigma (Taufkirchen)
Na <sub>2</sub> HPO <sub>4</sub>	Merck (Darmstadt)
KH <sub>2</sub> PO <sub>4</sub>	Merck (Darmstadt)
HCl	Merck (Darmstad)

### 2.3.2 RNA extraction

Phenol (Saturated with 0.1 M citrate Buffer, pH 4.3 +/- 0.2)	Sigma (Taufkirchen)
Sodium acetate	Sigma (Taufkirchen)
Chloroform (100%)	Merck (Darmstadt)
Isoamyl alcohol (100%)	Sigma (Taufkirchen)
Isopropranol (100%)	Sigma (Taufkirchen)
Glycogen (20 mg/ml)	Boehringer (Mannheim)
Ethanol (75%)	Merck (Darmstadt)
DEPC-treated H <sub>2</sub> O	Fresenius (Bad Homburg)

### 2.3.3 DNase treatment of total RNA

All components were included in the Atlas™ Pure Total Labelling System (#K1038-1)	Clontech (Heidelberg)
--	-----------------------

See chapter 2.4.4

### 2.3.4 Labelling of cDNA

$\alpha^{32}$  P dATP (3,000Ci/mmol, 10  $\mu$ Ci/ $\mu$ l) Amersham (Braunschweig)

All other components were included in the Clontech (Heidelberg)

Atlas Mouse 1.2 II Array Kit

See chapter 2.4.6

### 2.3.5 Column chromatography

All components were included in the

QIAquick PCR amplification Kit (Qiagene, (Hilden))

### 2.3.6 Preparation of the cDNA for hybridisation

2x Neutralizing solution (1M NaH<sub>2</sub>PO<sub>4</sub>, pH 7) Merck (Darmstadt)

10x Denaturing Solution (1M NaOH, 10mM EDTA) Merck (Darmstadt)

C<sub>0</sub>t-1 DNA Atlas Mouse 1.2 II Array Kit

### 2.3.7 Stripping the Arrays membranes

20 %SDS (Sodium Dodecyl Sulfate) Sigma (Taufkirchen)

20xSSC (NaCl,Na<sub>3</sub>Citrate·2H<sub>2</sub>O) Sigma (Taufkirchen)

### 2.3.8 cDNA synthesis from total RNA using RT enzyme (for PCR)

All components were included in the (Foster city, USA)

Applied Biosystems GeneAmp® RNA PCR kit.

See chapter 2.4.13

### 2.3.9 Real-time PCR

See chapter 2.4.12

### 2.3.10 Agarose gel electrophoresis

Electrophoresis Buffer 5xTBE

54g Tris base	Sigma (Taufkirchen)
27.5g boric acid	Sigma (Taufkirchen)
20 ml 0.5M EDTA pH (8.0)	Sigma (Taufkirchen)
in 1000ml aqua dest	

Gel-loading Buffer

900 µl 5xTBE	
100 µl Glycerine (98%)	Carl Roth (Karlsruhe)
Bromophenol blue (concentration of 0.25%)	Merck (Darmstadt)

DNA size standard (*Hinf*I Marker)

Per 50 µl- 10µl phiX 174 DANN /*Hinf*I Marker (1mg/ml) Promega (Mannheim)

10 µl 5xTBE

10 µl (gel-loading Buffer)
20 µl (Ampuwa H <sub>2</sub> O)

### 2.3.11 Immunohistochemistry

Tris washing buffer pH 7.6

(\* For preparing 20 liter washing buffer)

175.6g NaCl	Sigma (Taufkirchen)
18g Tris base	Sigma (Taufkirchen)
137g Tris HCL	Sigma (Taufkirchen)

2.5 liter aqua dest

Substrate solution:

Developing solution (NaCl 87g, Tris-HCl 15g, Tris-Base 49g, aqua dest 1750 ml) 70ml

N, N-Dimethyl formamide 600 ml Merck (Darmstadt)

2-Amino-2-methyl-1,3-Propanediol 25 ml Merck (Darmstadt)

Levamisole 40 mg Sigma (Steinheim)

Natriumnitrit 20mg Merck (Darmstadt)

aqua dest 500µl

Naphtol 50mg Sigma (Steinheim)

New-fuchsin 200µl Chroma -Gesellschaft (Koengene)

Tissue- Tek® Sakura Finetek (Zoeterwoude, the Netherlands)

### **2.3.12 Primers for TaqMan PCR**

\*All the primers are for mouse species.

\*Primers are from MWG-Biotech AG (Ebersberg, Germany)

**Table 2 A list of the primers used in this work.**

Gene <i>Gene Code</i>	Position + Length (Bp)	Sequence (5'– 3')
18s (house keeping ) <i>U30831</i>	218-289 Length-72	FP- AAA ACC AAC CCG GTC AGC C RP- CGA TCG GCC CGA GGT TAT CT
GAPDH (house keeping) <i>M32599</i>	411-531 Length-121	FP- GTG ATG GGT GTG AAC CAC GAG RP- CCA CGA TGC CAA AGT TGT CA
CD36 <i>L23108</i>	144-244 Length-101	FP- CCA CTG CTT TCA AAA ACT GGG RP- GCT GCT GTT CTT TGC CAC G
Apolipoprotein C II <i>Z15090</i>	202-305 Length-104	FP- GGT TGC CAA AGA CCT GTA CCA RP- TGC CTG CGT AAG TGC TCA TG
Protein S alpha <i>Z25469</i>	298-398 Length-101	FP- TCA AAG GCA ACT CGC CGT C RP- CAT TCA CTG GTG TGG CAC TGA
Cytochrome b-245 beta polypeptide <i>M31775</i>	107-207 Length-101	FP- TTT CGG CGC CTA CTC TAT CG RP- TCT GTC CAC ATC GCT CCA TG
NADH-ubiquinone oxidoreductase <i>Y07708</i>	46-158 Length-113	FP- GGT GTG CTT GGT CAT CCC C RP- CGC GTT CCA TCA GAT ACC ACT
Prosaposin <i>U23740</i>	117-220 Length-104	FP- GCA GTG CTG TGC AGA GAT GTG RP- TCG CAA GGA AGG GAT TTC G
Peptidylprolyl isomerase A <i>X52803</i>	306-406 Length-101	FP- ATG CTG GAC CAA ACA CAA ACG RP- GCC TTC TTT CAC CTT CCC AAA
Polypyrimidine tract binding protein <i>X52101</i>	496-596 Length-101	FP- TGG TGT GGT CAA AGG CTT CA RP- GCA GTT CAA TCA GCG CCT G
Integrin $\beta$ 2 <i>X14951</i>	195-295 Length-101	FP- GCA GAA GGA CGG AAG GAA CAT RP- CTA CCA CGG TGC CCC CTA C
Lectin galactose binding soluble Protein 1 <i>M57470</i>	255-355 Length-101	FP- CTT TCC AGC CTG GGA GCA T RP- GCG GTT TGG GAA CTT GAA TTC
Desmoglein 2 <i>AJ000328</i>	45-148 Length-104	FP- TCC TGC TTC CAC TCT GCA GTC RP- TGG GCA GAG GAC CTA TGC TT
Interleukin 9 receptor <i>M84746</i>	1283-1397 Length-115	FP- GGC AGC AGC GAC TAT TGC AT RP- ACA CAG GAA GGG CCA CAG G
G protein-coupled receptor 7 <i>U23807</i>	106-209 Length-104	FP- TGC AAG CTA ATT GTA GCC GT RP- TCT GCT GTG GCC AGA ACC A
Fibroblast growth factor 10 <i>D89080</i>	279-381 Length-103	FP- TGA GAA GAA CGG CAA GGT CAG RP- GAT GGC TTT GAC GGC AAC A
Interleukin 1 beta precursor <i>M15131</i>	605-707 Length-103	FP- CTT GGG CCT CAA AGG AAA GAA RP- CTT CTT TGG GTA TTG CTT GGG A
Cathepsin K <i>X94444</i>	374-476 Length-103	FP- CCC AGA AGG GAA GCA AGC A RP- CCG CAG GCG TTG TTC TTA TT
Cathepsin S <i>AJ223208</i>	7-87 Length-81	FP- TTG ATG GCA AAG ATT ACT GGC TT RP- TTC TTG CCA TCC GAA TGT ATC C
Acidic keratin complex 1 gene 16 <i>AF053235</i>	325-427 Length-103	FP- TCC TCA CAG CAC TCC TCT GGA RP- AGC TGG TTG AAC CTT GCT CCT
Vimentin <i>M26251</i>	134-225 Length-92	FP- AGA CGG TTG AGA CCA GAG ATG G RP- TGT TGC ACC AAG TGT GTG CAA T

## 2.4 Methods

### 2.4.1 Animal model of hypoxia

Male Balb/c AnNCr1BR –Mice (Charles River, Sulzfeld, Germany), 22-25 g, were placed in hypoxic chambers with reduced oxygen tension ( $FiO_2:0.10$ ). Oxygen pressure remained constant using an autoregulation control system ( $O_2$  control model 4010, Labotec, Göttingen).  $CO_2$  was continuously removed by soda lime (SodasorbR  $CO_2$  Absorbent, Grace, Columbia). Excess humidity in the recirculating system was prevented by condensation in a cooling system. Mice exposed to normobaric normoxia ( $FiO_2$  of 0.21 = control group) were kept in a similar chamber. After 1 or 21 days, the animals were intraperitoneally anaesthetised with 180 mg of sodium pentobarbital/kg body weight.

### 2.4.2 Bronchoalveolar lavage (BAL)

For BAL, the trachea was exposed and a small incision was made to insert a shortened 21-gauge cannula that was firmly fixed and then connected to a 1-ml insulin syringe filled with cold phosphate-buffered saline (PBS)-5 mM EDTA (pH 7.2). 300  $\mu$ l PBS was gently instilled into the lungs, withdrawn, followed by 400 and 500  $\mu$ l and then repeatedly with 500  $\mu$ l, until a total volume of 5ml was recovered. Cells gained by the BAL were kept during the whole process on ice. To remove the supernatant cells were centrifuged (1130 rpm, 5 min). The supernatant was then removed, 500 $\mu$ l cold saline added to the cells, followed by a second centrifugation, (1130 rpm, 5 min) and removal of the supernatant. Cells were counted using a *Neubauer* chamber and immediately afterwards stored in liquid nitrogen.

A crucial point of this work was to make sure that a large portion of the cells gained in the BAL are alveolar macrophages. For this reason, a sample containing 100  $\mu$ l cold saline and BAL-cells was taken (after the second centrifugation) for further investigation. Small portions of the sample were placed on a microscope slide, centrifuged in a cytocentrifuge (500 rpm, 5 min); air dried and then stained using the *Pappenheim stain*. *Pappenheim stain* is a combination of *May-Grünwald* and *Giemsa* stain and is generally used for blood smears. The cell nucleus is stained red-violet and the cytoplasm bright blue. After cells were stained, they were examined under the microscope, counted and differentiated.



### 2.4.3 Isolation of RNA from alveolar macrophages (AM)

The key to successful purification of intact RNA from cells is rapid preparation. Cellular RNAses should be inactivated as quickly as possible at the very first stage in the extraction process. Once endogenous RNAses have been destroyed, the immediate threat to the integrity of the RNA is greatly reduced, and purification can proceed at a more graceful pace.

Exogenous RNAses (for example those present on the human skin) are as harmful as the endogenous ones and therefore contamination must be avoided.

#### 2.4.3.1 Cell Lysis

The BAL containing-tubes were removed from the liquid nitrogen and a lysis buffer added to the cells. The buffer consist of 4M Guanidium Thiocyanat (GTC), 25mM Na<sub>3</sub> Citrate, 0.5% Lauroylsarcosin, 1M Tris-HCL) and β-Mercaptoethanol (Sigma, Taufkirchen Germany), for each sample (AM from 1 mouse)- 300 μl lysis Buffer and 2,4 μl β-Mercaptoethanol. Mercaptoethanol is a reduction agent and GTC is the cell lysis agent. Both agents reduce RNase activity. During the lysis step, probes were held at room temperature for 15 min, and then held on ice (during the whole extraction step), to protect RNA from degradation.

#### 2.4.3.2 Acid Phenol Guanidium Thiocyanate Chloroform Extraction

To isolate the RNA from DNA and cellular proteins, following reagents were added to cells (per one sample = 1 mouse)

Phenol (pH 4.3)	300 μl
Sodium-Acetate (2M, pH 4)	30 μl
Chloroform: Isoamyl alcohol (24:1)	90 μl

Tubes were briefly vortexed and centrifuged (15,000 rpm, 15 min, 4°C). The upper aqueous phase containing RNA was carefully transferred to a fresh tube.

An equal volume of isopropanol (≈300 μl), and 1.5 μl of glycogen was added to the extracted RNA, tubes were vortexed and stored for 1h at -20°C to allow precipitation of RNA. Following the precipitation step tubes were centrifuged (15,000 rpm, 15 min, 4°C). To collect the precipitated RNA, isopropanolol was removed carefully, (to avoid the losing of the pellet),

and the pellet was washed with 300  $\mu$ l 75% ethanol to remove remaining salt and isopropanolol rests. Tubes were then again centrifuged, and remaining ethanol removed. By holding the tubes open for a few min ethanol evaporated and pellet air-dried.

Finally, (glycogen) pellet was dissolved in 5  $\mu$ l of DEPC-treated H<sub>2</sub>O and the solution stored at -80°C.

#### 2.4.4 DNase treatment of total RNA

The removal of contaminating DNA from the RNA is a crucial factor in obtaining good results with Atlas Arrays. DNA was removed by a Danes treatment;

Total RNA	30 $\mu$ l
(5 $\mu$ l from each mouse x6=30 $\mu$ l)	
10x Danes I Buffer	4 $\mu$ l
(400mM Tris-HCl pH 7.5, 100mM NaCl, 60mM MgCl <sub>2</sub> )	
DNase I (1unit/ $\mu$ l)	2 $\mu$ l
(Deionized) H <sub>2</sub> O	4 $\mu$ l
<hr/>	
Total	40 $\mu$ l

Tubes were incubated at 37°C for 30 min, and the reaction was stopped by adding 4  $\mu$ l of 10x Termination Mix (0.1 M EDTA [PH 8.0], 1mg/ml glycogen).

To remove the degraded DNA, a second phenol-chloroform extraction followed the DNase treatment (as described in chapter 2.4.3.2).

#### 2.4.5 Spectrophotometry of isolated RNA

For measuring the amount and purity of the isolated RNA, UV absorption was recorded at 260 nm and 280 nm. The readings at 260 nm (OD<sub>260</sub>: Optical Density at 260 nm) were used to calculate the concentration of nucleic acid in the sample. An OD<sub>260</sub> of 1 corresponds to a concentration of 40 $\mu$ g/ $\mu$ l RNA. The OD<sub>260</sub>/OD<sub>280</sub> ratio provides an estimation of the purity of the nucleic acid. Pure preparations have OD<sub>260</sub>/OD<sub>280</sub> ratio values of 1.8-2. By significant

contamination with phenol or proteins the values will be less than those given above (because phenol as well as proteins has a maximum absorbance at 280nm).

1  $\mu$ l of RNA (aqueous solution) was 1:100 diluted in DEPC-treated H<sub>2</sub>O. Absorption at 260 nm and 280 nm was measured and corrected for those of the blank value (water sample). Concentration of the RNA was calculated using this equation-

$$\text{RNA } (\mu\text{g}/\mu\text{l}) = (\text{OD}_{260}^{\text{sample}} - \text{OD}_{260}^{\text{blank}}) \times 40\mu\text{g}/\mu \times 100$$

$$\text{Nucleic Acid Purity} = \frac{(\text{OD}_{260}^{\text{sample}} - \text{OD}_{260}^{\text{blank}})}{(\text{OD}_{280}^{\text{sample}} - \text{OD}_{280}^{\text{blank}})}$$

#### 2.4.6 Synthesis of radiolabelled cDNA using oligo (dT) primers

The following procedure enabled us to synthesise cDNA which is complementary to the mRNA isolated from AM, and to simultaneously label it with  $\alpha^{32}$  P-dATPs.

The  $\alpha^{32}$  P-dATPs are integrated in the newly formed cDNA strand like other dNTPs, and are complementary to the dUTP in the mRNA strand. The reaction is catalysed by a reverse-transcriptase.

Four different samples were simultaneously labelled (2 hypoxia, 2 normoxia mice) so the expression of different genes in hypoxia/normoxia could later be compared. Each sample contained the genetic material isolated from 6 mice, so that the total number of mice sacrificed to perform one assay (with 4 membranes) was 24.

2-5  $\mu$ l total RNA were mixed with 1  $\mu$ l Mouse 1.2 II CDS Primer mix in each tube and incubated in Thermoblock TDB120 at 70°C for 2 min. Due to the specificity of these CDS primers, hybridisation of non-mouse material with the mRNA could not take place. A second incubation at 50°C, again for 2 min, followed. During the second incubation, 1  $\mu$ l Molony Murine Leukaemia Virus Reverse Transcriptase (MMLV-RT, 100U/ $\mu$ l) was added to the Master Mix (MM).

### Preparation of MM-

5x reaction buffer	2 $\mu$ l
(250mM Tris-HCl [PH8.3], 375mM KCl, 15mM MgCl)	
10xdNTP Mix (for dATP labell)	1 $\mu$ l
5mM each dCTP, dGTP, dTTP)	
$\alpha^{32}$ P dATP (3,000Ci/mmol, 10 $\mu$ Ci/ $\mu$ l)	3.5 $\mu$ l
DTT (100mM)	0.5 $\mu$ l
<hr/>	
Total volume (for 1 sample)	7 $\mu$ l

After completion of the 2-min incubation at 50°C, 8  $\mu$ l of MM was added to each tube and incubated at 50°C for 35 min This reaction (cDNA and labelling) was then stopped by adding 1  $\mu$ l of 10x Termination Mix (0.1 M EDTA [PH8.0], 1mg/ml glycogen).

### 2.4.7 Column chromatography

To purify the labelled cDNA from unincorporated  $\alpha^{32}$  P-dATPs and small (<100bp) cDNA fragments, a QIAquick PCR amplification Kit was used in the following way:

1. Absorption of cDNA to a silica-gel membrane was achieved by adding 10 volumes of buffer PN to 1 volume of the cDNA sample. Tubes were then centrifuged (6000 rpm, 1 min). The PN buffer provided the correct salt concentration and pH for absorption of cDNA to the silica-gel membrane. Optimal absorption of nucleic acids to the membrane occurs in the presence of a high concentration of chaotropic salts at pH below 7.5. However, small cDNA fragments and nucleotides do not bind to the silica membrane.
2. Washing: 500  $\mu$ l ethanol containing PE buffer was added to the samples and centrifuged like in step 1 to wash salts away. This step was repeated twice followed by another centrifugation (13,000 rpm, 1 min) to remove any residual PE buffer, which may interfere with subsequent reactions.
3. Elution in low salt solutions: elution efficiency is strongly dependant on the salt concentration and pH of the elution buffer. It is most efficient under low salt concentration

and neutral pH (7-8.5). For elution, 100-200  $\mu$ l EB buffer (10mM Tris-Cl, pH 8.5) were added to the samples, which were then centrifuged (13,000 rpm, 1 min), giving the eluted purified cDNA.

The radioactivity of the 4 probes was measured with a liquid scintillation counter. This measurement allows a rapid evaluation of a successful incorporation of the  $\alpha^{32}$  P-dATPs. Furthermore, knowing the radioactive counts of the samples is a crucial factor to predict the time needed for exposure of the phosphorimager plates to the membranes (see below).

## **2.4.8 Array hybridisation**

Principles- The hybridisation of Atlas™ cDNA Expression arrays is a method for analyzing multiple genes simultaneously, by hybridisation of entire cDNA populations to nucleic acids arrays. This technology has a wide range of applications, including investigating of normal biological and disease processes and discovering potential therapeutic and diagnostic drug targets (see also chapter 1.5.5)

Identical nylon membranes (Mouse 1.2 II Atlas™ cDNA arrays containing 1,176 spots = genes) can be compared side by side, so that a comparison of expression profiles of different mRNA (in this work-hypoxia/normoxia) can be studied.

The cDNA fragments immobilized on the Atlas arrays are 200-600 bp in length and have been amplified from regions of the mRNA that lack the poly-A-tail, repetitive elements, or highly homologous sequences. In this way, non-specific hybridisation is minimized.

Different factors, mainly the quality of RNA, but also the correct hybridisation temperature, pH, low-viscosity of the hybridisation solution and the concentration of the probes are crucial factors for a successful and specific hybridisation.

### **2.4.8.1 Preparation of the hybridisation solution**

5 ml (for each sample) ExpressHyb-solution (Atlas™ Mouse 1.2 II arrays) were preheated in a water bath at 68°C. 52  $\mu$ l (for each sample) of sheared salmon testes (10.5 mg/ml, Sigma, Taufenkirchen, Germany) was heated at 95-100°C for 5 min and then quickly chilled on ice. Heat-denatured sheared salmon testes were then mixed with prewarmed ExpressHyb-solution and kept at 68°C until use.

Hybridisation bottles were filled with deionized water, and the membranes were placed into the bottles, adhering to the inside walls of the bottle without creating air pockets. Water was poured completely from the bottles and hybridisation solution prepared in the previous step was added to the bottles and distributed evenly over the membranes. Membranes were then prehybridised at 68°C for 30 min

#### **2.4.8.2 Preparation of radioactive labelled cDNA for hybridisation**

Each labelled probe (~110 µl) was mixed with 11 µl 10x denaturing Solution (1M NaOH, 10mM EDTA) and incubated at 68°C for 20 min 5 µl C<sub>0</sub>t-1 DNA (1mg/ml Mouse 1.2 II Atlas™ arrays) and 120 µl 2x neutralizing solution (1M NaH<sub>2</sub>PO<sub>4</sub>, pH 7) were added to each, and second incubation at 68°C for 10 min followed. C<sub>0</sub>t-1 DNA prevents non-specific hybridisation. Now the samples were finally suitable for hybridisation and pipetted carefully into the hybridisation bottles and well mixed. Hybridisation was performed overnight while bottles constantly being agitated in an oven at 68°C (Hybaid, Heidelberg, Germany).

On the next day the hybridisation solution was discarded into a radioactive waste container. 200 ml of pre warmed (at 68°C) Wash Solution 1 (2xSSC, 1% SDS) was poured into the bottles, which were then washed for 30 min with continuous agitation at 68°C. This step was repeated twice.

#### **2.4.9 Exposure of the phosphoimager plates to the membranes**

After washed, membranes were removed from the bottles and wrapped in to a transparent plastic foil, laid side by side and covered with a thin film of Wash Solution 1 to keep them wet. The radioactivity of the membranes was now measured by holding the β-γ-detector LB 122 ~1-2cm above. The radioactivity values (in counts per minute) were important for estimating how effective the hybridisation had been and the time needed for exposure of the plates (phosphoimaging screen). The plates were then laid over the plastic-wrapped membranes and packed together into a cassette for a time of exposure ranging from 1d to 15d (depending on the radioactive counts). Finally, the plates were scanned by the Phosphoimager FUJIX BAS 1000 so that the spatial distribution of radioactivity was represented by a grayscale image. After scanning, the membranes were stored at 4°C until stripping.

### 2.4.10 Stripping cDNA from the Atlas arrays

To reuse the membranes, they were stripped after every hybridisation. For this purpose 500 ml of 0.5% SDS was boiled in a 2-liter beaker on a hot plate. Membranes were removed from the plastic wrap and immediately placed in the boiling solution and boiled for 5-10 min. The beaker was removed from the hot plate and cooled for 10 min at room temperature. The membranes were rinsed in Wash Solution 1, wrapped and sealed again in a transparent plastic foil, and then stored at -20 °C until reuse. The efficiency of the stripping was checked using the  $\beta$ - $\gamma$ -detector LB 122; the stripping was repeated when radioactivity was still measured.

### 2.4.11 Image analysis and data processing

The investigation of such a large number of genes can hardly be done without the assistance of computer software developed for this purpose. The AtlasImage™ 2.0 (Clontech) is software for analysing the Atlas arrays in order to calculate normalised signal intensity values and intensity ratios as a measure for differential gene activity.

#### Background correction

For each spot  $i$  and each membrane  $k$ , the local background intensity  $B_{k,i}$  was subtracted from the corresponding spot (foreground) intensity  $F_{k,i}$  to obtain the background corrected intensity values

$$I_{k,i} = F_{k,i} - B_{k,i}$$

#### Normalising

It is necessary to normalise the signal intensity between two arrays being compared, especially when signal levels greatly differ. In this study, the “*global normalisation*” mode was used. This mode considers the signal values of all genes on the arrays. This approach assumes that although some genes are truly differentially expressed between two samples, the average activity of the genes represented on the membranes is more or less the same under treatment (hypoxia) and control (normoxia) conditions. The AtlasImage software normalises array 2 (hypoxia) with respect to array 1 (normoxia). The normalisation is done by multiplying the spot intensities of array 2 with a normalisation coefficient which is calculated-

$$\text{Normalizing Coefficient} = \frac{\sum_{i=1}^N I_{1,i}}{\sum_{i=1}^N I_{2,i}}$$

With  $F_{k,i}$  and  $B_{k,i}$ : foreground and background intensity of spot  $i$  at array  $k$ ;  
 $N$ : number of spots on the array (N=1176).

### Visualisation

The routine use of a variety of graphical displays is recommended to examine the outcome of the array results. Such displays can assist in deciding whether the experiment was successful, help in choosing appropriate analysis tools, and highlight specific experimental problems. Most of these graphical displays were first developed for the work with Microarrays, mainly because of large numbers of genes represented on each Microarray slide (few thousands), and the need to present the data obtained from these slides, in a form which is fast and easily understood for the viewer. Some of these displays were later “adopted” by scientists working with nylon arrays. In this work only summary displays are represented (e.g. for 1 day and for 21days). This form of data representation has become widely accepted for nylon arrays during the time this study was carried out, and was therefore performed when the experimental part of these work was completed.

The results of the array experiments are visualised in the form of MA-plots where the log intensity ratios (M) are plotted versus the average log intensities (A) with

$$M_i = \log_2 \left( \frac{I_{2,i}}{I_{1,i}} \right) = \log_2 I_{2,i} - \log_2 I_{1,i}$$

$$A_i = \log_2 \left( \sqrt{I_{2,i} \cdot I_{1,i}} \right) = \frac{1}{2} (\log_2 I_{2,i} + \log_2 I_{1,i})$$

MA plots allow recognising intensity dependant artifacts and bias in the data by visual inspection.

### Quality check

Prior to using statistical tests on the raw data, we selected the arrays most appropriate for analysis and excluded those that were not. For example, we omitted the experiments that



demonstrated a generally low spot-intensity of all genes close to the background intensity as a distinction between genuine signals and “noise” could not be safely performed.

Different background intensities between two membranes may further make a comparison of the signal strength of a single gene in normoxia/hypoxia difficult. Hence, to attain data representing the true biological activity of genes under hypoxia, a carefully selection of the row data is inevitable.

Statistical analysis

For the analysis the one-sample two-sided t-test ( $H_0: M=0$ ) was performed.

### **2.4.12 Real-time PCR**

The real-time PCR method was performed to confirm the array results for selected genes.

The principles of real-time PCR

Real-time PCR uses commercially available fluorescence-detecting thermocyclers to amplify specific nucleic acid sequences and measure their concentration simultaneously.

The technique applies oligonucleotides that anneal to an internal sequence within the amplified DNA fragment. The oligonucleotides, usually 20-24 bases in length, are coupled with a fluorescent dye at its 5' end (reporter) and a quenching group at its 3' end, which is blocked with  $PO_4$ ,  $NH_2$ , or a blocked base. The labelled oligonucleotide is added to the PCR together with primers required to drive the amplification of the target sequence. When both the fluorescent and quenching groups are present in close apposition on the intact probe, any emission from the reporter dye during the course of real-time PCR is absorbed by the quenching dye, and the fluorescent emission is low. As the reaction progresses, and the amount of target DNA increases, progressively greater amounts of oligonucleotide probe hybridise to the denatured target DNA. However, during the extension phase of the PCR cycle, the 5'→3' exonuclease activity of the thermostable polymerase cleaves the probe hybridised to the template strand. Because the reporter dye is no longer in close proximity to the quencher, it begins to fluoresce. The intensity of this fluorescence is directly proportional to the amount of target DNA synthesized during the course of the PCR.

The instrument plots the intensity of fluorescence signal (which is proportional to the amount of PCR-product) over the course of the entire PCR. The greater the initial concentration of

target sequence in the initial mixture is, the fewer is the number of cycles required to achieve a particular yield of amplified product. The initial concentration of target sequences can therefore be expressed as the fractional cycle number ( $C_T$ ) required achieving a present threshold of amplification.

An important factor in quantitative PCR is the definition of a reference sequence, so that later a ratio of the target sequence to this reference sequence can be achieved. Two types of reference sequences can be used: an endogenous standard and an externally added reference.

*Endogenous standard*- these are usually so called house keeping genes (see further information about house keeping genes below) that are not regulated and present in the same preparation of DNA/RNA of the target sequence. Quantification is achieved by comparing the amount of amplified product generated by the endogenous standard and the target sequence. The method works well, if the amplified products are measured during the exponential phase of the reaction, if the reference and target sequence are amplified with equal efficiency and if they are present in the sample at approximately equal concentrations.

However, these conditions are not always fulfilled because the amplified products are almost always different from the endogenous reference in size, sequence and abundance. In addition, the house keeping genes chosen, are often invariant in their level of expression from one sample to the other.

*Externally added reference*- is added in known amounts to a series of amplification reactions.

As the reference templates and the target sequences are present in the same amplification reaction and use the same primers, the effect of the variables mentioned earlier is nullified. To find out the ratio of target to reference sequence, a series of reactions is set up, containing different ratios of the reference and target molecules. A curve is calculated showing the relationship between the amount of amplified product and the amount of reference added to the reaction. The target sequence can be quantified by interpolation. Thus, in a reaction that yields equal amounts of two amplified products, the ratio of target molecules to reference molecules at the beginning of the PCR is one. However, this is only true if amplification efficiencies of the two PCR reactions are equal.

*House keeping genes* (=reference genes) are a set of predefined genes required for fundamental cellular processes in a wide range of cell types and tissues and whose expression is not generally dependant on the developmental stage or physiological or pathological state

of the tissue. Operationally, few if any genes truly fit such invariant expression, although genes such as actin, cyclophilin, GAPDH, are frequently used in this context. In this study 18S and GAPDH gene were used for that purpose:

- ◆ 18S ribosomal RNA- DNA coding for ribosomal RNA is present in region p12 on each of the satellited chromosomes, 13, 14, 15, 21 and 22. At the ribosomal RNA gene promoter, transcription initiation by RNA polymerase I allows synthesis of the 45S rRNA precursor molecule, which serves as the molecular precursor for the 18S, 5.8S and 28S ribosomal RNA components. 18S is, like GAPDH, an extensively used house keeping gene (Veiga-Crespo *et al.*, 2004; Yadetie *et al.*, 2004; Yamada *et al.*, 1997). 18S was also used as a reference gene by other groups who studied the influence of hypoxia on several genes (Popovici *et al.*, 1999; Razeghi *et al.*, 2003).
- ◆ GAPDH-Glyceraldehyde-3-phosphate dehydrogenase catalyzes an important energy-yielding step in carbohydrate metabolism, the reversible oxidative phosphorylation of glyceraldehyde-3-phosphate in the presence of inorganic phosphate and nicotinamide adenine dinucleotide (NAD). $\{D\text{-glyceraldehyde 3- phosphate} + \text{phosphate} + \text{NAD (+)} \leftrightarrow 3\text{- phospho-D-glycerol phosphate} + \text{NADH}\}$ .The enzyme is thought to be a tetramer of identical chains. GAPDH is widely used as a house keeping gene (Shen *et al.*, 2003; von Schnakenburg *et al.*, 2002). Regarding the influence of hypoxia on the expression of this gene, it should be mentioned that in recent years, some evidence showing an over-expression of GAPDH in cells exposed to hypoxia have been found. Furthermore, the GAPDH promoter region contains hypoxia responsive elements (Graven *et al.*, 1999). To investigate whether the use of GAPDH for our purposes was acceptable, we compared the amplification curves for GAPDH and 18S in real-time PCR. Since we could not demonstrate a regulation of this gene neither under 1 day hypoxia nor under 21 days of hypoxia (strong correlation of expression for GAPDH and 18S in normoxia and hypoxia), we figured that the use of GAPDH for AM was suitable in our setup. We calculated the mean value of the two reference genes that served as our reference.

### **2.4.13 cDNA synthesis from total RNA using RT enzyme**

Before being able to use the Real-time PCR technique, a further step was made- “translation” of the extracted RNA to cDNA. Using a Reverse-Transcriptase (RT) enzyme, a RNA-dependant-DNA-polymerase enzyme, RNA was transcribed to cDNA (c= copy, a complementary picture of the RNA). An important side effect of this step, is the fact that from this point on we no longer worked with a nucleic acid which is highly sensitive and prone to degradation ( through RNase), but with a stable, double stranded DNA molecule.

The enzyme used to catalyse this reaction, Murine Leukaemia Virus Reverse Transcriptase (MULV- RT), is an artificially mutated enzyme; by deletion or point mutation of its carboxyl-terminal domain (220 residues), accounting for its RNase H activity, this feature is inactivated. The inactivation dramatically increases the ability of the enzyme to catalyse the synthesis of cDNA at elevated temperatures (>42°C) and to generate a full-length cDNA molecules.

Depending on the purpose of the experiment, the primer for the first-strand cDNA synthesis can be specifically designed to hybridise to a particular gene, or it can bind generally to all RNA. Since we investigated expression of different genes and not only of a specific one, we used the random hexanucleotides for priming. They are capable of priming cDNA synthesis at many points along RNA templates, generate fragmentary copies of the entire population of RNA molecule and are useful when the target RNA is extremely long (recovering the whole mRNA length).

For the cDNA synthesis a GeneAmp® RNA PCR kit (Applied Biosystems, Foster, USA) was used.

Denaturation: extracted RNA dissolved in 10 µl H<sub>2</sub>O was incubated at 70°C for 10 min, then shortly (~ 5 min) ice cooled and centrifuged.

---

Mastermix: \_\_\_ per cup in 10  $\mu$ l dissolved RNA:

10xPCR Buffer II	2 $\mu$ l
25mM MgCl <sub>2</sub>	4 $\mu$ l
dNTP's (dATP,dCTP,dTTP,dGTP, each 10mM)	1 $\mu$ l
Random Hexamers	1 $\mu$ l
RNase Inhibitor	0.5 $\mu$ l
MuLV Reverse Transcriptase	1 $\mu$ l
RNase –free H <sub>2</sub> O	0.5 $\mu$ l
<hr/>	
Total	10 $\mu$ l

Cups were incubated in the TRIO Thermoblock TB-1 and the following program was activated:

<u>Temp(°C)</u>	<u>Time (min:sec)</u>
20.0	10:00 annealing
43.0	75:00 elongation
99.0	5:00 enzyme denaturation
4.0	end of program

Finally, cDNA was stored at -20°C.

---

Preparation of Master Mix (MM) for PCR:

2x PCR Master Mix Cyber® Green I Assays (Eurogenetec)	25µl
Forward Primer (200 nM)	1 µl
Reverse Primer (200 nM)	1 µl
1/2000 dilution (in DMSO) of Cyber® Green I	1.5 µl (1 in 66000)
RNAse-Free H <sub>2</sub> O	19.5 µl

---

Total	48 µl
-------	-------

Preparation of MM for house keeping genes:

2x qPCR™ -Mastermix (Eurogenetec)	25 µl
Forward Primer (900 nM)	4.5 µl
Reverse Primer (900 nM)	4.5 µl
Probe	1 µl
RNAse-Free H <sub>2</sub> O	13 µl

---

Total	48 µl
-------	-------

The MM for the house keeping genes and the gene of interest were pipetted in the following way; 48 µl of MM in each optical tube followed by 2 µl templates (cDNA from hypoxia/normoxia material) to a total volume of 50 µl. Tubes for the negative control assay contained only MM and 2 µl H<sub>2</sub>O instead of templates.

The following program was used for the PCR reaction:

<u>Temp(°C)</u>	<u>Time (min:sec)</u>	<u>Cycles</u>
50.0	2:00	1x
95.0	6:00 denaturation	1x
95.0	0:20 denaturation	} 45x
59.0	0:30 annealing	
73.0	0:30 elongation	

#### **2.4.14 Agarose gel electrophoresis**

Gel electrophoresis is used to separate, identify, and purify DNA fragments. To reassure that the correct products were amplified by the real-time PCR, an agarose gel electrophoresis was performed.

The agarose gel is a matrix in which the DNA is migrating in the presence of an electric field. The pore size of the gel is depending on the concentration of the gel (low concentration = large pore size), thus the DNA is sieved through the pores. In an aqueous solution and a neutral pH the DNA fragments are negatively charged (due to their sugar and phosphate residues) and are therefore migrating to the anode when they are in an electric field.

The following factors determine the rate of migration of DNA through the agarose gel-

- molecular size of the DNA
- concentration of the agarose
- conformation of the DNA
- applied voltage
- electrophoresis buffer and agarose type

To visualize the DNA in agarose gel, the fluorescent dye ethidium bromide is added. This dye contains a tricyclic planar group that intercalates between the stacked bases of the DNA. UV radiation at 302 nm is absorbed by the DNA. The energy is transferred to the dye which re-emits it as red- orange light with a maximum emission at wavelength of 590 nm, making the

dye-DNA complex visible. By comparing the DNA-bands obtained from the samples with a DNA fragment length marker, one can estimate the strands length of the DNA samples.

Generally, DNA from 50 bp to several mega bases in length can be separated on agarose gels.

Protocol:

1.25g agarose mixed in 60  $\mu$ l 0.5x TBE buffer were heated in a microwave until the agarose dissolved. Then, 1.6  $\mu$ l ethidium bromide (10 mg /ml Roth, Karlsruhe) was added and the solution was mixed by gently swirling. While the gel was left at room temperature for a couple of minutes to cool, an appropriate comb for forming the slots in the gel was placed in the mould. The agarose solution was then poured in to the mould and left for 30-45 min until the gel completely formed. A small amount of 0.5x TBE buffer was poured on top of the gel and the comb carefully removed.

The PCR samples (each contains 50  $\mu$ l) were mixed with 7  $\mu$ l of gel-loading buffer. 10  $\mu$ l of the sample mixture were carefully loaded in to the slots, one slot for each PCR sample. To enable the estimation of the DNA strand length, 2  $\mu$ l *Hinf* I marker was added in one slot. Finally, the lead of the gel tank was closed and the electrical leads attached (120V, 300 mA for 45 min). As electrophoresis was completed the gel was irradiated by UV light and photographed.

#### **2.4.15 Immunohistochemistry**

Immunohistochemistry (IHC), or immunocytochemistry, is a method for localising specific antigens in tissues or cells based on antigen-antibody recognition; it seeks to exploit the specificity provided by the binding of an antibody with its antigen at a light microscopic level. IHC has a long history, extending more than half a century from 1940, but it was not until the early 1990 when the method found general application in surgical pathology.

The basic principle of IHC, as with any other special staining method, is a sharp localisation of target components in the cell and tissue, based on a satisfactory signal- to- noise ratio. Amplifying the signal while reducing non-specific background staining is the major strategy to achieve a satisfactory and practically useful result.



#### **2.4.15.1 Blocking non-specific background staining**

There are two aspects to the blocking of background staining of tissues: non-specific antibody binding and the presence of endogenous enzymes. Non-specific antibody binding is generally more a problem using polyclonal antibody, because multiple “non-specific” antibodies may exist in the antiserum. If necessary, it is advisable to preincubate the tissue section with normal serum from the same species of animal in order to occupy “non-specific” binding sites before incubation with the primary antibody. Another form of non-specific binding results from the fact that antibodies are highly charged molecules and may bind non-specifically to tissue components bearing reciprocal charges (e.g., collagen). Such non-specific binding may lead to localisation of either the primary antibody or the labelled moiety, producing false-positive staining of collagen and other tissue components of sufficient degree to obscure specific staining. Pre-incubation with normal serum may also reduce this kind of non-specific binding.

Blocking endogenous enzyme activity is also important. The degree of susceptibility of an enzyme to denaturation and inactivation during fixation varies. Some, like peroxidase, are preserved in both paraffin and frozen sections; others, like alkaline phosphatase, are completely inactivated by routine fixation and paraffin-embedding procedures. Any residual activity of these endogenous enzymes must be abolished during immunostaining in order to avoid false-positive reactions when using the same or similar enzymes as labells. It is essential that blocking of endogenous enzymatic activity be carried out before the addition of enzyme-labelled antibody; otherwise, the enzyme labell is also inactivated by the blocking procedure, resulting in a false-negative result.

#### **2.4.15.2 Alkaline phosphatase anti alkaline phosphatase method**

The alkaline phosphatase anti alkaline phosphatase (APAAP) reagents consists of antibody against alkaline phosphatase (AP) and AP antigen in the form of a small, stable immune complex. This complex typically consists of two antibody molecules in the configuration shown in the figure below. The APAAP reagent and the primary antibody must be from the same species (or closely related species with common antigenic determinants), whereas the bridge antibody is derived from a second species and has specificity against the primary antibody and the immunoglobulin incorporated into the APAAP complex. The bridge antibody serves as a “specific glue” to bind the APAAP-labelled moiety to the primary

antibody, which, in turn, is bound to the antigen under study (Figure 4). This is the “classical” form of the APAAP method. In this work, though, commercially available AP- conjugated second antibody was used. We demonstrated a specific staining of epitopes on the AM, the use of a third antibody was therefore not justified.

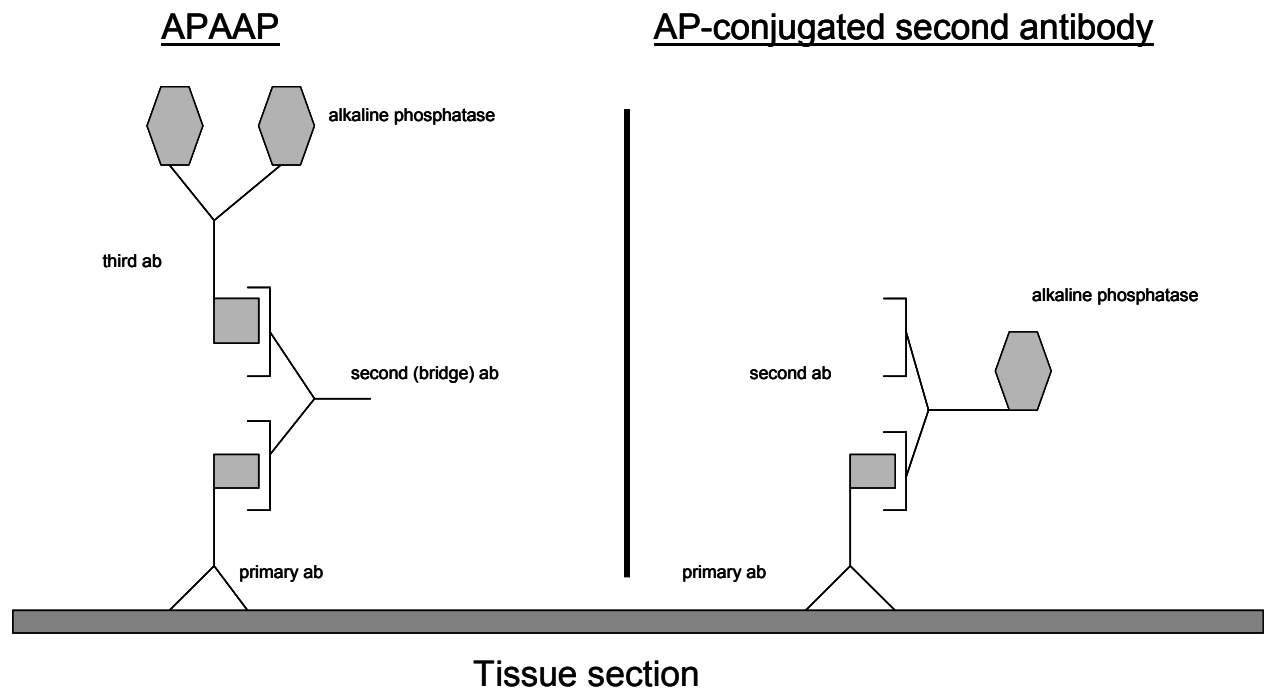


**Figure 4 The APAAP Immunohistochemistry method.** The “classical method” (left) and the AP- conjugated second antibody (right) used in this work. Ab= antibody

**Table 3 List of the antibodies used for staining**

Antigen/Protein	Primary antibody	Secondary antibody
<b>Vimentin</b>	Vimentin (c-20): sc-7557 Goat polyclonal anti-mouse  Each vial contains 200µg IgG in 1.0 ml of PBS containing 0,1% sodium azide and 0,2% gelatin Produced by Santa Cruz Biotechnology, INC	Anti-goat IgG F(ab') <sub>2</sub> [Rabbit] In buffer containing 0,05M Tris chlorid,0,15Msodium chlorid,0,0001M Zinc chloride,50%(v/v) Glycerol; pH 8 Stabilizer-10mg/ml Bovine Serum Albumin  Preservative-0,01%(w/v) sodium Azide
<b>Integrin β2</b>	Integrin β2 (k-19): sc-6625 Goat polyclonal anti-mouse  Each vial contains 200µg IgG in 1.0 ml of PBS containing 0,1% sodium azide and 0,2% gelatin Produced by Santa Cruz Biotechnology, INC	Anti-goat IgG F(ab') <sub>2</sub> [Rabbit] In buffer containing 0,05M Tris chlorid,0,15Msodium chlorid,0,0001M Zinc chloride,50%(v/v) Glycerol; pH 8 Stabilizer-10mg/ml Bovine Serum Albumin  Preservative-0,01%(w/v) sodium Azide

### Protocol

Lung tissue was obtained from mice treated in the same way described in chapter 2.4.1.

A total number of 12 mice were sacrificed for immunohistochemistry procedure (3 mice for 1day hypoxia, 3 mice for 1day normoxia, 3 for 21 normoxia and 3 for 21day hypoxia). After the peritoneal anaesthesia, the thorax was opened using small seizures, the lungs prepared and immediately fixed with preheated Tissue-Tek®.

The tissue was stored at -80 °C until sections were cut in a cryostat. 7-10 µm thick sections were used (sections are usually thinner), because cutting lung tissue, which is naturally air filled, in thinner sections, is often very difficult or impossible. Each section was placed on a microscope slide and air dried overnight at room temperature. Before being stained, the sections were fixed in ice cold acetone for 10 min and briefly air dried. For binding the primary antibody, sections stained for vimentin and integrin β2 were incubated in a dilution of (1:50). Slides were incubated for 30 min incubation in a humid chamber and then washed with Tris buffer. For the secondary, alkaline phosphatase conjugated antibody, a (1:100) dilution was used; slides were incubated for 30 min at room temperature and then washed with Tris buffer.

As for the negative controls, no primary antibody was introduced on the slides; slides were incubated solely with Tris buffer. For the second antibody, incubation was carried out as described above.

---

Finally, for staining, slides were incubated for 30 min in the following substrate solution:

Developing solution 70 ml

N, N-Dimethyl formamide 600 ml

Propandiol 25 ml

Levamisole 40 mg → Blocks endogenous AP activity

Natriumnitrit 20 mg

Aqua dest 500 µl

Naphtol 50 mg → Substrate

New-fuchsin 200 µl → Dye

In this procedure, epitopes were stained red (new-fuchsin), and slides were again washed with Tris-buffer. A counter- stain of the nuclei with haematoxylin completed the process, dyeing them blue.

After staining, slides were examined under a light microscope (magnitude x 200), and positive- stained- AM counted. The positive- stained- AM were grouped according to the strength of the staining (more than 50% of AM did not show a staining and were therefore not grouped for further analysis); 1-mild, 2-moderate and 3-strong staining. Every slide was observed under 5 fields of vision (1 field had an area of 0.196 mm<sup>2</sup>) with a total area of 0.98 mm<sup>2</sup>. The examination of the slides and cell counting was carried out by Prof. Dr. med RM Bohle, Institute for Pathology, university of the Saarland, Homburg, in a blinded way.

For the statistical tests only two groups of stained AM were considered, namely mild and moderate/strong. The moderate and strong stained AM were united into one group as there was only one single strongly stained macrophage seen in all slides. The Fischer's exact test (2-tailed) was performed for these two groups, to test whether there is a significant hypoxia dependant expression for the proteins stained.

## 3 Results

### 3.1 Bronchoalveolar lavage

Before exploring the gene expression of AM, we had to assure that the cells gained from BAL contain a major fraction of AM. For that reason, cells were counted and differentiated (as described in chapter 2.4.2.), in six different occasions. Counts from hypoxic and normoxic animals were compared in order to make sure that hypoxia does not affect cell numbers and type.

**Table 4** Cell counts from BAL AM= Alveolar Macrophages; Lymph= Lymphocytes; PMN=Polymorphonuclear leukocytes

<b>1 day</b>			<b>21 days</b>		
Date- 14/12/01	Normoxia	Hypoxia	Date- 05/01/02	Normoxia	Hypoxia
Cell Nr. (Mean)	329	380	Cell Nr. (Mean)	290	304
Cell Nr. (Min-Max)	270- 403	282- 497	Cell Nr. (Min-Max)	219-522	252-354
Cell type	AM-98% Lymph-1% PMN-1%	AM-97% Lymph-2% PMN-1%	Cell type	AM-98% PMN-2%	AM-99% PMN-1%
Date- 27/02/02	Normoxia	Hypoxia	Date- 08/02/02	Normoxia	Hypoxia
Cell Nr. (Mean)	276	257	Cell Nr. (Mean)	313	367
Cell Nr. (Min-Max)	241-384	220-371	Cell Nr. (Min-Max)	198-523	252-480
Cell type	AM-100%	AM-99% PMN-1%	Cell type	AM-99% Lymph-1%	AM-98% Lymph-2%
Date- 26/03/02	Normoxia	Hypoxia	Date- 26/02/02	Normoxia	Hypoxia
Cell Nr. (Mean)	242	272	Cell Nr. (Mean)	233	228
Cell Nr. (Min-Max)	166-304	166-411	Cell Nr. (Min-Max)	171-395	142-356
Cell type	AM-100%	AM-100%	Cell type	AM-98% Lymph-1% PMN-1%	AM-97% Lymph-2% PMN-1%
Mean	282.3	303.0	Mean	278.7	299.7
Standard deviation	35.8	54.8	Standard deviation	33.6	56.8

Table 4 shows that: first, all counts contained mainly (at least 97%) AM. Second, there was no significant distinction in cell numbers or type comparing BAL after 1 or 21 days. Third, hypoxia and normoxia did not differ in cell type or counts.

By doing this pre examination we could ascertain, that results and conclusions achieved using further methods, will be valid to gene expression of AM.

### **3.2 Hybridisation results**

A total number of 20 (10 for 1 day, 10 for 21 days) hybridisations was performed, each experiment contained 4 nylon membranes (2 hypoxia, 2 normoxia), laid side by side for analysis. Since the performance of the RT enzyme supplied by Clontech™ was inadequate, cDNA synthesis resulted in too low amounts of cDNA and poor incorporation of radiolabelled dATP. This in turn led to a weak hybridisation signal, and a low signal-to-noise ratio. Moreover, the low hybridisation signal made a longer exposition of the membrane inevitable, leading to an irregular background.

Therefore, the initially obtained hybridisation results were not adequate for further use and could not be used. Usable hybridisation results were obtained just after another RT-enzyme (supplied by Promega™) was applied. The remaining sample size allowed only a small number of hybridisations to be carried out for further analysis (between 3 to 5 per time point).

Figure 5 demonstrate the image obtained after the phosphoimager plates were scanned. Please note the major difference in signal intensity depending on the RT-enzyme used.

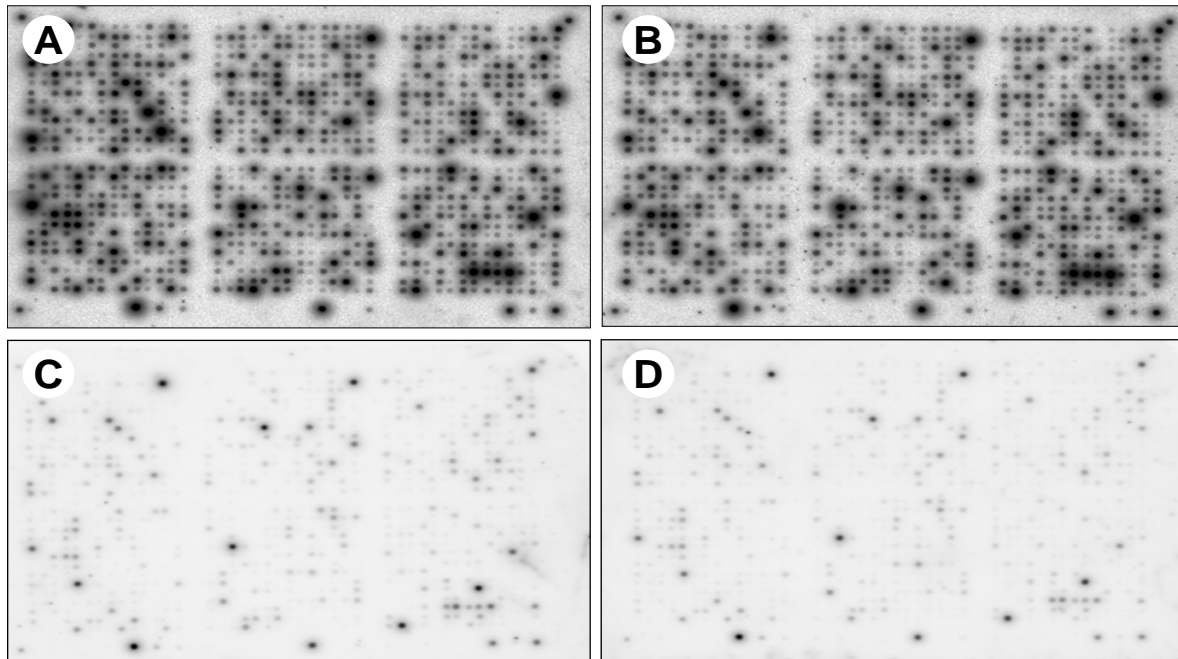


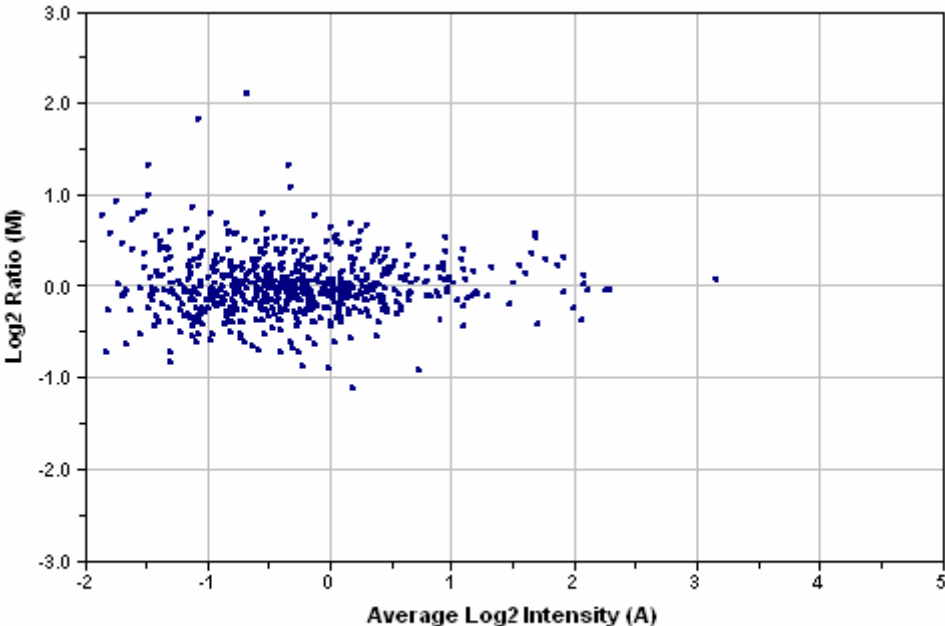
**Figure 5** Comparison of the images obtained using two different RT's: (A)- normoxia, and (B)- hypoxia. Using the RT supplied by Promega™; (C)- normoxia, and (D)- hypoxia using the RT supplied by Clontech™.

### 3.3 Arrays analysis

Figure 6 shows the M/A plots for the 1day/ 21days arrays. Only a small number of genes were influenced in their expression by hypoxia. Furthermore, intensity-dependant artefacts did not exist.

The use of statistical tests demonstrated the following; for 1 day not even one gene could be pointed out for demonstrating a statistical relevant regulation ( $P < 0.05$ ). As for the 21 days only one gene (Ia-associated invariant chain, gene code X05430) was selected ( $p = 0.0359$ ). Therefore, an alternative way for the selection of genes had to be used. For that purpose, we composed Table 5 and Table 6 including only genes that exhibit at least 3 times a ratio (normoxia/hypoxia)  $> 1$  or  $< 1$ , (i.e. showing a tendency to be hypoxia regulated). In that manner we introduced an instrument to identify (without using statistical methods) genes probably influenced by the lack of oxygen on their expression. A small number of candidates was selected from these tables for further analysis and validation by real-time PCR.

A)



B)

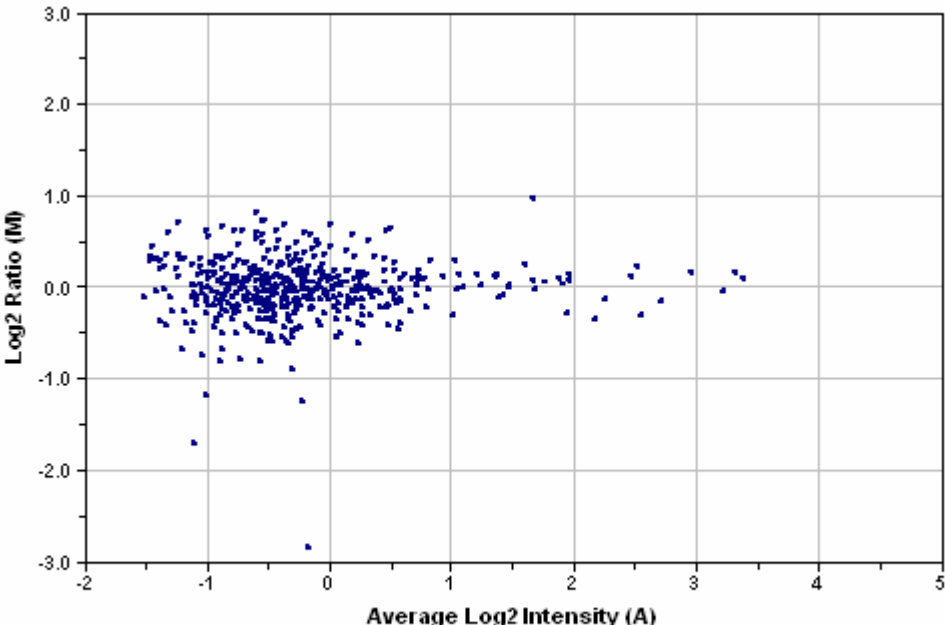


**Figure 6** M/A-plots of the nylon arrays results after 1d hypoxia (A) and 21d hypoxia (B). Each dot represents one gene (feature) spotted on the membrane.



Table 5 Regulated genes under hypoxia 1 day.

Gne Code*	Gne bankcode**	M <sup>1</sup>	SD <sup>2</sup>	P <sup>3</sup>	Gene
A01e	M63697	0.43	0.2091	0.6270	CD1d2 antigen
A01f	M58661	-0.30	0.1825	0.6837	CD24a antigen
A01j	U18372	0.16	0.1898	0.8486	CD37 antigen
A01n	S51806	-0.57	0.2031	0.6095	CD44 antigen precursor; phagocytic glycoprotein I
A02c	D16432	-0.47	0.2367	0.6549	Cd63 antigen
A02j	AF001041	0.21	0.1850	0.7788	CD83 antigen
A02n	L08115	0.33	0.2356	0.7523	CD9 antigen
A03f	X14951	-0.61	0.2684	0.6095	integrin beta 2 (ITGB2); cell surface adhesion glycoproteins
A03k	AB007599	-0.18	0.2214	0.8486	lymphocyte antigen 86 (LY86); MD1
A06e	M94087	0.48	0.1916	0.6095	activating transcription factor 4 (ATF4); TAXREB67 homolog
A06f	AB015140	0.71	0.2658	0.6095	aryl-hydrocarbon receptor repressor (AHR repressor; AHRR)
A06k	AF000998	0.42	0.2984	0.7468	circadian locomoter output cycles kaput
A06m	X79233	0.34	0.1889	0.6549	Ewing sarcoma homolog
A08j	D87964	0.10	0.1940	0.9140	TEA domain family member 3
A09l	X16834	-0.25	0.1658	0.7180	lectin galactose-binding soluble protein 3
B01k	Z25469	-1.21	0.4404	0.6095	protein S (alpha)
B04i	AB015800	0.22	0.2923	0.8507	solute carrier family 22 member 5 (SLC22A5); OCTN2
B07n	X70854	0.56	0.2354	0.6095	fibulin 1
B08h	U35035	0.04	0.1781	0.9736	matrilin 1; cartilage matrix protein 1
B10g	X05430	-0.48	0.1697	0.6095	Ia-associated invariant chain
B10j	M25244	-0.21	0.1764	0.7628	lysosomal membrane glycoprotein 1
B10n	X90582	0.26	0.2092	0.7533	signal sequence receptor delta
B11k	M31775	-0.45	0.2102	0.6095	cytochrome b-245 alpha polypeptide
B12e	L06465	-0.33	0.2071	0.7000	cytochrome c oxidase polypeptide VI a1 (COX6A1)
B14h	M60847	-0.09	0.3218	0.9697	lipoprotein lipase
B14i	X51547	-0.64	0.1861	0.6095	P lysozyme structural
C01b	AF002718	0.10	0.1854	0.9138	ATPase inhibitor
C02a	M16229	0.62	0.2457	0.6095	mitochondrial malate dehydrogenase
C03f	M65034	0.51	0.2552	0.6549	fatty acid binding protein intestinal
C03i	D29639	-0.49	0.3536	0.7523	hydroxylacyl-Coenzyme A dehydrogenase-dehydrogenase
C03k	X70100	-0.13	0.2287	0.9014	keratinocyte lipid binding protein
C04e	U27340	0.39	0.2259	0.6549	prosaposin
C06d	M63244	0.36	0.2410	0.7328	erythroid aminolevulinic acid synthase 2
C06j	X13752	-0.32	0.2452	0.7523	delta-aminolevulinic acid dehydratase
C08g	M61704	0.37	0.1822	0.6356	alkaline phosphatase 5
C09h	L10244	-0.26	0.2093	0.7533	spermidine/spermine N1-acetyl transferase
C09m	X52803	-0.18	0.1689	0.7811	peptidylprolyl isomerase A
C10n	M73329	-0.61	0.1974	0.6095	endoplasmic reticulum protein
C11k	X81987	-0.42	0.1738	0.6095	ribosomal protein L6
C12b	X03039	-0.17	0.2245	0.8507	eukaryotic translation initiation factor 4A1
C12n	AF067834	-0.45	0.2166	0.6356	caspase 8
C13d	U19463	-0.27	0.1503	0.6549	tumor necrosis factor alpha-induced protein 3 (TNFAIP3; TNFIP3)
C14e	X75947	0.66	0.2411	0.6095	poly(rC) binding protein 2
D01c	X53476	-0.87	0.2600	0.6095	high mobility group protein 14 (HMG14)
D03c	X59927	1.12	0.2643	0.5805	fibroblast growth factor receptor 4 (FGFR4)
D07m	U26176	1.05	0.3224	0.6095	somatostatin receptor 4
D10e	U40811	0.34	0.2251	0.7209	endothelial differentiation sphingolipid G protein-coupled receptor 1
D11g	U28772	0.24	0.1971	0.7533	olfactory receptor 10
D12e	AF102533	0.47	0.2891	0.7086	olfactory receptor F7
D13a	M60909	0.16	0.1730	0.8282	retinoic acid receptor alpha
D14i	D89080	0.21	0.1983	0.7938	fibroblast growth factor 10 (FGF10)
E01c	AF092734	0.45	0.1670	0.6095	growth differentiation factor 11 (GDF11)
E02i	U15209	-0.27	0.1912	0.7399	small inducible cytokine A9
E02k	M13177	0.69	0.1970	0.6095	transforming growth factor beta 1 (TGF-beta 1; TGFB1)
E03e	AF070988	0.29	0.1442	0.6270	wingless-related MMTV integration site 2b protein (WNT2B)
E05h	M15131	-0.48	0.2878	0.6837	interleukin 1 beta precursor (IL1-beta; IL1B)
E06c	X94322	0.40	0.2637	0.7328	melanoma inhibitory activity protein (MIA)
E08c	U43187	0.43	0.2124	0.6270	mitogen-activated protein kinase kinase 3
E11k	AF031147	0.15	0.1746	0.8447	phosphodiesterase 9A (PDE9A)
E12b	D16301	0.18	0.1786	0.8049	caltractin; 20-kDa calcium-binding protein
F02e	AB009459	0.79	0.2839	0.6095	mannan-binding lectin serine protease 2 (MASP2)
F02m	D10445	-0.72	0.2914	0.6095	protein C
F04m	D84096	0.28	0.2359	0.7639	ubiquitin c-terminal hydrolase related polypeptide
F05e	AF090691	0.35	0.2719	0.7523	cystatin 8 (cystatin-related epididymal spermatogenic)
F06l	X63535	0.42	0.3109	0.7523	AXL receptor tyrosine kinase
F07m	U58884	0.55	0.2470	0.6270	drebrin-like
F09j	M26251	-0.52	0.1946	0.6095	vimentin (VIM)
F09m	U04443	-0.57	0.2493	0.6095	non-muscle myosin light chain 3
F12f	L07063	-0.17	0.2493	0.8752	FK506 binding protein 6 (65 kDa)
F12i	AF022371	-0.59	0.2473	0.6095	interferon activated gene 203
F13d	U41805	-0.41	0.2202	0.6549	lymphocyte antigen 84 ligand
F14d	L27990	-1.08	0.5596	0.6549	Sjogren syndrome antigen A1

\* =Gene code given on the Clontech arrays

<sup>1</sup>M= Ratio log<sub>2</sub>(<sup>H</sup>/<sub>N</sub>)

\*\* = Gene code from the gene bank

<sup>2</sup>SD= Standard deviation<sup>3</sup>P value of the one-sample two-sided t-test(H<sub>0</sub>:M=0)

**Table 6** Regulated genes under hypoxia 21 days.

Gne Code*	Gne bankcode**	M <sup>1</sup>	SD <sup>2</sup>	P <sup>3</sup>	Gene
A01d	M62542	-0.85	0.3364	0.5948	CD19 antigen
A01n	S51806	-0.34	0.2504	0.6131	CD44 antigen precursor; phagocytic glycoprotein I (PGP1)
A02j	AF001041	-0.49	0.2842	0.5948	CD83 antigen
A03f	X14951	-0.23	0.2328	0.7299	integrin beta 2 (ITGB2); cell surface adhesion glycoproteins
A03h	M76124	-0.86	0.3143	0.5948	lymphocyte antigen 74 (LY74)
A03m	AJ223765	-0.44	0.2847	0.5956	lymphocyte antigen 94 (LY94); activating receptor 1 (mAR1)
A09b	AF132483	-0.15	0.2349	0.8176	cyclin-dependent kinase 6
A10l	AF013107	-0.74	0.3142	0.5948	a disintegrin & metalloproteinase domain 7 (ADAM7)
A12e	L38281	-0.48	0.2990	0.5948	immunoresponsive gene 1
B10g	X05430	1.39	0.2419	<b>0.0358</b>	Ia-associated invariant chain
B10n	X90582	0.18	0.2857	0.8176	signal sequence receptor delta
B12c	X54691	0.14	0.2836	0.8741	cytochrome c oxidase polypeptide IV (COX4)
B12e	L06465	0.35	0.2405	0.6012	cytochrome c oxidase polypeptide VI a1 (COX6A1)
B12g	U37721	0.28	0.2353	0.6630	cytochrome c oxidase polypeptide VIIIa (COX8A)
B12i	X55771	-0.57	0.2858	0.5948	testis cytochrome c
B12k	AI256292	-0.22	0.2873	0.7788	clone 1889103 (IMAGE Consortium mouse liver cDNA clone)
C02b	M29462	0.52	0.3331	0.5956	soluble malate dehydrogenase
C03k	X70100	0.19	0.2388	0.7788	keratinocyte lipid binding protein
C05m	J02623	-0.18	0.2859	0.8176	soluble glutamate oxaloacetate transaminase 1
C09i	AF036894	0.28	0.2960	0.7450	sphingosine phosphate lyase 1
C14a	U72032	0.54	0.3412	0.5948	eosinophil-associated ribonuclease 1
D01i	U35730	-1.00	0.2899	0.3659	jerky
D04e	L26349	-0.44	0.2850	0.5956	tumor necrosis factor receptor superfamily member 1A
D04f	L12120	-0.57	0.2928	0.5948	interleukin 10 receptor alpha precursor ( IL10R- alpha; IL10RA)
D04g	U53696	-0.33	0.2986	0.6865	interleukin 10 receptor beta ( IL10R- beta; IL10RB)
D05i	Z15119	-0.63	0.2927	0.5948	5-hydroxytryptamine receptor 2C receptor (5HT2C; HTR2C)
D07d	X78936	-0.84	0.2887	0.5768	parathyroid hormone receptor
D07e	D50872	-0.46	0.2852	0.5948	platelet-activating factor receptor
D07m	U26176	-0.72	0.3156	0.5948	somatostatin receptor 4
D08h	X55674	-1.02	0.3836	0.5948	dopamine receptor 2
D08j	U23807	-1.49	0.4639	0.4743	G protein-coupled receptor 7
D09a	U51908	-0.50	0.2921	0.5948	neurotensin receptor 2
D10e	U40811	-0.73	0.2875	0.5948	endothelial differentiation sphingolipid G protein-coupled receptor 1
D10m	M14215	0.57	0.3232	0.5948	low-affinity IgG Fc receptor III (FCGR3)
D11g	U28772	-0.69	0.3363	0.5948	olfactory receptor 10
D11h	X89689	-0.45	0.3021	0.6012	olfactory receptor 24
D12a	AF102520	-0.30	0.2917	0.7278	olfactory receptor B7
D13a	M60909	-0.38	0.2400	0.5948	retinoic acid receptor alpha
D14i	D89080	-1.08	0.3794	0.5768	fibroblast growth factor 10 (FGF10)
E01h	M74181	-0.70	0.3429	0.5948	hepatocyte growth factor-like
E02i	U15209	-0.43	0.2862	0.6012	small inducible cytokine A9
E03e	AF070988	-0.40	0.2903	0.6131	wingless-related MMTV integration site 2b protein (WNT2B)
E05h	M15131	-0.64	0.3139	0.5948	interleukin 1 beta precursor (IL1-beta; IL1B)
E08c	U43187	-0.40	0.2899	0.6131	mitogen-activated protein kinase kinase kinase 3
E09k	U53276	0.48	0.2991	0.5948	protein phosphatase 1 catalytic subunit, gamma isoform
E10d	S53270	-0.36	0.2423	0.6012	cell line NK14 derived transforming oncogene
E11b	U85021	-0.73	0.3143	0.5948	adenylate cyclase 8
E12b	D16301	-0.38	0.2872	0.6174	caltractin; 20-kDa calcium-binding protein
E14k	X74154	-0.40	0.2927	0.6131	cellular retinol-binding protein 2
F03d	D50411	-0.71	0.3400	0.5948	a disintegrin and metalloproteinase domain 12 (ADAM12)
F04c	D38117	-0.38	0.2537	0.5956	calpain 2 (CAPN2)
F04l	AJ000990	0.55	0.3050	0.5948	cysteine protease 1 (PRCS1); preprolegumain; legumain
F05b	M93264	-0.49	0.3022	0.5948	alpha-2-macroglobulin
F07l	AB011678	-0.29	0.2947	0.7371	X-linked doublecortin (DCX; DCN); X-linked lissencephaly protein (LISX)
F08l	AF053235	-0.68	0.3299	0.5948	acidic keratin complex 1 gene 16 (KRT1-16)
F09g	D49733	-0.53	0.2875	0.5948	lamin A
F09j	M26251	-0.41	0.2488	0.5948	vimentin (VIM)
F10e	M57590	-0.54	0.3027	0.5948	fast skeletal troponin C
F13k	U69172	0.10	0.2852	0.9000	palate, lung & nasal epithelium-expressed transcript
F14e	U95114	-0.22	0.2893	0.8020	sperm specific antigen 1
G11	X51703	0.22	0.2351	0.7421	ubiquitin; UBA52; UBB; UBC; UBCEP1
G47	L31609	0.38	0.2459	0.5955	40S ribosomal protein S29 (RPS29)

\* =Gene code given on the Clontech arrays

\*\* = Gene code from the gene bank

<sup>1</sup>M= Ratio  $\log_2(\frac{H}{N})$ <sup>2</sup>SD= Standard deviation<sup>3</sup>P value of the one-sample two-sided t-test( $H_0:M=0$ )

The tables demonstrate that only very few genes expressed a tendency of hypoxia- induced regulation. In addition, a careful look at the log-ratios of these genes that were filtered and

were included in the tables shows that many of them had a log-ratio (M) close to 0, i.e., the observed regulation was only weak.

### 3.4 PCR results

After analysis of the nylon arrays, real-time PCR was performed for confirmation. Genes for PCR analysis were selected using the following criteria:

- Genes listed in Table 5 and Table 6 as described earlier.
- Genes that we found to be hypoxia-dependant regulated in pulmonary vessels or alveolar septa; Cytochrome b-245  $\alpha$  polypeptide (Gene bank code M31775) was found to be hypoxia-regulated in vessels (Fink *et al.*, 2002). We therefore tested it in this work aiming to understand its possible regulation in AM. New data suggested that other genes like CD36 (L23108), Prosaposin (U23740), IL-9RC (M84746),(Kwapiszewska *et al.*, 2005) are hypoxia-regulated in alveolar septum or in lung vessels and were therefore investigated in this work as well.

The results are demonstrated in Figure 7.

#### 1 day

For most of the genes tested, real-time PCR resulted in a variable relative expression. Moreover, only few genes showed the same tendency (up / down) in regulation by PCR and arrays analysis {Cytochrome b245 alpha (M31775), G Protein coupled Receptor 7 (U23807), NADH Ubiquinone oxidoreductase (Y07708), Peptidylprolyl isomerase A (X52803) and Polypyrimidine tract binding protein (X52101)}. Regarding only the last two, the ratios were nearly equal. For all other genes tested, including vimentin (M26251) and integrin  $\beta$ 2 (X14951) that were further investigated by immunohistochemistry, a remarkable difference occurred comparing array and PCR calculated expression change. However, the average regulation factors determined by the real-time PCR results were close to 1 (i.e.  $\Delta\Delta$ CT-values were close to 0), indicating a very weak if any regulation.

21 days

PCR results for the gene expression after 21 days of hypoxia did not differ considerably from those of 1 day in the fact that most expression changes could not be confirmed. Most of the genes investigated showed  $\Delta\Delta\text{CT}$ -values close to 0. The regulation of Cathepsin S precursor (AJ223208), FGF 10 (D89080), CD 36 (L23108), G Protein coupled Receptor 7 (U23807), Peptidylprolyl isomerase A (X52803), Cathepsin K (X94444), Apolipoprotein C II (Z15090) was further supported by the PCR assays.

G Protein coupled Receptor 7 (U23807) was the only gene underlying probably a real hypoxia dependant regulation with a reduction of m-RNA levels after 1 and 21 days of hypoxia.

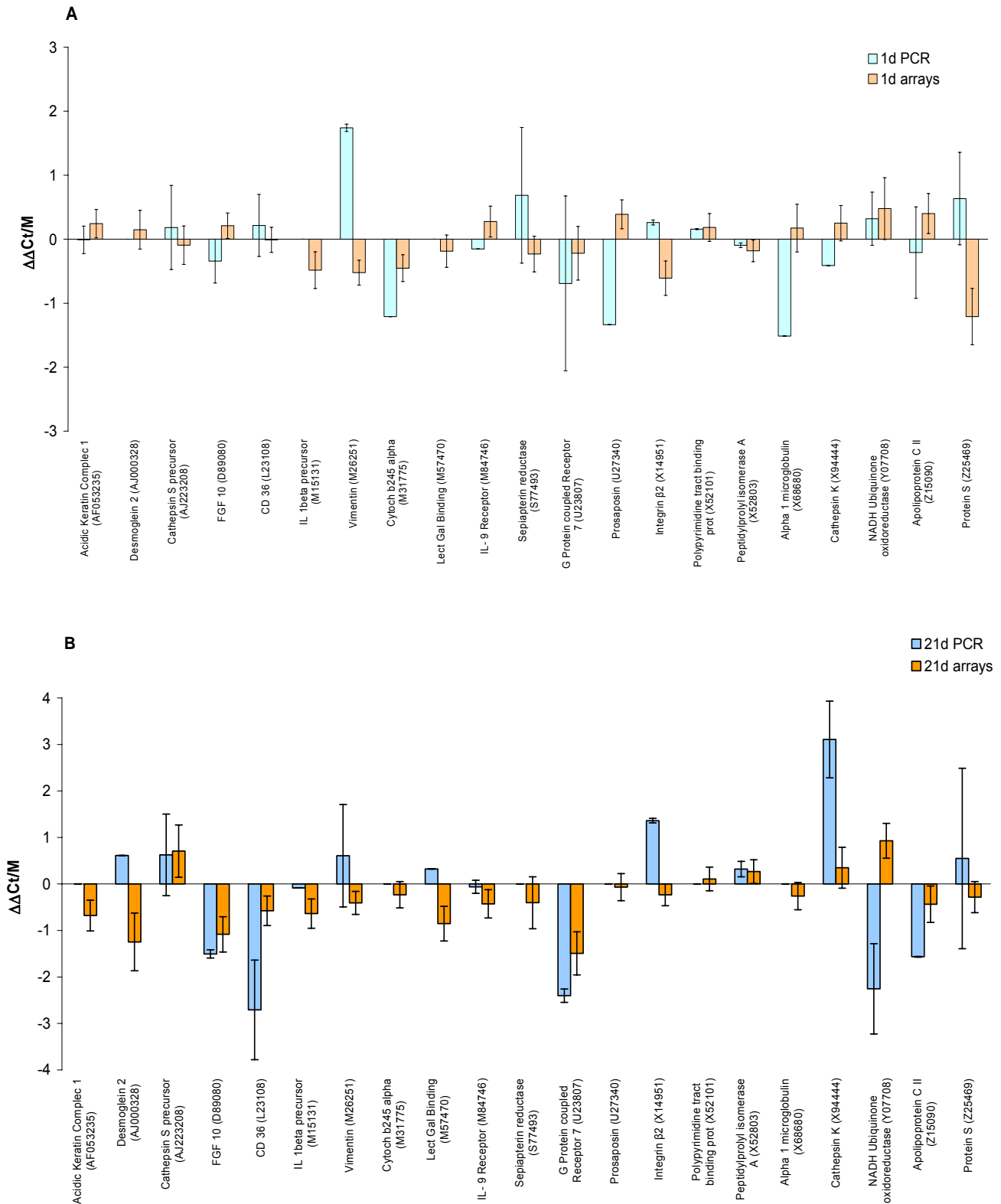
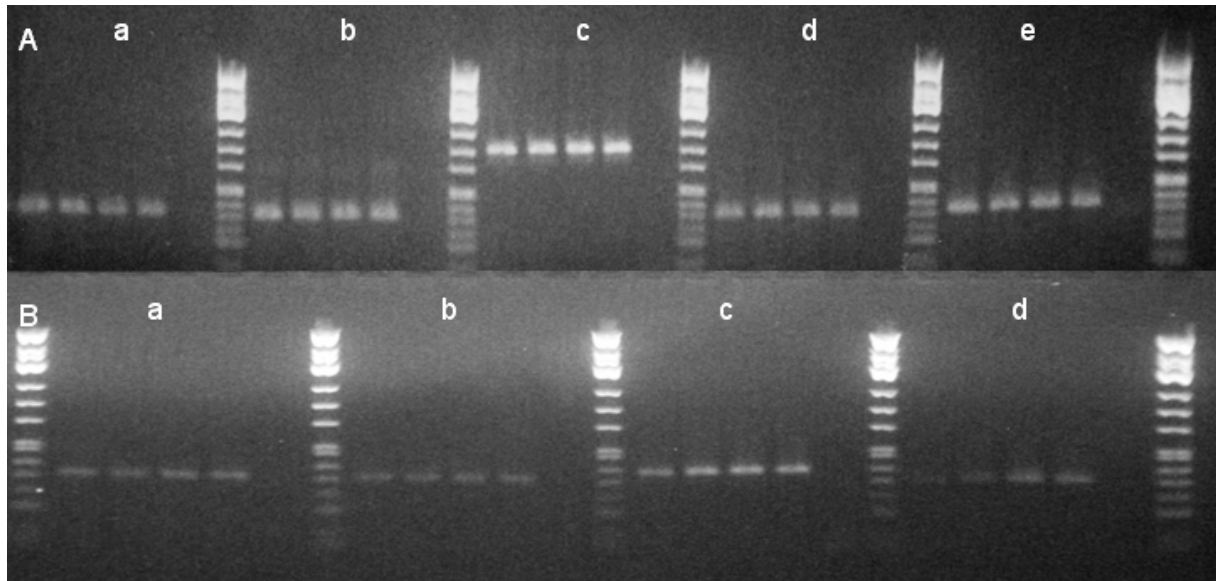


Figure 7

**A Comparison of array and PCR results for A- 1 day, B- 21 days.** On the x axis the genes are listed, on the y axis  $\Delta\Delta Ct = \Delta Ct$  (target gene) -  $\Delta Ct$  (reference/house-keeping gene) or (M) = average  $\log_2$ -ratio calculated for the membranes.



**Figure 8** Gel electrophoresis of selected genes performed after PCR assay (A) 1 day, and (B) 21 days. For each of the genes tested, the 2 most left bands represent the PCR product of normoxia, followed by two PCR products of hypoxia and a negative control. (A)- a.- G protein coupled receptor 7, b. Polypirimidin tract binding protein, c. Acidic keratin complex, d. Sepiapterin reductase e. Prosaposin. (B)-a.-Desmoglein 2, b.- Cathepsin K, c.- IL-9 receptor, d.- Il 1 beta precursore.

Each PCR assay was completed by gel electrophoresis (as described in chapter 2.4.14). For each one of the genes tested with PCR, PCR products of the two hypoxia and normoxia samples and a negative control were carried out, as demonstrated in Figure 8 .

### 3.5 Immunohistochemistry

To measure the protein expression level, immunohistochemistry staining was carried out for vimentin and integrin  $\beta 2$  (as described in chapter 2.4.15). More than 50% of the AM did not show a staining for vimentin /integrin  $\beta 2$  (personal communication Prof. Dr. med. R.M. Bohle, director of the department of pathology, University of the Saarland, Homburg) and were excluded from counting, the total amount of AM (hypoxia/normoxia) was in a comparable range. Figure 9 demonstrates the immunoreactivity of AM stained for vimentin after 1 and 21 days hypoxia.

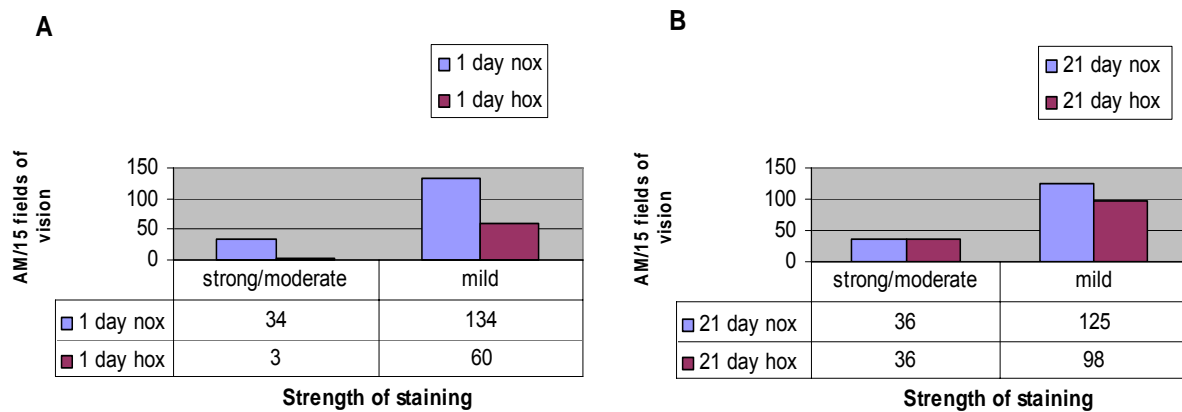


**Figure 9 Immunoreactivity for AM stained for Vimentin.** A- 1day hox/nox, p-value = 0.004 (Fischer's exact test, 2-tailed), B-21 days hox/nox, p-value = 0.414 (Fischer's exact test, 2-tailed).

The influence of acute hypoxia (1day) could clearly be seen as decrease of vimentin on the protein level ( $p=0.004$ ), while the impact of longer term hypoxia (21days) seemed to be weaker and was not significant ( $p=0.414$ ). These findings support the array results rather than the PCR results.

The influence of hypoxia on the expression pattern of integrin  $\beta 2$ , shown in Figure 10 was different than vimentin. On protein level, acute hypoxia led to a reduction of  $\beta 2$  expression in AM ( $p=0.693$ ), and to a significant ( $p=0.032$ ) up-regulation of integrin  $\beta 2$  after 21 days of hypoxia.

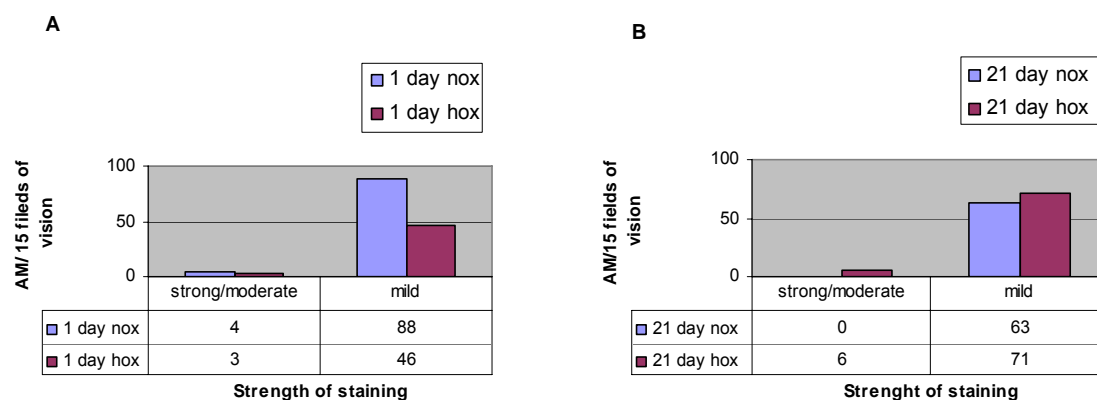


**Figure 10 Immunoreactivity for AM stained for Integrin  $\beta 2$ .** A- 1day hox/nox, p-value = 0.693 (Fischer's exact test, 2-tailed), B-21 days hox/nox, p-value = 0.032 (Fischer's exact test, 2-tailed).

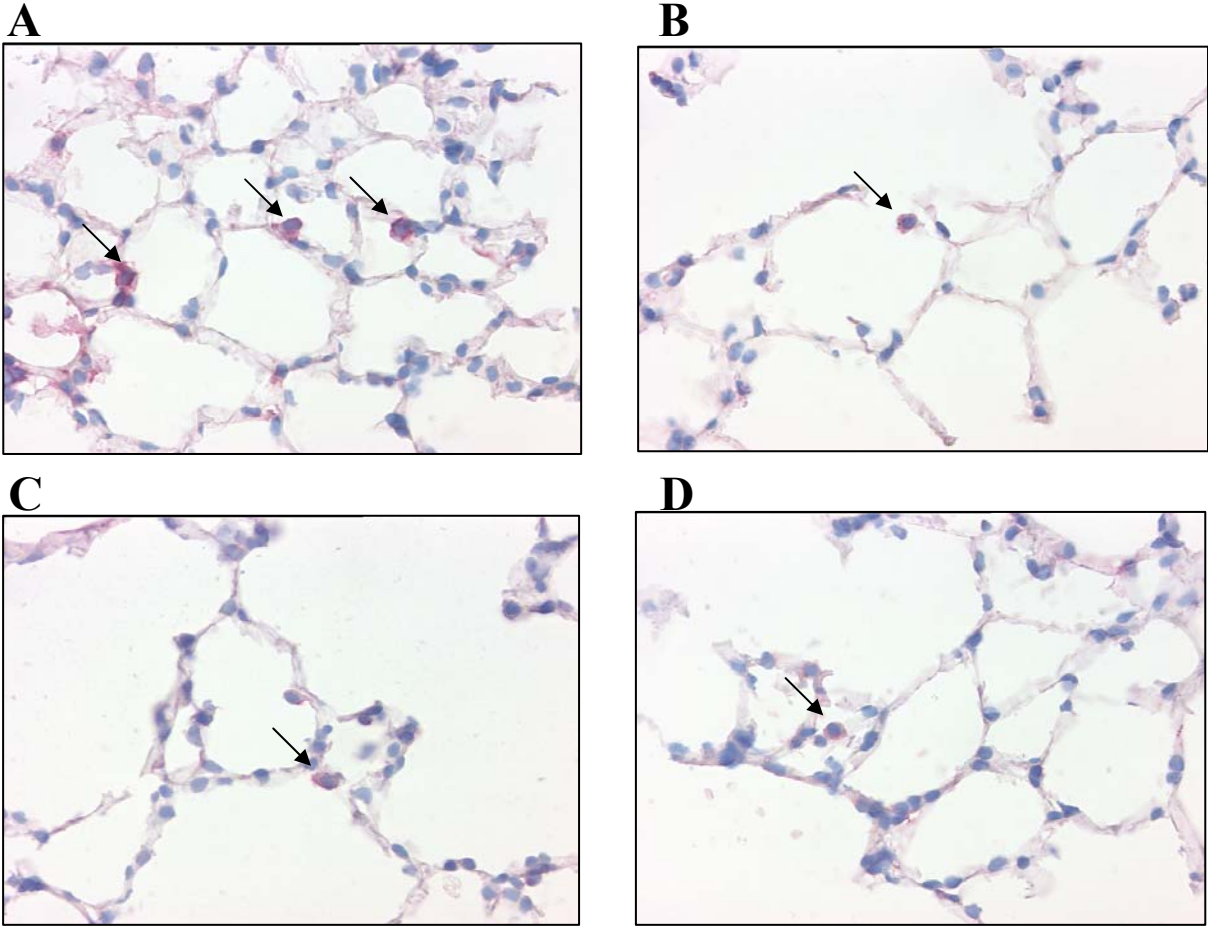


**Figure 11** AM stained for vimentin magnitue x 400 (A-normoxia, B-hypoxia 1day), and integrin (C-normoxia D-hypoxia 1day) as seen under the microscope. Arrows mark the stained AM



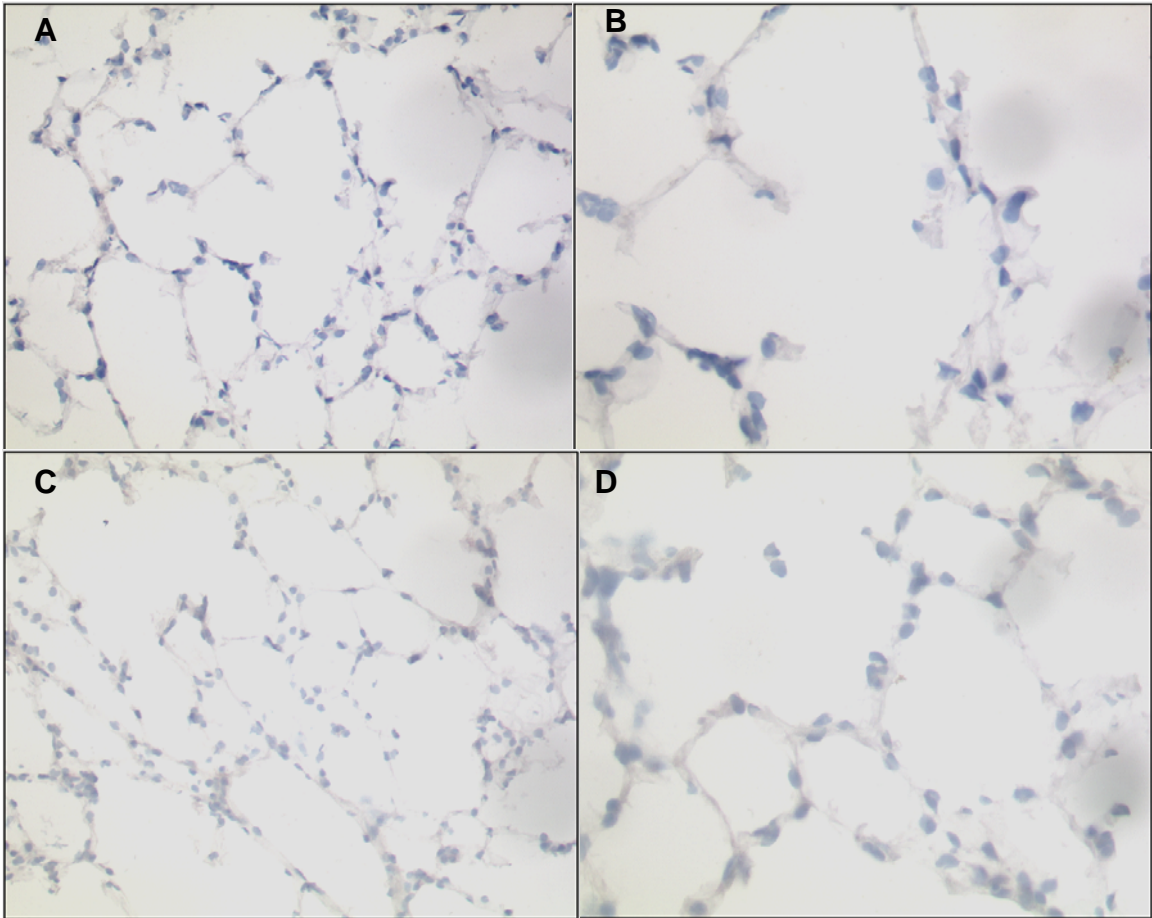


**Figure 12** Negative control of the immunohistochemistry, no use of the primary antibody (A- integrin 1 day magnitude x 200, B- integrin 1 day magnitude x 400, C- vimentin 21 days magnitude x 200 and D-vimentin 21 days magnitude x 400)

## 4 Discussion

### 4.1 Methodical aspects and limitation of the study

The lung is an important target organ for systemic inflammatory mediators released after major trauma and severe infections. Hypoxia is a well studied factor known to mediate lung injury. Most studies investigating the role of hypoxia in initiating pulmonary damage have not solely examined the influence of hypoxia but rather the combination of hypoxia and other factors known to trigger an inflammatory reaction like lipopolysaccharide (Hempel *et al.*, 1994; Hempel *et al.*, 1996; VanOtteren *et al.*, 1995). However, some studies demonstrated that hypoxia can solely induce lung inflammation and secretion of pro-inflammatory mediators (Hirani *et al.*, 2001; Madjdpour *et al.*, 2003). The role of AM in mediating and regulating the inflammatory processes in the lungs is only partially revealed. In fact, AM can phagocyte cells, and be powerful secretors when activated, releasing cytokines that recruit other cells, altering the adhesion and permeability of blood vessels etc.

The aim of this study was to extend the current knowledge about the hypoxia-dependant gene expression in AM. New hypoxia-regulated candidate genes should be identified using the Microarray technology. cDNA arrays are a powerful tool for analysing gene expression or monitoring gene regulation. The nylon membrane based arrays used in this work, the so-called nylon arrays, were proven to be sensitive, reproducible and inexpensive. Since Microarrays are a new and fast developing technique in molecular biology, it is not surprising that nylon arrays have been partly replaced by a new generation of Microarrays using glass carriers. The advantage of glass arrays is the higher spot density (up to 170,000 spots per slide) which allows a comprehensive genome screen at once and therefore a detailed reflection of underlying processes. Furthermore, the use of competitive hybridisation of the fluorophor-labelled RNA- or cDNA sample on one slide and of local background normalisation overcomes the problems of different background levels between two arrays. However, high density glass Microarrays were not available at the beginning of this work. Nevertheless, nylon arrays have proven to be a powerful tool for investigating the expression and regulation of a large number of genes to screen for candidate genes. They can be used as

an efficient filter to point out hypoxia-dependant regulated genes. However, screening many genes at a time will inevitably yield false-positive results. Therefore, results for interesting candidates which should further be analyzed, e.g. by protein analysis or in knock-out/knock-down experiments, need to be validated by an independent experiment. For this purpose, during the last decade quantitative real-time PCR became the standard.

Initially, material for each 10 experiments per time point (1d and 21d hypoxia, including a technical replication = total of 80 membranes or individual hybridisations, respectively) was collected. The data obtained from the arrays turned out to be of insufficient quality. Since the performance of the RT-enzyme supplied by Clontech™ was inadequate, cDNA synthesis resulted in too low amounts of cDNA and poor incorporation of radiolabelled dATP. This in turn led to a weak hybridisation signal and a low signal-to-noise ratio (see Table 5). The high and irregular background observed in many hybridisations is caused by long exposure time and reduction in washing stringency due to the low enzyme performance. The initially obtained results could thus not be used for further analysis and an essential part of the samples was lost before the reason for the bad results was identified. The subsequent application of an enzyme from another supplier (Promega) finally gave usable results (see Table 5). However, the remaining sample size (3 to 5 experiments per time point) was too small to allow the identification of regulated genes by statistical means with adequate power. Accordingly, the statistical analysis for differential expression under hypoxic conditions revealed only a single candidate (Ia-associated invariant chain,  $p=0.0359$ , see chapter 3.2) at the desired level of significance ( $\alpha=0.05$ ). In order to extract as much information as possible, further candidates were selected using only the information about the direction of regulation (see chapter 3.3). The candidates showing a consistent direction in at least three experiments are shown in Table 6 and Table 5.

The differential expression of the selected candidates should be validated by real-time PCR. Although candidates with a more than 2-fold difference in expression between hypoxia and normoxia were expected to be found and to be subsequently validated by real-time PCR, hypoxia turned out to be only a weak stimulus in AM. Most candidates from the hybridisation experiments showed less than 2-fold differences. Such small effects require large sample sizes to yield statistically significant results from quantitative real-time PCR. Unfortunately, there was not enough sample material available to provide enough data for a statistical analysis with adequate power. Additionally, some samples showed very low expression yielding Ct values

that were not useable for a quantitative analysis. Consequently, it is not surprising that the results of the Microarray experiments and the real-time PCR show just a weak correlation.

Additionally, the differential expression of some further genes was analyzed by real-time PCR. Some of these genes were previously investigated by members of our research group that examined the hypoxia dependant gene expression in lung vessels and alveolar septa. A small number of the genes, which seemed to play an important role in the adaptation of lung vessels to hypoxia, were also examined in this work. Examples are CD 36 that was found to be initially upregulated under hypoxia in intrapulmonary arteries while at later time period (21 days) downregulated (Kwapiszewska *et al.*, 2005). Additionally, Prosaposin and Cytochrome b-245  $\alpha$  polypeptide was shown to be regulated by hypoxia in intrapulmonary arteries (Fink *et al.*, 2002). Because of the same reasons as discussed above, the real-time PCR did not provide enough evidence to identify a differential expression of these genes as well. The data do neither allow to conclude that these genes are not regulated in AM, nor that they are regulated. However, this work demonstrates that the sample size must be considerably increased to study hypoxia-dependant gene regulation in AM in future studies.

## 4.2 Genes selected for immunohistochemistry

Only some antibodies (for vimentin and integrin  $\beta$ 2) for performing the immunohistochemistry were available, for all other candidates no antibodies existed at the time of practical work. Therefore, immunohistochemistry was performed only for these two proteins. Following is a literature research summing the current knowledge about them and evidences for hypoxia- dependant regulation.

### 4.2.1 Vimentin

The cytoskeleton of all metazoan cells contains three major filament systems: actin microfilaments (MFs), microtubules (MTs) and intermediate filaments (IFs). The name “intermediate filaments” comes from their diameter (10-12 nm) being intermediate between that of MTs (25 nm) and MFs (7-10 nm). The integrated network formed by the three-filament system is responsible for the mechanical integrity of the cell and is crucially involved in such processes as cell division, motility and plasticity.

IF's subunit proteins have been subdivided into three major groups on the basis of the assembly properties, gene, and sequence structure: the keratins, the neurofilament-like proteins, and the vimentin-related proteins.

At present, IFs are the least characterised structures of the three-filament system. Nevertheless, we can say that they exhibit unique structural features clearly differentiating them from the two other filament systems. First, the elementary “building block” of both MFs and MTs are represented by globular proteins, a monomeric actin and a  $\alpha\beta$ -tubulin heterodimer, respectively. However, the elementary unit of IFs is a very elongated (ca.45 nm) and thin (ca. 2-3 nm) rod-like dimer. The axes of the elementary dimers are aligned approximately parallel to the filament axis, while the filament width is controlled by a specific lateral association of the dimers. Second, both actin MFs and MTs are polar, which allows an active transport of associated motor proteins, such as myosins and kinesins, along these filaments. On the contrary, assembled IFs have no polarity, as individual dimers are oriented in both “up” and “down” directions along the filament. Third, in vivo IFs appear to be the most dynamic of the three filament types. In particular, reversible dissociation –association of IF dimers can occur along the entire filament length and not just at the two ends as in MTs and MFs.

All IF proteins exhibit a characteristic “tripartite” structure (Figure 13), which includes the highly  $\alpha$ -helical, centre domain (the “rod”), and the non-helical “head” and “tail” domains located at either end of the rod domain.

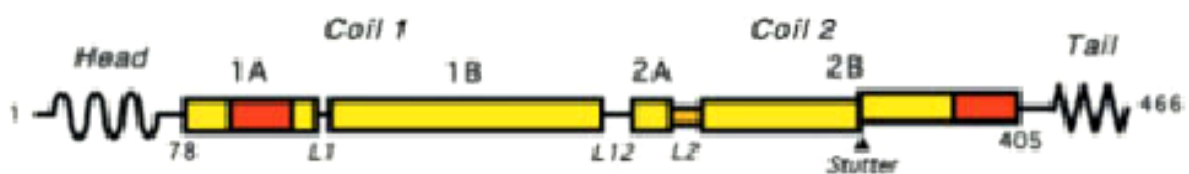


**Figure 13** Schematic diagram of human Vimentin. The central rod domain is predicted to consist of two subdomains, coil 1 and coil 2, that are predicted to be largely  $\alpha$ -helical (rectangles). Two highly conserved regions are darkish highlighted. Taken from (Strelkov SV et al 2003).

Vimentin IFs are expressed in many mesenchymal cell types during development and are the only IFs type found in a variety of cells, including fibroblasts, endothelial cells, macrophages (in particular, multinucleated giant cells), neutrophils, and lymphocytes. Although vimentin

---

IFs are clearly not required for the survival of individual cells (vimentin null or knockout mutations in transgenic mice failed to provide the functional significance of vimentin), at present there is no consensus on the functional role of this IF protein.

#### 4.2.1.1 What are the possibly roles of vimentin?

- ◆ At the cellular level vimentin IF forms associations with other organelles, mostly with other components of the cytoskeleton and membrane adhesions. It was thought, that vimentin would have a significant influence on cell morphology and cytoskeleton organisation. But is it really the case? A work comparing the distribution of cytoplasmic organelles, including microfilaments and microtubules, in cell lines that either contain vimentin or lack any detectable IFs, failed to find any obvious difference that could be associated with vimentin expression (Colucci-Guyon *et al.*, 1994; Sarria *et al.*, 1994). Other works demonstrated a normal microtubules and microfilaments organisation in fibroblasts lacking vimentin. Even when examining the widely accepted assumption that IFs have an important role in protecting cells against physical injury some questions about the role of vimentin are raised. Numerous studies have shown that mutations or lack of IF protein desmin or epidermal keratin leads to an increased fragility of these cells in response to mechanical stress. On the other hand, knockout mutation of other IF proteins (inclusive vimentin) failed to reveal a similar “fragility” phenotype.
- ◆ A number of studies have indicated some interaction between vimentin IFs and chaperone or stress proteins. The organisation of IFs, including vimentin, is affected by conditions, such as heat shock or other agents that elicit a stress response. Hsc70, for example, a member of the large heat shock protein family, seems to co localize with vimentin after cells were exposed to hyperthermia. The functional significance of such interactions remains unclear.
- ◆ When exposed to cytopathic/inflammatory agent (Toxin B from *Clostridium difficile*), human macrophages and monocytes showed a reorganisation of the components building the cytoskeleton; tubulin, actin, vimentin (Siffert *et al.*, 1993). New evidences (Bravo *et al.*, 2003) gives further support to the theory that vimentin is involved in cellular stress reaction; by inducing a renal injury scientists showed a tubulointerstitial

accumulation of macrophages and lymphocytes, and an increase (8 to 20 times) of vimentin, heat shock protein 60 and 70 expression in the renal cortex.

- ◆ An interesting work (Mor-Vaknin *et al.*, 2003) suggests a new role of vimentin in activated macrophages. The work demonstrates that vimentin, which was first phosphorylated at serine and threonine residues by protein kinase c, is secreted from macrophages. These findings are consistent with previous observations showing that phosphorylation of vimentin affects its intracellular localisation and redistribute the cytoskeleton (Ciesielski-Treska *et al.*, 1991; Owen *et al.*, 1996). Moreover, the activation of macrophages with the pro-inflammatory cytokine tumour necrosis factor  $\alpha$  showed to trigger vimentin extracellular secretion and vimentin seemed to be involved in bacterial killing and generation of oxidative metabolites. A lately published paper (Xu *et al.*, 2004) gives some further evidence that vimentin can be secreted into the extra cellular matrix. It was found that the antigen of PAL-E antibody, a marker used for almost 20 years to identify blood and lymph vessels, is a secreted form of vimentin. Its secretion is restricted to a distinct population of blood endothelial cells and activated macrophages, and PAL-E reactive vimentin found in circulating human blood. This secreted form of vimentin seems to be a product of cell-specific posttranslational modification and not to arise from an endothelial cell-specific m-RNA.

Taken together, there are some evidences that vimentin is involved, alone or via interactions with other proteins in the cellular response to stress factors like heat or inflammation; it can also be secreted by some cells including macrophages. Further studies are needed to evaluate the significance of these findings.

A totally different perspective to the function of vimentin in macrophages is demonstrated in works investigating atherosclerotic lesions (Heidenthal *et al.*, 2000; Muller *et al.*, 2001). A membrane protein on the cell surface of macrophages, binding oxidised and acetylated but not native LDL, was identified as vimentin. Only oxidised LDL, but not native or acetylated LDL, induced apoptosis of human macrophages, a process involving the cleavage of vimentin into fragments of 48-50, 46, 29 and 26 kDa. Although it is yet too early to be able to evaluate these phenomena, vimentin may play a role in membrane-associated steps involved in the intracellular processing of modified

LDL, contributing to its unregulated uptake and intracellular retention by cells of the atherogenic plaque.

Antibodies directed to the Sa antigen are highly specific for rheumatoid arthritis (RA) and can be detected in approximately 40% of RA sera. It was just recently discovered (Vossenaar *et al.*, 2004), that Sa antigen is citrullinated vimentin (which means that some of its arginine residues are deiminated to citrulline residues). This modification of vimentin has also been described as occurring in dying macrophage (Asaga *et al.*, 1998; Vossenaar *et al.*, 2004). It is known that citrullination of the amino terminal head domain by peptidylarginine deiminase induces disassembly of the vimentin filaments *in vitro*. Therefore, citrullination may be involved in the disassembly of the vimentin cytoskeleton during cell death, when the network of vimentin filaments collapses into perinuclear aggregates. Taken together, this new information makes citrullinated vimentin an interesting candidate autoantigen in RA and may provide new insights into the potential role of citrullinated synovial antigens and the antibodies directed to them in the pathophysiology of RA.

#### **4.2.1.2 Vimentin and hypoxia**

A fascinating study (Krishnamachary *et al.*, 2003) demonstrated an influence of hypoxia and hypoxia inducible factor-1 (HIF-1) on the m-RNA levels of vimentin in human colon carcinoma cells. The study showed that hypoxia or HIF-1 overexpression stimulates invasion by human colon carcinoma cells, whereas a small interfering RNA directed against HIF-1 could inhibit this process. They also revealed that HIF-1 regulates the expression of genes encoding cathepsin D, fibronectin1, some keratins, vimentin and some other proteins, all playing a role in the pathophysiology of tumour invasion. Reprogramming of IFs expression (due to intratumoural hypoxia or HIF-1 activity) leads to the production of vimentin, which either alone or in combination with specific keratins, promotes tumour cell invasion. Similar findings are described by (Luo *et al.*, 2006) regarding human prostate cancer cells. It was shown that over-expression of HIF-1 stimulates the invasion potency of these cells and that vimentin expression is HIF-1 regulated. Our findings regarding the hypoxia induced regulation of vimentin m-RNA und protein are not supported by the studies listed above. Evidences suggesting that the regulation of vimentin is stress-dependant, and that such stress may lead to a reorganisation of intracellular structures including cytoskeleton and vimentin



filaments are also favouring our data, because hypoxia must be seen a form of cellular stress. In which way the regulation of vimentin in AM under hypoxia is involved in lung damage or in the attempt of the organism to cope with it, is still not clear, just like the question whether it can also initiate the secretion of vimentin from AM into the extracellular matrix (as described in some of the works). Our data indicates a suppression of vimentin m-RNA and protein by a lack of oxygen. The papers dealing with the induction of vimentin through HIF-1 are suggestive of a mechanism leading to an up-regulation of this gene. Although it may seem to be a contradiction, it does not necessarily have to be one since the records implicating HIF-1 regulation of vimentin were made in tumour cells. Further studies taking a closer look at the regulation in non-tumour cells need to evaluate the exact mechanism in which hypoxia influences vimentin.

#### **4.2.2 Integrin $\beta$ 2**

Integrins are a large family of surface receptors that are localised on the plasma membrane and share common features in molecular structure and functions. Integrins are involved in cell interactions with extracellular matrix glycoproteins (collagen, fibronectin, laminin etc.). Some integrins are also involved in intercellular interactions (via binding to counter-receptors on other cells). In their capacity as adhesions receptors that organise the cytoskeleton, integrins play an important role in controlling various steps in the signalling pathways that regulate processes as diverse as proliferation, differentiation, apoptosis, and cell migration.

All integrins share certain structural resemblance. Each receptor is a heterodimer consisting of one  $\alpha$ - and one  $\beta$ -subunit (Figure 14). Each subunit is an integral transmembrane polypeptide that contains three domains: glycosilated extracellular domain (which consists of more than 90% of the whole molecule), hydrophobic transmembrane domain (responsible for membrane anchoring) and endo- (or cytoplasmatic) domain, localised in the cytoplasm.

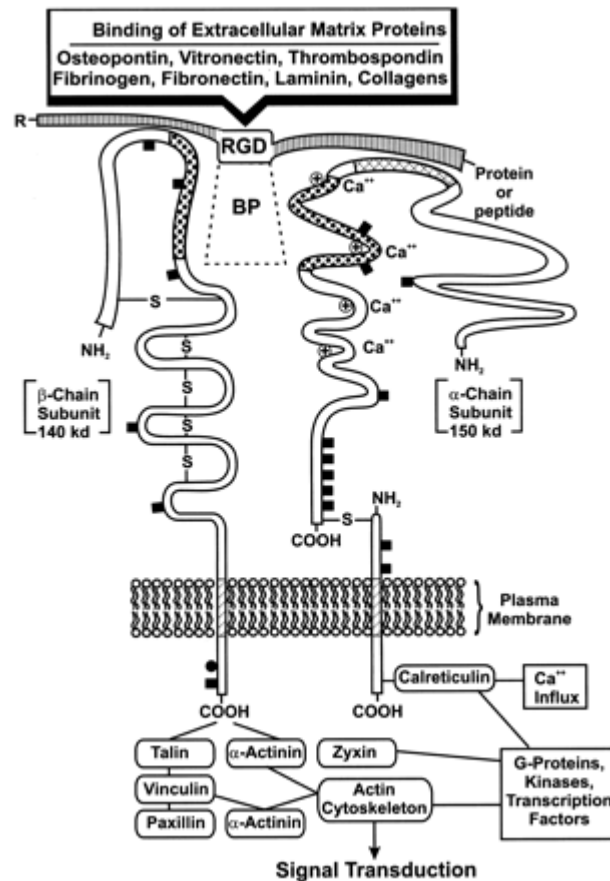


**Figure 14** A diagrammatic representation of a universal integrin receptor heterocomplex. The  $\alpha$ - and  $\beta$ -chains are displayed as noncovalently linked parallel subunits with insertions through the cell membrane. The long extracellular domains of both chains are contrasted with their short intracytoplasmic subunit chains. The binding pocket (BP) is depicted as the stippled portion of the opposing sides of both the  $\alpha$ - and  $\beta$ -chains. The various extracellular matrix protein ligands are contained within the rectangular box at the top of the diagram. An RGD-containing peptide (adhesion inhibitor) is interposed between the ligand and the Integrin binding site. Taken from (van der Flier *et al.*, 2001).

Analysis of the human genome suggests the possibility of existence of 24 $\alpha$  – and 9 $\beta$  –integrin subunits. At the present time, 18 $\alpha$  and 8 $\beta$  subunits forming 24 heterodimers have been recognised. In most cases, only one or a few  $\alpha$ – subunits may bind certain  $\beta$ –subunits and these  $\alpha$ –subunits do not form dimer(s) with other  $\beta$  –subunits.

This feature of integrin dimer formation underlines integrin subdivisions into separate  $\beta$  – subfamilies. Table 7 shows that  $\beta$ 1 and  $\beta$ 2 –subfamilies consist of 12 and four members, respectively.

Most integrins do not exhibit unique ligand specificity. Usually, each matrix protein may bind to several receptors and each integrin shows affinity to several of these proteins. It is hard to interpret the multiple ligand specificity of the integrin family. Whether integrins should be considered only as “anchors” responsible for cell adhesion to the matrix substrate is still not clear. The development of the theory that integrins are components of cell signalling well explains this phenomenon. Certain evidence exists that integrin receptors exhibit common ligand specificity may transduce various intracellular signals controlling physiological reactions.

**Table 7 Integrins and their ligands.** Please notice that only some of the integrins known today are displayed here. Taken from (Berman *et al.*, 2003).

Integrins		Ligands
$\beta$ subunit	$\alpha$ subunit	
$\beta 1$	$\alpha 1$	Native collagene, Laminin
	$\alpha 2$	Native collagen, Laminin
	$\alpha 3$	Native collagen, Laminin, Fibronectin
	$\alpha 4$	Fibronectin (splicing domain)
	$\alpha 5$	Fibronectin (RGD-containing domain)
	$\alpha 6$	Laminin
	$\alpha 7$	Laminin
	$\alpha 8$	Fibronectin, Vitronectin
	$\alpha 9$	Tenascin
	$\alpha 10$	Collagene
	$\alpha 11$	Collagene
$\beta 2$	$\alpha v$	Vitronectin, Fibronectin, Osteoponin
	$\alpha L$	ICAM-1, ICAM-2, ICAM-3
	$\alpha M$	ICAM-1, VCAM-1, Fibrinogene, C3b
	$\alpha X$	C3b
	$\alpha D$	ICAM-3, VCAM-1

The signal function of integrins can be defined as their ability to mediate the influence of extracellular matrix on intracellular processes modifying cell behaviour. This influence is mutual and intracellular biochemical reactions, which employ integrins as substrate, modify their conformation and, consequently, cell interaction with matrix. Thus, two pathways of signal transduction are generally recognised: *outside- in and inside- out*.

The mechanism in which integrins are being activated is crucial to their function and should be therefore shortly discussed. This is mostly important on leukocytes, where integrins play a key role in binding of leukocytes to epithelial cells, as the first step on their way from the blood vessels to the periphery, due to cellular damage, inflammation etc.

Integrins expressed on leukocytes, such as LFA-1 (leukocytes function-associated antigen-1) = (CD11a/CD18), are usually in inactive state, ensuring that these cells do not bind inappropriately to their ligands. Two mechanisms have been proposed to explain how leukocytes bind their ligand. First, the integrin can undergo conformational change that increases affinity of individual integrins to their ligands. It has been demonstrated, that the so called  $\alpha I$  domain (half of all integrins  $\alpha$ - subunits contain an additional, “inserted” (I) domain, which is a nucleotide binding fold with a metal binding site), serves as the principal ligand-binding site for those integrins that possess it. When  $\alpha I$  domain- containing integrins is activated, the conformation of this domain is altered, to expose or alter ligand-binding sites. Second, stimulation of leukocytes causes clustering of integrins, resulting in increased avidity (regardless of affinity status) providing stronger adhesion at sites of cell-cell contact. The clustered form of LFA-1 was shown to be essential for adhesion to ICAM-1. The exact mechanism of clustering remains to be fully clarified, but agents, which disrupts the cytoskeleton, affect clustering, indicating that cytoskeletal reorganisation is involved (Ross *et al.*, 1992). Thus, the nonactive integrin is restrained by the cytoskeleton and an activating agonist causes release of the cytoskeleton tether, which in turn, leads to integrin mobility on the cell membrane and clustering.

One of the most important features of leukocytes is their ability to adhere to other cells or to the extracellular matrix. For that purpose, they utilize members of three major groups of adhesion molecules, namely integrins, selectins, and members of the immunoglobulin superfamily. From the currently 8 known  $\beta$  integrin subunits, only  $\beta 2$  and  $\beta 7$  are expressed exclusively on leukocytes. Integrin  $\beta 2$  seems to be an important player in the process enabling leukocytes (particularly Polymorphonuclear leukocytes= [PMN]) to leave the intravascular lumen and migrate towards the apical epithelial membrane. This occurs in three sequential stages-

1. Adhesions: of PMNs to the endothelial cells in the intravascular lumen,
2. Migration: transendothelial migration of PMNs across the epithelia,
3. Post migration: after migration PMNs reach the lumen and contact the apical epithelial membrane. The initial step, which consists of firm adhesion of PMNs to the basolateral epithelial membrane, appears to be mediated exclusively by the leukocyte integrin  $\beta 2$  (CD11b/CD18). It was demonstrated, for example, that by adding integrin  $\beta 2$  (CD11b/CD18) monoclonal antibodies, ca. 90% of in vitro PMNs- migration across intestinal epithelial monolayers could be blocked. The epithelial

expressed basolaterally ligand for  $\beta 2$  (CD11b/CD18) that mediates PMN adhesion during early stages of migration has to be yet identified (might include multiple fucosylated proteoglycan(s)). ICAM-1, the best-characterized cellular ligand for (CD11b/CD18) is normally not expressed on intestinal epithelia, and as its expression is induced it is up regulated on the apical rather than basolateral surface. However, it might be different in the airways, where epithelia can have more flattened morphology and up regulation of ICAM-1 expression is localised at the apical region of the cell boundaries (Taguchi *et al.*, 1998). Moreover, ICAM-1 expression is strongly induced by viral infections of airway epithelial cells (Wegner *et al.*, 1990) in a NF- $\kappa$ B-dependant fashion, so that ICAM-1 may play a role in PMN transepithelial migration in the lungs (Jahn *et al.*, 2000).

During the second phase, the transepithelial migration of PMNs, integrin  $\beta 2$  does not appear to take part.

Finally, after migrating PMNs reach the apical epithelial plasma membrane, they may destroy luminal pathogens. But how do PMNs retained at the apical epithelial surface? Leukocyte receptors, such as ICAM-1 on the apical surface (that are markedly up regulated under inflammatory conditions and after microbial infection), would be accessible as a ligand for integrin  $\beta 2$  (CD 11b/CD 18). Under these conditions, ICAM-1 might serve as a foothold for PMNs and macrophages on the luminal surface, serving to retain them in the site of inflammation.

#### **4.2.2.1 The important role of integrin $\beta 2$ in disease**

The medical importance of leukocyte integrins is most evident from the clinical condition known as leukocyte adhesion deficiency type 1 (LAD-1), a life threatening condition, in which a mutation is found in the common CD18 polypeptide. LAD is characterized by the inability of leukocytes, in particular neutrophilic granulocytes, to emigrate from the bloodstream towards sites of inflammation. Infectious foci are nonpurulent and may eventually become necrotic because of abnormal wound healing. When the  $\beta 2$  integrins (CD11/CD18) expression on leukocytes is completely absent, patients often die within the first year. However, low levels of  $\beta 2$  expressions may result in a milder clinical picture of recurrent infection, which offers a better prognosis.

#### 4.2.2.2 Integrin $\beta 2$ and alveolar macrophages

A number of works investigating the influence of smoking on alveolar macrophages (AM), and the expression of their surface adhesion molecules (CD11/CD18), revealed some interesting findings. Hoogsteden *et al.* demonstrated increased numbers of macrophages in bronchoalveolar lavage (BAL) of smokers (compared with those of healthy, non smoker individuals), which is probably the effect of increased recruitment of blood monocytes to the alveoli (Hoogsteden *et al.*, 1991). Schaberg *et al.* also showed that BAL of smoker individuals contain more AM, and that more AM (from smokers) express (CD11/CD18) adhesion molecules (Schaberg *et al.*, 1992), suggesting a role for these molecules in the “fight” of AM against exogenous agents causing lung damage (like smoking). AM adhesion molecules and their ligands seem to be also involved in other diseases affecting the lungs. Striz *et al.* demonstrated a higher expression of the  $\alpha$  chain (CD11b) and of ICAM-1 (a ligand of the CD11/CD18 family), on AM in active pulmonary sarcoidosis, compared with their expression in inactive form of the disease or with AM from healthy probands (Striz *et al.*, 1992).

Laundahl *et al.* were also interested to find how the activation of AM influences the expression of their CD 11b/CD 18 complexes (Lundahl *et al.*, 1996). They first compared the expression of these molecules on resting AM and blood monocytes (BMs), and demonstrated a higher expression of CD 11b/CD 18 on AM (although no significant difference of the adhesion of the two cell population was demonstrated). After cells were activated (using N-formyl-methionyl-leucyl-phenylalanine or phorbol-12-myristate-13-acetate and ionomycin) a significantly higher surface expression of CD 11b/CD 18 on BMs but not on AM was detected. The cellular adherence of BMs, but not AM, increased after activation. These findings might be interpreted as a mechanism supporting the accumulation and recruitment of leucocytes into an affected organ through a higher expression of adhesion molecules on BMs supporting their migration from the blood vessels to the periphery.

Other works dealing with the function of AM in host defence and inflammatory response further reveal the task of adhesion molecules. Albert *et al.* looked into the expression of the different CD11/CD18 family members in primates (Albert *et al.*, 1992). They established that AM constitutively express predominantly CD11a/CD18 (=LFA-1) surface antigens and mRNA. Concerning the function of integrins in activated AM, they demonstrated that AM chemotaxis was markedly inhibited by a monoclonal antibody to CD18, and adhesion of AMs to an alveolar epithelial cell monolayer is partly but not completely dependant on the  $\beta 2$

integrins (CD18). Milne et al. further confirmed the role of CD18 in the recruitment of leukocytes to the airways (Milne *et al.*, 1994). Using antibodies against CD 18, they decreased the number of eosinophiles in BAL from Guinea pigs exposed to an agent causing airway eosinophilia and bronchial hyperresponsiveness. Another work (Paine *et al.*, 2002) also demonstrated the importance of the adhesion molecules for the mobility of AM and their phagocytic activity in the alveoli. The authors showed a significantly reduced phagocytic activity of AM in ICAM-1 deficient mice compared to the control, or when alveolar epithelial cells were treated with a neutralizing anti-ICAM-1 antibody. The study indicates that ICAM-1 on the AEC surface promotes mobility of AM in the alveoli and is crucial for the efficient phagocytosis of particles by AM. ICAM-1 is an important ligand of the CD11/CD18 integrin receptor and this study further demonstrates the significant role of adhesion molecules in inflammatory response carried out by AM.

In recent years it has become apparent that adhesion pathways not only provide a mechanism for translocation of leukocytes from blood to the inflammatory sites but also participate in intracellular signalling of leukocytes, which can result in cytokine production. Schmal et al. demonstrated the binding interaction between AM and soluble ICAM-1, which resulted in generation of two major inflammatory cytokines- Tumour Necrosis Factor- $\alpha$  (TNF- $\alpha$ ) and the chemokine Macrophages Inflammatory Protein-2 (MIP-2) (Schmal *et al.*, 1998). Both the binding interactions and the cytokines production appear to be CD 18 dependant. Mulligan et al. had similar results and proved a neutrophil accumulation, which is also  $\beta$ 2 integrin-dependant (Mulligan *et al.*, 1992). Furthermore, the generation of these two cytokines is Nuclear Factor- $\kappa$ B (NF- $\kappa$ B) dependant (the promoter region of both MIP-2 and TNF- $\alpha$  contain a consensus motif for NF- $\kappa$ B) (Schmal *et al.*, 1998). NF- $\kappa$ B is known to play a major role in AM mediated lung injury. On the other hand, one should also consider that the cytotoxicity of AM is not exclusively CD 18 dependant; Hirano et al. validated a lipopolysaccharide (LPS) - dependant activation of AM (Hirano, 1998). But stimulated AM generate NO (which mediates the tumouricidal activity of activated macrophages) in a CD- 18 independant way (Jungi *et al.*, 1997).

#### 4.2.2.3 Integrin $\beta$ 2 und hypoxia

Inflammatory responses are associated with significant changes in tissue metabolism. In particular, metabolic shifting during inflammation can results in significant tissue hypoxia.

The following association motivated scientists to look whether the function of leukocytes, and their expression of adhesion molecules is hypoxia induced. This mechanism was investigated by (Kong *et al.*, 2004). The exposure of the promonocytic cell line U937 to hypoxia resulted in increased adhesion to activated endothelium, in a CD18 dependant manner. Comparable results regarding hypoxia- treated PMN were also described by ((Montoya *et al.*, 1997). Using real-time PCR an elevation of CD18 mRNA under hypoxia was also demonstrated, as well as elevated CD18 protein expression (Scannell *et al.*, 1995). In addition, the first group also identified a binding site for HIF-1 in the CD18 gene. In this way a mechanism of recruiting leukocytes to a site of inflammation/ hypoxia was revealed: hypoxia as a stress factor can regulate the expression of adhesion molecules on leukocytes, thus supporting their migration from the vessels towards this site. Again, hypoxia proves to have a very similar effect to that of inflammation. This data was partly supported by our findings; on the protein level a significant hypoxia-dependant up-regulation of integrin  $\beta 2$  was demonstrated after a long period (21 days), but not for 1 day hypoxia or for the changes on the mRNA level.

### 4.2.3 CD 74 antigen

CD 74 antigen (invariant polypeptide of major histocompatibility complex, class II antigen-associated /Gene bank code X05430) was the only gene that demonstrated a statistically significant ( $p=0.0359$ ) hypoxia induced regulation in the arrays analysis for 21 days (Table 6) and was also included in the analysis for 1 day (Table 5). For that reason it should be shortly mentioned.

CD 74 is a nonpolymorphic type II integral membrane protein; it has a short N-terminal cytoplasmic tail of 28 amino acids, followed by a single 24 amino acids transmembrane region and an approximately 150 amino acids luminal domain. Surface expression of newly synthesized CD 74 followed by rapid internalisation to the endosomal pathway. CD 74 remains on the cell-surface for a very short time. The surface half -life of CD 74 was calculated to be fewer than 10 minutes.

CD 74 was thought to mainly function as an MHC class II chaperone, which promotes endoplasmic reticulum (ER) exit of MHC class II molecules, directing them to the endocytic compartments, preventing peptide binding in the ER, and contributes to peptide editing in the MHC class II compartment (Stumptner-Cuvelette *et al.*, 2002). However, CD 74 was lately shown to have a role as an accessory- signaling molecule. CD 74 was reported to be a high



affinity binding protein for the proinflammatory cytokine macrophage migration inhibitory factor (MIF), providing evidence for a role in signal transduction pathways. Moreover, helicobacter pylori was recently shown to bind to CD 74 on gastric epithelial cells and to stimulate interleukin 8 production (Beswick *et al.*, 2005). CD 74 also regulates the B-Cell differentiation by inducing a pathway leading to the activation of transcription mediated by the NF- $\kappa$ B p65/REIA homodimer and its coactivator, TAF<sub>II</sub> 105 in CD 74-transfected 293 cells and in B-Cells.

Starlets and coworkers have demonstrated a CD 74 induced signal cascade resulting in NF- $\kappa$ B activation, entry of the stimulated cells into the S phase, elevation of DNA synthesis, cell division and augmented expression of BCCL-X<sub>L</sub>, thus showing that CD 74 functions as a survival receptor (Lantner *et al.*, 2007; Starlets *et al.*, 2006)

The results of the arrays analysis in this study suggest a hypoxia dependant regulation of this gene (a current literature search could not provide further evidence for this finding). Nevertheless, a further investigation is necessary using a larger number of samples so a statistically significant result can be made for 1 and not only for 21 days. Moreover, a real-time PCR diagnosis (which was not performed in this study because of the lack of primers) should be performed to verify the array results. Future studies could perhaps confirm if a CD 74 mediated activation of NF- $\kappa$ B exists also under hypoxia as it was demonstrated in the above mentioned works.

## 5 Summary

The lung is an organ continuously exposed to infectious or non-infectious inflammatory stimuli. Hypoxia turned out to be a trigger of inflammatory reaction solely or in concert with other stimuli. Therefore, effective defence mechanisms are necessary for a successful confrontation with and repair of inflammation-mediated damages.

AM are key players in the cellular arm of the immune system assisting the lung in fighting inflammation-mediated damage. Not only their direct effect of phagocytosis makes AM indispensable, but rather their ability to initiate an appropriate reaction by the secretion of many mediators, thus recruiting more AM and other player important for an efficient and fast response.

To increase current knowledge about the genes involved in the hypoxia mediated- activation of AM, three well established techniques were applied; 1. Microarrays to screen hypoxia-regulated genes, 2. real-time PCR for confirmation of array results and 3. immunohistochemistry to reveal the hypoxia- initiated changes on the protein level.

Although nylon arrays have proven to be highly sensitive and reproducible, technical problems disallowed the identification of regulated genes by statistical means (as only a small number of samples could be used for analysis). Therefore, an alternative way for screening was used to extract as much information as possible from the remaining samples.

Since hypoxia turned out to be a weak stimulus for gene expression in AM, most candidates selected via arrays for further validation using PCR, showed less than 2-fold differences. To demonstrate such a minor effect, large sample sizes would be required; due to practical reasons, this that was not available. Consequently, the results of the Microarrays and the PCR showed only a low degree of correlation.

On the protein level, acute hypoxia (1 day) initiated a statistically significant reduction of vimentin expression in AM and a tendency of reduction after 21 days of hypoxia. Further studies will be necessary to evaluate the effects demonstrated in this work, since current information regarding the hypoxia- dependant regulation of vimentin (mediated via HIF-1) was detected in tumour cells.

As for integrin  $\beta$ 2, its HIF-1- mediated, hypoxia- dependant up-regulation to enhance the recruitment of leukocytes to the site of inflammation was demonstrated before. This finding

was supported by our immunohistochemistry results after long-term, but not after acute hypoxia.

The data collected in this study did not allow to conclude (by statistical means) whether the genes tested are hypoxia-regulated or not. Future studies should rely on a larger sample sizes to answer this question.

## 6 Zusammenfassung

Die Lunge ist permanent infektiösen und nicht- infektiösen entzündlichen Stimuli ausgesetzt. Es hat sich herausgestellt, dass auch Hypoxie- allein oder gemeinsam mit anderen Stimulatoren- eine solche entzündliche Reaktion hervorzurufen vermag. Um entstandene Schäden erfolgreich reparieren zu können, sind effektive Abwehrmechanismen erforderlich.

AM als zellulärer Arm des Immunsystems unterstützen die Lunge in entscheidender Weise bei der Bekämpfung dieser Entzündungsreize. Nicht nur ihre Fähigkeit zur Phagozytose macht sie unverzichtbar, sondern vielmehr ihre indirekte Beteiligung an vielerlei Prozessen durch die Sekretion zahlreicher Mediatoren, die durch Rekrutierung anderer AM und weiterer wichtiger Komponenten zu einer schnellen und effizienten Reaktion führt.

Ziel dieser Arbeit war es, den jetzigen Wissensstand über die an der Hypoxie-induzierten Aktivierung der AM beteiligten Gene zu vergrößern. Drei bewährte Methoden wurden hierfür eingesetzt: 1. Microarrays, um Hypoxie-induzierte Gene zu filtern, 2. real-time PCR zur Validierung der Arrays Ergebnisse 3. Immunhistochemische Färbung um die Hypoxie-induzierte Veränderung auf Proteinebene aufzudecken.

Obwohl sich Nylonarrays in ihrer Anwendung bewährt haben und reproduzierbare Ergebnisse liefern, haben in dieser Studie technische Probleme die statistisch signifikante Identifikation potentiell regulierter Gene unmöglich gemacht. Um möglichst viele Informationen aus den erhaltenen Daten zu gewinnen, mußte hier ein anderer Weg für die Selektion von Kandidatengenomen beschränkt werden.

Da sich Hypoxie als ein schwacher Stimulus für die Genexpression in AM erwiesen hat, zeigten die meisten (anhand der Arrays ausgewählten) Kandidaten eine Regulation um weniger als Faktor 2. Um solche geringen Effekte mittels PCR bestätigen zu können, wäre eine größere Proben-Anzahl erforderlich gewesen. So ließ sich in der vorliegende Studie nur eine schwache Korrelation zwischen den Array- und PCR- Ergebnissen zeigen.

Auf Proteinebene konnte unter akuter Hypoxie (1 Tag) eine statistische signifikante Reduktion der Vimentin- Expression nachgewiesen werden, welche auch tendenziell unter chronischer Hypoxie noch vorlag (wenn auch nicht statistisch signifikant). Weitere Studien sind erforderlich, um die hier mittels immunhistochemischer Färbung gezeigten Effekte zu verifizieren, da aktuelle Studien eine andere-, HIF-1 vermittelte Regulation des Vimentins in

Tumorzellen nachgewiesen haben. Für Integrin  $\beta 2$  wurde eine HIF-1- vermittelte, Hypoxie-abhängige gesteigerte Leukozyten-Rekrutierung zum Entzündungsfokus jüngst publiziert. Die vorliegende Studie unterstützt dieses Ergebnis zumindest für die chronische Hypoxie-Exposition.

Die in dieser Arbeit erhobene Daten, erlauben keine statistisch gefestigten Aussagen hinsichtlich der potentiellen Hypoxie-bedingten Regulation der hier untersuchten Gene. Künftige Studien sollten daher auf einer größeren Probenanzahl basieren.

---

## 7 References

- Albert, R. K., Embree, L. J., McFeely, J. E. & Hickstein, D. D. (1992). Expression and function of beta 2 integrins on alveolar macrophages from human and nonhuman primates. *Am J Respir Cell Mol Biol*, **7**(2), 182-9.
- Archer, S. L., Reeve, H. L., Michelakis, E., Puttagunta, L., Waite, R., Nelson, D. P., Dinauer, M. C. & Weir, E. K. (1999). O<sub>2</sub> sensing is preserved in mice lacking the gp91 phox subunit of NADPH oxidase. *Proc Natl Acad Sci U S A*, **96**(14), 7944-9.
- Asaga, H., Yamada, M. & Senshu, T. (1998). Selective deimination of vimentin in calcium ionophore-induced apoptosis of mouse peritoneal macrophages. *Biochem Biophys Res Commun*, **243**(3), 641-6.
- Beck-Schimmer, B., Schimmer, R. C., Madjdpour, C., Bonvini, J. M., Pasch, T. & Ward, P. A. (2001). Hypoxia mediates increased neutrophil and macrophage adhesiveness to alveolar epithelial cells. *Am J Respir Cell Mol Biol*, **25**(6), 780-7.
- Berman, A. E., Kozlova, N. I. & Morozevich, G. E. (2003). Integrins: structure and signaling. *Biochemistry (Mosc)*, **68**(12), 1284-99.
- Beswick, E. J., Bland, D. A., Suarez, G., Barrera, C. A., Fan, X. & Reyes, V. E. (2005). *Helicobacter pylori* binds to CD74 on gastric epithelial cells and stimulates interleukin-8 production. *Infect Immun*, **73**(5), 2736-43.
- Bonizzi, G., Dejardin, E., Piret, B., Piette, J., Merville, M. P. & Bours, V. (1996). Interleukin-1 beta induces nuclear factor kappa B in epithelial cells independently of the production of reactive oxygen intermediates. *Eur J Biochem*, **242**(3), 544-9.
- Bonizzi, G., Piette, J., Schoonbroodt, S., Greimers, R., Havard, L., Merville, M. P. & Bours, V. (1999). Reactive oxygen intermediate-dependent NF-kappaB activation by interleukin-1beta requires 5-lipoxygenase or NADPH oxidase activity. *Mol Cell Biol*, **19**(3), 1950-60.
- Bravo, J., Quiroz, Y., Pons, H., Parra, G., Herrera-Acosta, J., Johnson, R. J. & Rodriguez-Iturbe, B. (2003). Vimentin and heat shock protein expression are induced in the kidney by angiotensin and by nitric oxide inhibition. *Kidney Int Suppl*(86), S46-51.
- Brennan, P. & O'Neill, L. A. (1995). Effects of oxidants and antioxidants on nuclear factor kappa B activation in three different cell lines: evidence against a universal hypothesis involving oxygen radicals. *Biochim Biophys Acta*, **1260**(2), 167-75.
- Chen, C. C. & Manning, A. M. (1995). Transcriptional regulation of endothelial cell adhesion molecules: a dominant role for NF-kappa B. *Agents Actions Suppl*, **47**, 135-41.
- Ciesielski-Treska, J., Ulrich, G. & Aunis, D. (1991). Protein kinase C-induced redistribution of the cytoskeleton and phosphorylation of vimentin in cultured brain macrophages. *J Neurosci Res*, **29**(3), 362-78.

- Colucci-Guyon, E., Portier, M. M., Dunia, I., Paulin, D., Pournin, S. & Babinet, C. (1994). Mice lacking vimentin develop and reproduce without an obvious phenotype. *Cell*, **79**(4), 679-94.
- DiChiara, M. R., Kiely, J. M., Gimbrone, M. A., Jr., Lee, M. E., Perrella, M. A. & Topper, J. N. (2000). Inhibition of E-selectin gene expression by transforming growth factor beta in endothelial cells involves coactivator integration of Smad and nuclear factor kappaB-mediated signals. *J Exp Med*, **192**(5), 695-704.
- Fan, J., Ye, R. D. & Malik, A. B. (2001). Transcriptional mechanisms of acute lung injury. *Am J Physiol Lung Cell Mol Physiol*, **281**(5), L1037-50.
- Fink, L., Kohlhoff, S., Stein, M. M., Hanze, J., Weissmann, N., Rose, F., Akkayagil, E., Manz, D., Grimminger, F., Seeger, W. & Bohle, R. M. (2002). cDNA array hybridization after laser-assisted microdissection from nonneoplastic tissue. *Am J Pathol*, **160**(1), 81-90.
- Goldberg, M. A., Dunning, S. P. & Bunn, H. F. (1988). Regulation of the erythropoietin gene: evidence that the oxygen sensor is a heme protein. *Science*, **242**(4884), 1412-5.
- Graven, K. K., Yu, Q., Pan, D., Roncarati, J. S. & Farber, H. W. (1999). Identification of an oxygen responsive enhancer element in the glyceraldehyde-3-phosphate dehydrogenase gene. *Biochim Biophys Acta*, **1447**(2-3), 208-18.
- Heidenthal, A. K., Weber, P. C., Lottspeich, F. & Hrboticky, N. (2000). The binding in vitro of modified LDL to the intermediate filament protein vimentin. *Biochem Biophys Res Commun*, **267**(1), 49-53.
- Hempel, S. L., Monick, M. M., He, B., Yano, T. & Hunninghake, G. W. (1994). Synthesis of prostaglandin H synthase-2 by human alveolar macrophages in response to lipopolysaccharide is inhibited by decreased cell oxidant tone. *J Biol Chem*, **269**(52), 32979-84.
- Hempel, S. L., Monick, M. M. & Hunninghake, G. W. (1996). Effect of hypoxia on release of IL-1 and TNF by human alveolar macrophages. *Am J Respir Cell Mol Biol*, **14**(2), 170-6.
- Hirani, N., Antonicelli, F., Strieter, R. M., Wiesener, M. S., Ratcliffe, P. J., Haslett, C. & Donnelly, S. C. (2001). The regulation of interleukin-8 by hypoxia in human macrophages--a potential role in the pathogenesis of the acute respiratory distress syndrome (ARDS). *Mol Med*, **7**(10), 685-97.
- Hirano, S. (1998). Nitric oxide-mediated cytotoxic effects of alveolar macrophages on transformed lung epithelial cells are independent of the beta 2 integrin-mediated intercellular adhesion. *Immunology*, **93**(1), 102-8.
- Ho, V. T. & Bunn, H. F. (1996). Effects of transition metals on the expression of the erythropoietin gene: further evidence that the oxygen sensor is a heme protein. *Biochem Biophys Res Commun*, **223**(1), 175-80.
- Hofer, T., Wenger, H. & Gassmann, M. (2002). Oxygen sensing, HIF-1alpha stabilization and potential therapeutic strategies. *Pflugers Arch*, **443**(4), 503-7.

- Hoogsteden, H. C., van Hal, P. T., Wijkhuijs, J. M., Hop, W., Verkaik, A. P. & Hilvering, C. (1991). Expression of the CD11/CD18 cell surface adhesion glycoprotein family on alveolar macrophages in smokers and nonsmokers. *Chest*, **100**(6), 1567-71.
- Hur, E., Chang, K. Y., Lee, E., Lee, S. K. & Park, H. (2001). Mitogen-activated protein kinase kinase inhibitor PD98059 blocks the trans-activation but not the stabilization or DNA binding ability of hypoxia-inducible factor-1alpha. *Mol Pharmacol*, **59**(5), 1216-24.
- Jahn, H. U., Krull, M., Wuppermann, F. N., Klucken, A. C., Rosseau, S., Seybold, J., Hegemann, J. H., Jantos, C. A. & Suttorp, N. (2000). Infection and activation of airway epithelial cells by Chlamydia pneumoniae. *J Infect Dis*, **182**(6), 1678-87.
- Jungi, T. W., Sager, H., Adler, H., Brcic, M. & Pfister, H. (1997). Serum factors, cell membrane CD14, and beta2 integrins are not required for activation of bovine macrophages by lipopolysaccharide. *Infect Immun*, **65**(9), 3577-84.
- Kallio, P. J., Okamoto, K., O'Brien, S., Carrero, P., Makino, Y., Tanaka, H. & Poellinger, L. (1998). Signal transduction in hypoxic cells: inducible nuclear translocation and recruitment of the CBP/p300 coactivator by the hypoxia-inducible factor-1alpha. *Embo J*, **17**(22), 6573-86.
- Koay, M. A., Gao, X., Washington, M. K., Parman, K. S., Sadikot, R. T., Blackwell, T. S. & Christman, J. W. (2002). Macrophages are necessary for maximal nuclear factor-kappa B activation in response to endotoxin. *Am J Respir Cell Mol Biol*, **26**(5), 572-8.
- Kong, T., Eltzschig, H. K., Karhausen, J., Colgan, S. P. & Shelley, C. S. (2004). Leukocyte adhesion during hypoxia is mediated by HIF-1-dependent induction of beta2 integrin gene expression. *Proc Natl Acad Sci U S A*, **101**(28), 10440-5.
- Koong, A. C., Chen, E. Y., Mivechi, N. F., Denko, N. C., Stambrook, P. & Giaccia, A. J. (1994). Hypoxic activation of nuclear factor-kappa B is mediated by a Ras and Raf signaling pathway and does not involve MAP kinase (ERK1 or ERK2). *Cancer Res*, **54**(20), 5273-9.
- Krishnamachary, B., Berg-Dixon, S., Kelly, B., Agani, F., Feldser, D., Ferreira, G., Iyer, N., LaRusch, J., Pak, B., Taghavi, P. & Semenza, G. L. (2003). Regulation of colon carcinoma cell invasion by hypoxia-inducible factor 1. *Cancer Res*, **63**(5), 1138-43.
- Kwapiszewska, G., Wilhelm, J., Wolff, S., Laumanns, I., Koenig, I. R., Ziegler, A., Seeger, W., Bohle, R. M., Weissmann, N. & Fink, L. (2005). Expression profiling of laser-microdissected intrapulmonary arteries in hypoxia-induced pulmonary hypertension. *Respir Res*, **6**, 109.
- Lantner, F., Starlets, D., Gore, Y., Flaishon, L., Yamit-Hezi, A., Dikstein, R., Leng, L., Bucala, R., Machluf, Y., Oren, M. & Shachar, I. (2007). CD74 induces TAp63 expression leading to B-cell survival. *Blood*, **110**(13), 4303-11.
- Leeper-Woodford, S. K. & Detmer, K. (1999). Acute hypoxia increases alveolar macrophage tumor necrosis factor activity and alters NF-kappaB expression. *Am J Physiol*, **276**(6 Pt 1), L909-16.



- Leeper-Woodford, S. K. & Mills, J. W. (1992). Phagocytosis and ATP levels in alveolar macrophages during acute hypoxia. *Am J Respir Cell Mol Biol*, **6**(3), 326-34.
- Lentsch, A. B., Shanley, T. P., Sarma, V. & Ward, P. A. (1997). In vivo suppression of NF-kappa B and preservation of I kappa B alpha by interleukin-10 and interleukin-13. *J Clin Invest*, **100**(10), 2443-8.
- Lopez-Barneo, J., Pardal, R. & Ortega-Saenz, P. (2001). Cellular mechanism of oxygen sensing. *Annu Rev Physiol*, **63**, 259-87.
- Lundahl, J., Hallden, G. & Skold, C. M. (1996). Human blood monocytes, but not alveolar macrophages, reveal increased CD11b/CD18 expression and adhesion properties upon receptor-dependent activation. *Eur Respir J*, **9**(6), 1188-94.
- Luo, Y., He, D. L., Ning, L., Shen, S. L., Li, L. & Li, X. (2006). Hypoxia-inducible factor-1alpha induces the epithelial-mesenchymal transition of human prostatecancer cells. *Chin Med J (Engl)*, **119**(9), 713-8.
- Madjdpour, C., Jewell, U. R., Kneller, S., Ziegler, U., Schwendener, R., Booy, C., Klausli, L., Pasch, T., Schimmer, R. C. & Beck-Schimmer, B. (2003). Decreased alveolar oxygen induces lung inflammation. *Am J Physiol Lung Cell Mol Physiol*, **284**(2), L360-7.
- Maxwell, P. H., Wiesener, M. S., Chang, G. W., Clifford, S. C., Vaux, E. C., Cockman, M. E., Wykoff, C. C., Pugh, C. W., Maher, E. R. & Ratcliffe, P. J. (1999). The tumour suppressor protein VHL targets hypoxia-inducible factors for oxygen-dependent proteolysis. *Nature*, **399**(6733), 271-5.
- Michiels, C. (2004). Physiological and pathological responses to hypoxia. *Am J Pathol*, **164**(6), 1875-82.
- Milne, A. A. & Piper, P. J. (1994). The effects of two anti-CD18 antibodies on antigen-induced airway hyperresponsiveness and leukocyte accumulation in the guinea pig. *Am J Respir Cell Mol Biol*, **11**(3), 337-43.
- Montoya, M. C., Luscinskas, F. W., del Pozo, M. A., Aragonés, J. & de Landazuri, M. O. (1997). Reduced intracellular oxidative metabolism promotes firm adhesion of human polymorphonuclear leukocytes to vascular endothelium under flow conditions. *Eur J Immunol*, **27**(8), 1942-51.
- Mor-Vaknin, N., Punturieri, A., Sitwala, K. & Markovitz, D. M. (2003). Vimentin is secreted by activated macrophages. *Nat Cell Biol*, **5**(1), 59-63.
- Muller, K., Dulku, S., Hardwick, S. J., Skepper, J. N. & Mitchinson, M. J. (2001). Changes in vimentin in human macrophages during apoptosis induced by oxidised low density lipoprotein. *Atherosclerosis*, **156**(1), 133-44.
- Mulligan, M. S., Varani, J., Warren, J. S., Till, G. O., Smith, C. W., Anderson, D. C., Todd, R. F., 3rd & Ward, P. A. (1992). Roles of beta 2 integrins of rat neutrophils in complement- and oxygen radical-mediated acute inflammatory injury. *J Immunol*, **148**(6), 1847-57.

- Owen, P. J., Johnson, G. D. & Lord, J. M. (1996). Protein kinase C-delta associates with vimentin intermediate filaments in differentiated HL60 cells. *Exp Cell Res*, **225**(2), 366-73.
- Paine, R., 3rd, Morris, S. B., Jin, H., Baleeiro, C. E. & Wilcoxon, S. E. (2002). ICAM-1 facilitates alveolar macrophage phagocytic activity through effects on migration over the AEC surface. *Am J Physiol Lung Cell Mol Physiol*, **283**(1), L180-7.
- Parsey, M. V., Kaneko, D., Shenkar, R. & Abraham, E. (1999). Neutrophil apoptosis in the lung after hemorrhage or endotoxemia: apoptosis and migration are independent of interleukin-1beta. *Chest*, **116**(1 Suppl), 67S-68S.
- Popovici, R. M., Irwin, J. C., Giaccia, A. J. & Giudice, L. C. (1999). Hypoxia and cAMP stimulate vascular endothelial growth factor (VEGF) in human endometrial stromal cells: potential relevance to menstruation and endometrial regeneration. *J Clin Endocrinol Metab*, **84**(6), 2245-8.
- Razeghi, P., Essop, M. F., Huss, J. M., Abbasi, S., Manga, N. & Taegtmeyer, H. (2003). Hypoxia-induced switches of myosin heavy chain iso-gene expression in rat heart. *Biochem Biophys Res Commun*, **303**(4), 1024-7.
- Richard, D. E., Berra, E., Gothie, E., Roux, D. & Pouyssegur, J. (1999). p42/p44 mitogen-activated protein kinases phosphorylate hypoxia-inducible factor 1alpha (HIF-1alpha) and enhance the transcriptional activity of HIF-1. *J Biol Chem*, **274**(46), 32631-7.
- Ross, G. D., Reed, W., Dalzell, J. G., Becker, S. E. & Hogg, N. (1992). Macrophage cytoskeleton association with CR3 and CR4 regulates receptor mobility and phagocytosis of iC3b-opsonized erythrocytes. *J Leukoc Biol*, **51**(2), 109-17.
- Sarria, A. J., Lieber, J. G., Nordeen, S. K. & Evans, R. M. (1994). The presence or absence of a vimentin-type intermediate filament network affects the shape of the nucleus in human SW-13 cells. *J Cell Sci*, **107** ( Pt 6), 1593-607.
- Scannell, G., Waxman, K., Vaziri, N. D., Zhang, J., Kaupke, C. J., Jalali, M. & Hect, C. (1995). Effects of trauma on leukocyte intercellular adhesion molecule-1, CD11b, and CD18 expressions. *J Trauma*, **39**(4), 641-4.
- Schaberg, T., Lauer, C., Lode, H., Fischer, J. & Haller, H. (1992). Increased number of alveolar macrophages expressing adhesion molecules of the leukocyte adhesion molecule family in smoking subjects. Association with cell-binding ability and superoxide anion production. *Am Rev Respir Dis*, **146**(5 Pt 1), 1287-93.
- Schmal, H., Czermak, B. J., Lentsch, A. B., Bless, N. M., Beck-Schimmer, B., Friedl, H. P. & Ward, P. A. (1998). Soluble ICAM-1 activates lung macrophages and enhances lung injury. *J Immunol*, **161**(7), 3685-93.
- Schwartz, M. D., Moore, E. E., Moore, F. A., Shenkar, R., Moine, P., Haenel, J. B. & Abraham, E. (1996). Nuclear factor-kappa B is activated in alveolar macrophages from patients with acute respiratory distress syndrome. *Crit Care Med*, **24**(8), 1285-92.

- Sen, R. & Baltimore, D. (1986). Multiple nuclear factors interact with the immunoglobulin enhancer sequences. *Cell*, **46**(5), 705-16.
- Shen, Z. Y., Xu, L. Y., Chen, M. H., Cai, W. J., Shen, J., Chen, J. Y. & Zeng, Y. (2003). Cytogenetic and molecular genetic changes in malignant transformation of immortalized esophageal epithelial cells. *Int J Mol Med*, **12**(2), 219-24.
- Shenkar, R. & Abraham, E. (1999). Mechanisms of lung neutrophil activation after hemorrhage or endotoxemia: roles of reactive oxygen intermediates, NF-kappa B, and cyclic AMP response element binding protein. *J Immunol*, **163**(2), 954-62.
- Siffert, J. C., Baldacini, O., Kuhry, J. G., Wachsmann, D., Benabdelmoumene, S., Faradji, A., Monteil, H. & Poindron, P. (1993). Effects of Clostridium difficile toxin B on human monocytes and macrophages: possible relationship with cytoskeletal rearrangement. *Infect Immun*, **61**(3), 1082-90.
- Starlets, D., Gore, Y., Binsky, I., Haran, M., Harpaz, N., Shvidel, L., Becker-Herman, S., Berrebi, A. & Shachar, I. (2006). Cell-surface CD74 initiates a signaling cascade leading to cell proliferation and survival. *Blood*, **107**(12), 4807-16.
- Strelkov, S. V., Herrmann, H. & Aebi, U. (2003). Molecular architecture of intermediate filaments. *Bioessays*, **25**(3), 243-51.
- Striz, I., Wang, Y. M., Kalaycioglu, O. & Costabel, U. (1992). Expression of alveolar macrophage adhesion molecules in pulmonary sarcoidosis. *Chest*, **102**(3), 882-6.
- Stumptner-Cuvelette, P. & Benaroch, P. (2002). Multiple roles of the invariant chain in MHC class II function. *Biochim Biophys Acta*, **1542**(1-3), 1-13.
- Taguchi, M., Sampath, D., Koga, T., Castro, M., Look, D. C., Nakajima, S. & Holtzman, M. J. (1998). Patterns for RANTES secretion and intercellular adhesion molecule 1 expression mediate transepithelial T cell traffic based on analyses in vitro and in vivo. *J Exp Med*, **187**(12), 1927-40.
- Tan, C. C. & Ratcliffe, P. J. (1991). Effect of inhibitors of oxidative phosphorylation on erythropoietin mRNA in isolated perfused rat kidneys. *Am J Physiol*, **261**(6 Pt 2), F982-7.
- van der Flier, A. & Sonnenberg, A. (2001). Function and interactions of integrins. *Cell Tissue Res*, **305**(3), 285-98.
- Vanden Hoek, T. L., Becker, L. B., Shao, Z., Li, C. & Schumacker, P. T. (1998). Reactive oxygen species released from mitochondria during brief hypoxia induce preconditioning in cardiomyocytes. *J Biol Chem*, **273**(29), 18092-8.
- VanOtteren, G. M., Standiford, T. J., Kunkel, S. L., Danforth, J. M. & Strieter, R. M. (1995). Alterations of ambient oxygen tension modulate the expression of tumor necrosis factor and macrophage inflammatory protein-1 alpha from murine alveolar macrophages. *Am J Respir Cell Mol Biol*, **13**(4), 399-409.
- Veiga-Crespo, P., Poza, M., Prieto-Alcedo, M. & Villa, T. G. (2004). Ancient genes of *Saccharomyces cerevisiae*. *Microbiology*, **150**(Pt 7), 2221-7.

- 
- von Schnakenburg, C., Strehlau, J., Ehrich, J. H. & Melk, A. (2002). Quantitative gene expression of TGF-beta1, IL-10, TNF-alpha and Fas Ligand in renal cortex and medulla. *Nephrol Dial Transplant*, **17**(4), 573-9.
- Vossenaar, E. R., Despres, N., Lapointe, E., van der Heijden, A., Lora, M., Senshu, T., van Venrooij, W. J. & Menard, H. A. (2004). Rheumatoid arthritis specific anti-Sa antibodies target citrullinated vimentin. *Arthritis Res Ther*, **6**(2), R142-50.
- Vossenaar, E. R., Radstake, T. R., van der Heijden, A., van Mansum, M. A., Dieteren, C., de Rooij, D. J., Barrera, P., Zendman, A. J. & van Venrooij, W. J. (2004). Expression and activity of citrullinating peptidylarginine deiminase enzymes in monocytes and macrophages. *Ann Rheum Dis*, **63**(4), 373-81.
- Wang, G. L. & Semenza, G. L. (1993). Desferrioxamine induces erythropoietin gene expression and hypoxia-inducible factor 1 DNA-binding activity: implications for models of hypoxia signal transduction. *Blood*, **82**(12), 3610-5.
- Wegner, C. D., Gundel, R. H., Reilly, P., Haynes, N., Letts, L. G. & Rothlein, R. (1990). Intercellular adhesion molecule-1 (ICAM-1) in the pathogenesis of asthma. *Science*, **247**(4941), 456-9.
- Weih, F., Carrasco, D., Durham, S. K., Barton, D. S., Rizzo, C. A., Ryseck, R. P., Lira, S. A. & Bravo, R. (1995). Multiorgan inflammation and hematopoietic abnormalities in mice with a targeted disruption of RelB, a member of the NF-kappa B/Rel family. *Cell*, **80**(2), 331-40.
- Weissmann, N., Schermuly, R. T., Ghofrani, H. A., Hanze, J., Goyal, P., Grimminger, F. & Seeger, W. (2006). Hypoxic pulmonary vasoconstriction--triggered by an increase in reactive oxygen species? *Novartis Found Symp*, **272**, 196-208; discussion 208-17.
- Wenger, R. H., Marti, H. H., Schuerer-Maly, C. C., Kvietikova, I., Bauer, C., Gassmann, M. & Maly, F. E. (1996). Hypoxic induction of gene expression in chronic granulomatous disease-derived B-cell lines: oxygen sensing is independent of the cytochrome b558-containing nicotinamide adenine dinucleotide phosphate oxidase. *Blood*, **87**(2), 756-61.
- Xu, B., deWaal, R. M., Mor-Vaknin, N., Hibbard, C., Markovitz, D. M. & Kahn, M. L. (2004). The endothelial cell-specific antibody PAL-E identifies a secreted form of vimentin in the blood vasculature. *Mol Cell Biol*, **24**(20), 9198-206.
- Yadatie, F., Sandvik, A. K., Bergum, H., Norsett, K. & Laegreid, A. (2004). Miniaturized fluorescent RNA dot blot method for rapid quantitation of gene expression. *BMC Biotechnol*, **4**, 12.
- Yamada, H., Chen, D., Monstein, H. J. & Hakanson, R. (1997). Effects of fasting on the expression of gastrin, cholecystokinin, and somatostatin genes and of various housekeeping genes in the pancreas and upper digestive tract of rats. *Biochem Biophys Res Commun*, **231**(3), 835-8.
- Yamamoto, Y., Konig, P., Henrich, M., Dedio, J. & Kummer, W. (2006). Hypoxia induces production of nitric oxide and reactive oxygen species in glomus cells of rat carotid body. *Cell Tissue Res*, **325**(1), 3-11.

- 
- Zampetaki, A., Mitsialis, S. A., Pfeilschifter, J. & Kourembanas, S. (2004). Hypoxia induces macrophage inflammatory protein-2 (MIP-2) gene expression in murine macrophages via NF-kappaB: the prominent role of p42/ p44 and PI3 kinase pathways. *Faseb J*, **18**(10), 1090-2.

## 8 Curriculum Vitae

### Personal details

Name	Zeev Israeli
Place of birth	Zefat (Israel)
Date of birth	21.10.1972
Status	married + 3

### School

1978- 1984	primary school in Ayelet- haschahar
1984-1990	high school in Kefar- blum
1990-1995	serving in the Israeli defense force

### Study

1996-1999	faculty of Dentistry in the Tel-Aviv university Israel
1999	learning the German language in Frankfurt am Main
2000-2004	study of human Medicine in the Justus-Liebig Universität Gießen
2004-2005	practical year in the Department of pediatric Uniklinik Gießen and in the Hospital in Bad-Homburg v.d.H
2005	final national exam in Bad-Homburg v.d.H

### Professional experience

7/2005-12/2007	working in the Department for Gastroenterology Med.Klinik II, städtische Kliniken Frankfurt Höchst
Since 1/2008	Department for Kardiology Med.Klinik I, städtische Kliniken Frankfurt Höchst

## 9 Acknowledgments

For guiding me in the long process of writing this work I would like to thank Prof .Dr. med Ludger Fink.

For a careful reading of this manuscript and for the statistical analysis of the results I thank Dr.rer.nat. Jochen Wilhelm.

For technical support and creative ideas while doing the bronchoalveolar lavage I thank Karin Quanz.

For helping me at the very first steps of the lab work and giving me a very clear plan of the way the trials should be performed, as well as the mental supporting in moments of despair I thank Maria Magdalena Stein.

For all my colleges and co-worker who supported me in the experimental part of this work I thank Jai Prakash Moyal, Grazyna Kwapiszewska, Stefanie and Jens Wolff, Elena Hartmann and Esther Kuhlmann.

For financial support of this work I thank Prof. Dr. med. Andreas Schulz, director of the pathology institute in Gießen, Prof. Dr.med Werner Seeger, director of Med. Klinik II Gießen.

For carrying out the immunohistology and its analysis I thank Prof. Dr. med. Rainer Maria Bohle.

For technical assistance in establishing many of the figures and tables in this work I thank my brothers.

Last but not least for my wife who supported me during the long period of time in which I was studying, especially for being a great mother to our sons and for the long days she had to spend alone with them.